Washington University in St. Louis
Washington University Open Scholarship

Arts & Sciences Electronic Theses and Dissertations | Arts & Sciences

Spring 5-15-2017

Regulation of the Pro-Tumorigenic Senescence-Associated Secretory Phenotype

Kevin Flanagan
Washington University in St. Louis

Follow this and additional works at: https://openscholarship.wustl.edu/art_sci_etds

 Part of the Cell Biology Commons

Recommended Citation
Flanagan, Kevin, "Regulation of the Pro-Tumorigenic Senescence-Associated Secretory Phenotype" (2017). *Arts & Sciences Electronic Theses and Dissertations*. 1101.
https://openscholarship.wustl.edu/art_sci_etds/1101

This Dissertation is brought to you for free and open access by the Arts & Sciences at Washington University Open Scholarship. It has been accepted for inclusion in Arts & Sciences Electronic Theses and Dissertations by an authorized administrator of Washington University Open Scholarship. For more information, please contact digital@wumail.wustl.edu.

WASHINGTON UNIVERSITY IN ST. LOUIS

Division of Biology and Biomedical Sciences
Molecular Cell Biology

Dissertation Examination Committee:
Sheila A. Stewart, Chair
Kendall Blumer
Milan Chheda
Robert Mecham
Joshua Rubin
Jason Weber

Regulation of the Pro-Tumorigenic Senescence-Associated Secretory Phenotype

by

Kevin Colin Flanagan

A dissertation presented to
The Graduate School
of Washington University in
partial fulfillment of the
requirements for the degree
of Doctor of Philosophy

May 2017
St. Louis, Missouri

TABLE OF CONTENTS

LIST OF FIGURES

CHAPTER 2: c-Myb is a novel regulatory of the senescence-associated secretory phenotype

CHAPTER 3: p38MAPK plays a crucial role in stromal mediated tumorigenesis

LIST OF TABLES

CHAPTER 2: c-Myb is a novel regulatory of the senescence-associated secretory phenotype

CHAPTER 3: p38MAPK plays a crucial role in stromal mediated tumorigenesis

ACKNOWLEDGMENTS

I would like to thank my advisor, Sheila Stewart, for welcoming me into her lab and supporting me the whole way. Without her expertise, encouragement, advice, and direction, I would not have succeeded in my Ph.D. nor learned how to be an effective, focused researcher. I would also like to thank the members of my thesis committee over the course of my research—Kendall Blumer, Josh Rubin, Jason Weber, Bob Mecham, Milan Chheda, Tatiana Efimova, and Andrey Shaw. Their expertise and advice kept me on track and taught me how to approach research questions and overcome problems.

Thank you to my workplace proximity associates in the Stewart Lab for being my friends, colleagues, and mentors. I learned so much from them, starting with Elise Alspach, with whom I worked throughout her time in lab. Not only did she lay the groundwork and begin what became my thesis, she guided me along the way on issues both technical and bigger picture. Likewise, I would like to thank Mira Pazolli, Yujie Fu, Daniel Teasley, Megan Ruhland, Hayley Moore, Bhavna Murali, Shankar Parajuli, Qihao Ren, and all of the other members of the Stewart lab over the years for their scientific help, criticism, and making work fun, especially when it otherwise wasn't. Each of them contributed to my growth as a scientist and to making graduate school a better place in their own way. I'd also like to specifically thank my undergraduate students Hui Huang and Talon Trecek, and Laura Arthur, who rotated in our lab and helped with my project. Similarly, I'd like to thank Roberto Tapia, who worked with me

for a year when everything seemed like it wasn't working, but he stayed positive and helped me do the same. His help was invaluable.

I'd also like to thank the rest of my friends, fellow graduate students, and the many members of the BRIGHT and ICCE institutes who were a constant source of help and reagents. Thank you also to the many other professors, post-docs, staff members, and students who helped me in countless big and small ways, both in science and in life. Thank you to my many teachers over the years, both formal and informal. I am grateful from funding from NIH Cellular Biochemical and Molecular Sciences Pre-doctoral Training Grant T32 GM007067 and NIH F31 CA189669.

I'd like to thank my parents, who taught me the importance of education and made it possible for me to get a great one. Specifically, I'd like to thank my mom, Jan Flanagan, the only scientist I knew growing up, for being a role model and giving me—whether through genes or environment—an interest in science and biology. I'd like to thank my dad, Jim Flanagan, for teaching me the value of working hard and working well, and of making time for things that are important. Thank you to my brothers and their families for being role models, a welcome distraction from science, for intentionally misunderstanding what I do in lab, and for celebrating my victories and sometimes letting me forget my failures. I'd also like to thank my parents-in-law and the entire Berlage family for making me one of their own and supporting and helping me along the way.

Finally, I'd like to thank my wife, Laura, and my daughter, Clare. Laura followed me to St. Louis and has been my biggest supporter in graduate school and life. She put up with weekends in lab and cells that always needed to be split. She endured pushed back deadlines, delayed dinner times, and patiently avoided asking when I would graduate. She encouraged me and motivated me. Clare inspired me, cheered me, and reminded me that there are more important things than failed experiments.

Kevin C. Flanagan

Washington University in St. Louis

May 2017

ABSTRACT OF THE DISSERTATION

Regulation of the pro-tumorigenic senescence-associated secretory phenotype

by

Kevin Colin Flanagan

Doctor of Philosophy in Biology and Biomedical Sciences

Molecular Cell Biology

Washington University in St. Louis, April 2017

Dr. Sheila A. Stewart, Chair

Tumorigenesis results from the convergence of cell autonomous mutations and corresponding stromal changes that promote tumor cell growth. Mutations and stromal changes both accumulate with age and together account for the dramatic increase in cancer incidence with age. One change that occurs with age is the accumulation of stromal senescent cells. Senescent stromal cells secrete pro-tumorigenic factors collectively termed the senescence-associated secretory phenotype (SASP). The SASP impacts every stage of tumorigenesis and is a promising therapeutic target. As such, it is important to understand how the SASP is regulated.

Many but not all SASP factors are regulated transcriptionally by NF-kB and its upstream activator p38MAPK. However, many pro-tumorigenic SASP factors, including osteopontin (OPN), are not dependent on NF-κB or other canonical SASP regulators such as ATM, leaving the regulation of these factors an open question. Here, I report that the transcription factor c-Myb regulates OPN, IL-6, IL-8 and other SASP factors.

The regulation of OPN is direct as c-Myb binds to the OPN promoter in senescent cells, and this binding is required for promoter activation. Further, OPN is also regulated by the known SASP regulator C/EBPβ. In response to senescence, the full-length activating C/EBPβ isoform LAP2 increases binding to the OPN, IL-6, and IL-8 promoters. Using a microarray and RNAi approach, we identified 57 additional putative c-Myb-dependent SASP factors and 125 additional putative C/EBPβ SASP factors. There is a high degree of overlap between c-Myb- and C/EBPβ-dependent factors. The importance of both c-Myb and C/EBPβ is underscored by our finding that the depletion of either factor reduces the ability of senescent fibroblasts to promote the growth of preneoplastic epithelial cells.

Furthermore, I describe a post-transcriptional SASP mRNA stability regulator pathway. This pathway is dependent on p38MAPK, but is distinct from p38MAPK's role in NF-κB transcription of SASP factors. In fully senescent fibroblasts, p38MAPK regulates the removal of mRNA-destabilizing protein AUF1 from the 3'-UTRs of numerous SASP factor mRNAs, resulting in increased mRNA stability. Given p38MAPK's role in both transcriptional and post-transcriptional regulation of the SASP, we tested the ability of p38MAPK inhibitors to inhibit tumor growth. Treatment of mice with an orally-administered p38MAPK inhibitor significantly decreased tumor growth in senescent fibroblast-supported xenograft models. Importantly, p38MAPK inhibition acts upon the microenvironment by removing stromal support of tumor growth. Interestingly, p38MAPK inhibition also inhibits the tumor promoting activities of cancer-associated fibroblasts (CAFs). CAFs have a secretory profile similar to senescent fibroblasts. This

work indicates that p38MAPK inhibition is a viable therapeutic for targeting both senescent fibroblast and CAF stromal support of tumor cell growth.

CHAPTER 1

Introduction and Significance

Cellular senescence is a stress-response

Eukaryotic cells have evolved numerous strategies to overcome the insults and stresses presented by the environment, repeated DNA replication and cell division, and DNA mutations. In multicellular organisms, it is critical to maintain functional tissues and avoid proliferation of dysfunctional cells. One method organisms have developed is the induction of senescence. Senescence, a permanent cell cycle arrest characterized by a number of phenotypic changes, was first observed *in vitro* by Leonard Hayflick in 1965 (1). Although it had previously been believed that mammalian cells could undergo an unlimited number of cell divisions *in vitro*, Hayflick demonstrated that normal human cells will no longer divide after approximately 40-60 divisions. This limit is known as the Hayflick limit and was the first description of cellular senescence. Although it was widely assumed to be an artifact of tissue culture, it is now known that senescence occurs both *in vitro* and *in vivo,* where it plays important roles. It was later shown that the senescence Hayflick observed was induced by the shortening and eventual loss of telomeric DNA (2). More recent findings indicate that it is the loss of telomeric integrity, and not telomeric shortening *per se*, that can drive entrance into senescence. In the decades since it was first described, significant progress has been made in understanding the phenotypes associated with senescence, the mechanisms driving senescence, and the physiological and pathological roles of senescence.

In addition to telomere shortening or dysfunction, cellular senescence can be caused by DNA double strand breaks, epigenetic alterations to chromatin, oxidative or metabolic stress, tumor suppressor expression, and oncogene activation (3). When it occurs in

incipient tumor cells, senescence is a potent anti-tumor mechanism which prevents continued proliferation of cells with dysfunctional telomeres, extensive and persistent DNA damage, oncogene activation, or other stresses which could lead to the formation of tumors. Interestingly, senescent cells are resistant to apoptosis, another important tumor suppressive mechanism (4). Although senescent cells do not divide, they remain metabolically active and generally adapt a number of senescence-associated phenotypes, including a flattened morphology, the presence of heterochromatic foci (SAHFs), positive senescence-associated β-galactosidase staining, and an altered gene expression and secretion profile termed the senescence-associated secretory phenotype (SASP; ref. 8–12).

Although many cellular insults can induce senescence, they all converge on two related pathways which activate the senescence program. The tumor suppressors p53 and Rb are both critical for the induction of senescence in most contexts. p53 is commonly activated in response to DNA damage, excessive reactive oxygen species (ROS), or activation of oncogenes such as Ras (9). In turn, p53 activates $p21^{Cip1}$, a cyclin-dependent kinase inhibitor, which arrests the cell cycle (10). Likewise, Rb, which prevents progression of the cell cycle from G1 to S, is activated by $p16^{INK4A}$ in response to a variety of stresses. Although p16 is not required for the induction of senescence, p16 is often used as a marker of senescence, particularly *in vivo*. While the p53 and Rb pathways are interconnected, they act mostly independently to induce senescence and, in the right context, activation of either pathway alone is sufficient to induce senescence.

Senescence plays important physiological and pathological roles

While senescence was first described and characterized *in vitro*, it is now known to occur *in vivo*, where it impacts a diverse and growing list of physiological processes and is implicated in multiple pathologies. For instance, senescent cells are important for normal mammalian development, including in the apical ectodermal ridge and structures in the ear (11, 12). A recent report also indicates that senescence can also act as an antiviral mechanism (13). Further, clearance of senescent cells from mice inhibits wound repair (14). Interestingly, while short-lived senescent cells seem to be important for wound healing, the persistent presence and accumulation of senescent cells can contribute to tissue dysfunction. While many senescent cells are rapidly cleared by the immune system, senescent cells do accumulate with age (15–17), potentially altering the microenvironment and contributing to many age-related diseases.

Indeed, work using various senescent cell clearing models in mice has indicated that clearance of senescent cells reverses multiple aging phenotypes. Using a transgenic mouse model which activates a suicide gene in response to AP20187 (AP) treatment in $p16^{INK4A}$-expressing cells (INK-ATTAC), Baker *et al.* selectively removed p16-positive senescent cells from young and old mice (18). Treatment of progeroid mice with AP starting at weaning resulted in significantly delayed aging phenotypes such as sarcopenia, cataracts, and loss of adipose tissue. Further, starting AP treatment at five months of age in the same progeroid mice significantly increased adipose tissue, the size of muscle fibers, and resulted in increased treadmill exercise test performance at

ten months, indicating that elimination of senescence cells in this setting can not only delay but also rescue aging phenotypes associated with this mouse model.

Similar results were obtained in naturally aged mice (19). Indeed, clearance of $p16^{INK4A}$-positive cells resulted in increased lifespan and healthspan as measured by numerous metrics including delayed cataracts and increased activity and exploratory behavior. These studies and others indicate that senescent cells play an important role in aging and can contribute to diverse aging phenotypes including cardiac aging, glomerulosclerosis, decreased motor activity, cancer, and overall lifespan (20, 21). Further, not only can elimination of senescent cells inhibit or delay aging phenotypes, it can also reverse some aging phenotypes, making senescent cells an appealing therapeutic target.

Indeed, in the last two years there has been increasing research on “senolytic” drugs, those that target and selectively kill senescent cells (20–23). Senescent cells are resistant to apoptosis (4). Most senolytic drugs sensitize senescent cells to apoptosis by targeting apoptotic proteins such as Bcl-2 family members (22). Treatment with two senolytic drugs which target Bcl-2 proteins can improve cardiovascular function and reduce aortic calcification, phenocopying improvements seen in genetic models of senescent clearance (23). Likewise, a recent report indicates FOXO4 is elevated in senescent cells and is required for senescent cell resistance to apoptosis (20). Treatment with a peptide which blocked interaction between FOXO4 and p53 resulted in selective apoptosis of senescent cells. Treatment with this peptide improved multiple

measures of health in both progeroid and naturally aged mice, including restoring hair growth and improving renal function. Further, treatment reduced chemotherapy side-effects such as liver damage. Together with models of genetic clearance of senescent cells, research using senolytic drugs has demonstrated that in addition to the important physiological and anti-tumor roles of senescent cells, senescent cells contribute to numerous aging phenotypes and pathologies. Further, while senolytic drugs are far from use in the clinic, recent work has demonstrated that it is possible to selectively target senescent cells and that senolytic drugs hold great promise in the treatment of many diseases.

Therefore, it is important to understand the mechanisms by which senescent cells promote the varied aging phenotypes described. Senescent cells may contribute to aging and tissue function decline simply by taking the place of a healthy, proliferating cell, particularly progenitor and stem cells (24). However, while the mere accumulation of non-dividing cells may play a role, there is significant evidence that senescent cells play an active role in many disease states. In fact, senescent cells have an altered secretory profile known as the senescence-associate secretory phenotype (SASP; ref 8). The SASP can alter local tissue homeostasis and promote disease states through a diverse set of mechanisms (5–8, 17, 24–26).

The senescence-associated secretory phenotype is pro-tumorigenic

The SASP consists of numerous inflammatory, mitogenic, and ECM-remodeling factors that are upregulated at the mRNA and protein levels and can promote tumor initiation

and development (6, 27, 28). The specific factors which are upregulated depends on the cell and tissue type as well as the means of senescence induction (29, 30). However, many “canonical” SASP factors, such as IL-6 and IL-8, are commonly upregulated in many contexts. Taken together, the known functions of SASP factors can impact every stage of tumorigenesis and progression, including tumor initiation, expansion, vascularization, local invasion, and metastasis (6, 7, 24, 25, 28).

Senescence is a potent tumor suppressive mechanism and yet, through the SASP, is also potently tumor promoting. This apparent paradox is explained by the differing effect of senescence in a cell autonomous versus a cell non-autonomous setting. Senescence does prevent cancer initiation in incipient tumor cells that senesce. However, when they arise in the stromal compartment senescent cells can promote tumor development in other nearby cells. Indeed, work over the last decade has demonstrated the importance of the stroma in tumorigenesis (31).

Traditionally, cancer has been thought of as a disease of a single, typically epithelial, cell which accumulates mutations and begins to proliferate uncontrollably. However, more recent work has indicated that a carcinoma arises and progresses through a complex process of communication between the incipient tumor cell and its microenvironment, which consists of stromal cells such as fibroblasts, immune cells, vasculature, the extracellular matrix, and other epithelial cells. Furthermore, communication between the incipient tumor cell and the microenvironment is bidirectional (32). Clearly nascent tumors can shape their microenvironment in many

ways such as inhibiting the immune response and promoting vascularization. However, stromal cells also direct the evolution of nascent tumors. For instance, when non-tumor forming pre-neoplastic epithelial cells are injected into a mouse either alone or with normal fibroblasts, they are unable to establish tumors. However, if the same pre-neoplastic epithelial cells are coinjected with tumor-educated cancer-associated fibroblasts (CAFs), which themselves are not cancerous, the CAFs will promote the formation of tumors by the pre-neoplastic cells (33). This work indicates that the stroma plays an active role and can drive epithelial cells to form tumor cells when they otherwise would not.

Interestingly, fibroblasts can also restrain tumor growth. Coinjection of tumor-forming epithelial cells with normal fibroblasts can inhibit tumor formation. Perhaps even more strikingly, injection of blastocysts with teratocarcinoma cells will form mosaic mice which, despite containing teratocarcinoma cells, are tumor free (34). Thus, stromal fibroblasts can either promote or repress tumor initiation and growth, indicating that the stroma and tumor microenvironment plays an important role in cancer biology. Indeed, senescent stromal cells also promote tumorigenesis. Coinjection of senescent fibroblasts with pre-neoplastic epithelial cells will drive increased tumor initiation and growth in a similar manner to coinjection of CAFs (7, 8, 28). So while senescence can prevent tumor formation in a cell autonomous manner, this mechanism comes at a cost to the organism as senescent stromal cells can promote the development of tumors in nearby tissue.

The evolution of a senescence mechanism which provides a benefit to the organism but is also detrimental can be explained by the hypothesis of antagonistic pleiotropy. Antagonistic pleiotropy suggests that natural selection favors traits that increase fitness during reproductive years even if they come at a cost later in life. Cancer is a disease of aging, with the vast majority of cases occurring after peak reproductive years (35). Senescence helps prevent the formation of tumors in younger individuals, allowing them to have a healthy reproductive lifespan. However, as the individual ages senescent cells accumulate in their tissues and begin to affect physiology, including promoting tumorigenesis (17, 36). Because this cost is delayed until after reproduction it is not strongly selected against during evolution. Thus, cancer is a disease of the aged in part because senescence both prevents cancer formation in young individuals and can promote it cell non-autonomously in aged individuals.

Senescence, via the SASP, can promote cancer via multiple mechanisms. For instance, senescent fibroblasts can directly promote cell growth as well as promote EMT, an important step in metastasis (7, 28). In addition, senescent fibroblasts can induce local immune invasion, resulting in increased myeloid cell populations and immunosuppression (17). This occurs even in the absence of a tumor and creates a tumor-permissive environment. Senescence can also promote migration and invasion of tumor cells (8, 37). This work and more, along with studies demonstrating that clearance of senescent cells can positively impact multiple aging phenotypes, suggests that targeting senescent stromal cells via the SASP may be a powerful therapeutic opportunity.

The SASP is regulated by multiple pathways

In order to target the SASP therapeutically, it is vital to understand how it is regulated. The regulation of SASP induction is complex and incompletely understood. One potent inducer of senescence is persistent DNA-damage and the subsequent DNA-damage response (DDR) signaling. ATM is a central mediator of the DDR and is required for the induction of many SASP factors, including IL-6 and IL-8 (38). However, many SASP factors do not require ATM for their induction. For instance, the induction of Osteopontin (OPN) does not require ATM activity (39). Many SASP factors are transcriptionally activated by NF-κB and C/EBPβ (39–42). NF-κB seems to act in the same pathway as ATM, as ATM depletion decreases NF-κB activity in senescent cells (40). As with ATM, a subset of SASP factors, including OPN, are NF-κB-independent (39). NF-κB is also downstream of another important SASP regulator, the stress-induced kinase p38MAPK (40). Depletion of p38MAPK prevents the induction of many SASP factors, and constitutive activation of p38MAPK signaling results in SASP induction even in the absence of additional senescence cues. Further, ATM is not required for p38MAPK activation or activation of the SASP by p38MAPK, suggesting that ATM and p38MAPK act in parallel pathways to activate NF-κB signaling. While p38MAPK induces many SASP factors, at the protein level only 25 of 37 SASP factors studied required p38MAPK signaling, suggesting that, like ATM and NF-κB, it is far from a universal SASP regulator (40). Many of the SASP factors regulated by ATM, p38MAPK, and NF-κB are inflammatory genes, while many matrix remodeling proteins and growth factors are independent of these pathways.

NF-κB, while not a universal SASP regulator, is a key regulator of the SASP. The regulation of NF-κB in senescent cells is complex, however. In addition to the roles ATM and p38MAPK play in activating NF-κB in response to senescence, feedback loops also modulate NF-κB activity. In response to senescence, NF-κB promotes transcription of SASP factors such as IL-6 and IL-1α. These factors are important for reinforcing senescence and promoting the SASP (41, 43). IL-1α in particular is upregulated by senescent cells and further promotes NF-κB and C/EBPβ activity, leading to further activation of the SASP (43). This positive feedback loop is mediated in part by mTOR, which promotes IL-1α translation (44). Inhibition of mTOR suppresses the upregulation of many NF-κB-dependent SASP factors. Thus, the NF-κB-dependent arm of the SASP is regulated by many factors at numerous levels. Still, NF-κB-dependent SASP factors represent only a subset of all SASP factors. For instance, only 35% of studied factors are mTOR-dependent, all of them also being NF-κB-dependent (44). Thus, there is considerable need to understand how NF-κB-independent SASP factors are regulated.

OPN is protumorigenic and distinctively regulated

The lack of broad SASP regulators on which nearly all SASP factors are dependent suggests that the SASP is not regulated by a single program but rather many overlapping regulatory mechanisms. This notion is further supported by the diversity of specific SASP factors which are conditionally upregulated depending on the cell type and senescence inducer. One such factor is osteopontin (OPN), a protumorigenic protein which has numerous physiological and pathological roles, including regulating

bone turnover, cell adhesion and migration, and inflammation (45–48). OPN is a secreted matrix protein that may anchor osteoclasts to the matrix (47), is upregulated in response to wounds, acts to recruit immune cells, can suppress apoptosis, and is upregulated in a number of cancer types (46, 49–52). OPN is also robustly upregulated in response to stress-induced, replicative, and oncogene-induced senescence in human cells (28).

Previous work in our lab demonstrated that in a two-stage skin carcinogenesis model, stromal cells stained positive for SA-βgal and $p16^{INK4A}$ prior to the appearance of hyperplasia. This work further demonstrates that senescent cells can play a role in promoting carcinogenesis and are not simply a by-product of tumor formation. Importantly, stromal cells staining positive for $p16^{INK4A}$ also stained positive for OPN, indicating that *in vivo* senescent mouse skin cells express OPN and that it may be playing a role in promoting tumorigenesis (28). Further, human AK and SCC skin lesions displayed coincident stroma cell staining for $p16^{INK4A}$ and OPN, suggesting that in human pre-neoplasias and neoplasias, stromal senescent cells express OPN and that OPN may be important in human tumorigenesis (53). Using *in vitro* cocultures assays and *in vivo* xenografts, our lab demonstrated that knocking down OPN in BJ fibroblasts eliminated the ability for senescent fibroblasts to promote the growth of preneoplastic HaCaT skin epithelial cells. Thus, OPN is necessary for senescent-fibroblast promoted preneoplastic cell growth in this context.

Additionally, treatment of pre-neoplastic HaCaT or N.p.c.T epithelial cells with recombinant human OPN (rhOPN) is sufficient to induced growth *in vitro* in the absence of senescent fibroblasts (28). In this context, rhOPN acts to promote cell growth via the MAPK pathway via the CD44 receptor (53). However, the growth induction using rhOPN did not recapitulate the magnitude of growth induction by senescent fibroblasts, suggesting that either additional factors secreted by senescent cells also play important roles, or that, given OPN is a highly modified protein, the rhOPN lacked some important post-translational modifications to achieve maximal growth promotion. These data together demonstrate that, at least in this skin carcinoma context, OPN is an important SASP factor for the promotion of pre-neoplastic cell growth by senescent cells. OPN is an extracellular matrix-associated protein and can promote cell migration (48). In fact, its expression correlates with tumor cell migration and invasion in squamous cell carcinoma (54), raising the possibility that senescent fibroblast-derived OPN may promote tumor invasion and metastasis in addition to cell proliferation. However, this possibility remains an untested area for future study.

Given senescent-derived OPN's ability to promote tumorigenesis, it is important to understand how OPN is regulated in senescent cells. However, the regulation of OPN in response to senescence is not understood. SASP regulators ATM and NF-κB are not required for OPN induction in response to senescence (39). Other SASP regulators, such as C/EBPβ, have not been studied in conjunction with OPN. Indeed, there are no known regulators of OPN in response to senescence.

The transcription factor C/EBPβ has three isoforms and regulates the SASP

One possible regulator of OPN is the transcription factor C/EBPβ. C/EBPβ belongs to the C/EBP family of transcription factors which also includes C/EBPα, C/EBPγ, C/EBPδ, C/EBPε, and C/EBPζ, each representing a distinct gene locus (55, 56). C/EBP transcription factors bind to DNA as a dimer and can do so as homodimers or as heterodimers consisting of two different C/EBP isoforms (57). C/EBPβ itself consists of three different isoforms translated from the same mRNA using alternative translation start sites. Two of the isoforms, LAP and LAP2 (Liver Activating Protein 1 and 2, respectively), contain the transactivation domain and activate transcription when they bind to promoters (55, 56). Although there is evidence for unique roles between LAP and LAP2 and distinct molecular targets, little is known about these differences nor their functional importance. The third isoform, LIP (Liver Inhibitory Protein), lacks the transactivation domain and acts in a dominant negative fashion to inhibit the activity of LAP and LAP2 (58). LIP can bind both to DNA as well as to the LAP and LAP2 isoforms. A C/EBPβ heterodimer consisting of LIP and one of the activating isoforms is unable to activate transcription (58). In addition to its known ability to regulate numerous genes such as cytokines as well as SASP factors specifically, C/EBPβ has been shown to regulate OPN in liposarcomas and lung cancer cells (59, 60). In addition to dimerizing with itself or other C/EBP family members, C/EBPβ also frequently interacts with other transcription factors, including the proto-oncogene c-Myb (61). With c-Myb, C/EBPβ coactivates transcription of several genes, including mim-1 and ChAT (62–64).

The transcription factor c-Myb is a proto-oncogene

One possible regulator of SASP factors is the transcription factor c-Myb. C-Myb is a proto-oncogene and is the mammalian homologue of the Avian myeloblastosis virus (AMV) v-*myb* oncogene (65, 66). V-*myb* is a 45 kD truncation of c-Myb and causes leukemia in various bird species (65, 67). Normal, endogenous, cellular c-Myb is highly conserved in animals, and Myb family members and homologues are present in a wide variety of species, including plants (68, 69).

Human c-Myb is a 75 kD DNA-binding protein consisting of three major domains: a DNA-binding domain (DBD), a negative regulatory domain (NRD), and a transactivation domain (TAD; ref. 65). C-Myb has multiple isoforms due to alternative splicing and is subject to numerous post-translational modifications, including phosphorylation and sumoylation, which can regulate its localization and activity (70–74). In addition, c-Myb cooperates and interacts with many other transcription factors to regulate transcription (75).

In mammals, c-Myb is best studied in hematopoietic development (76). c-Myb is critical for hematopoietic differentiation, including that of B cells and T cells (77–81). Additionally, it plays important roles in proliferation and expansion of certain cell lineages and low expression results in a myeloproliferative phenotype (82). Importantly, the role of c-Myb varies among different cell types, with many different transcriptional targets depending on context (83). More recent work has shown that c-Myb has roles in

differentiation, proliferation, and stem cell maintenance in settings such as colon crypt epithelial cells (84–86), neural progenitors and stem cells (87), and melanocytes (88).

Additionally, c-Myb is a known regulator of OPN in hepatocellular carcinoma and melanoma models (89, 90). However, c-Myb is poorly characterized in fibroblasts and has not been studied in mammalian cell senescence. C-Myb was first characterized as being expressed and having roles in fibroblasts in 1997, where it was shown to regulate cell-cycle progression and intracellular calcium levels (91). C-Myb has not been studied as a regulator of OPN in fibroblasts.

As a transcription factor, c-Myb binds to DNA as monomer (92). In a manner somewhat unusual for a transcription factor, however, c-Myb often binds to promoter regions without activating transcription (93). Instead, it may serve to prime promoters for co-activation by other transcription factors (94). Supporting this idea, c-Myb is known to interact with a number of other transcription factors including CBP, p300 and, as mentioned, C/EBPβ (61, 95). Given their previously reported abilities to regulate OPN in other contexts, I hypothesized that c-Myb and C/EBPβ regulate OPN in response to senescence. In addition, I hypothesized that other SASP factors may also be activated by c-Myb and C/EBP in response to senescence.

This thesis work focuses on better understanding the regulation of the SASP. I investigate the transcriptional regulation of SASP factors including OPN by the novel SASP regulator c-Myb. In addition, I describe a post-transcriptional regulatory role for

p38MAPK. Further, I investigate the potential efficacy of using drugs that target the p38MAPK pathway as a cancer therapy. This work expands the understanding of SASP regulation and advances our ability to understand and combat the contributions of the SASP to diseases of aging.

REFERENCES

1. Hayflick L. 1965. The limited in vitro lifetime of human diploid cell strains. Exp Cell Res 37:614–36.

2. Watson J. 1972. Origin of concatemeric T7 DNA. Nat New Biol 18:197–201.

3. Campisi J. 2005. Senescent cells, tumor suppression, and organismal aging: good citizens, bad neighbors. Cell 120:513–22.

4. Wang E. 1995. Senescent Human Fibroblasts Resist Programmed Cell Death, and Failure to Suppress bell Is Involved. Cancer Res 55:2284–2292.

5. Pazolli E, Stewart SA. 2008. Senescence: the good the bad and the dysfunctional. Curr Opin Genet Dev 18:42–7.

6. Coppé J-P, Desprez P-Y, Krtolica A, Campisi J. 2010. The senescence-associated secretory phenotype: the dark side of tumor suppression. Annu Rev Pathol 5:99–118.

7. Coppé J-P, Kauser K, Campisi J, Beauséjour CM. 2006. Secretion of vascular endothelial growth factor by primary human fibroblasts at senescence. J Biol Chem 281:29568–74.

8. Coppé J-P, Patil CK, Rodier F, Sun Y, Muñoz DP, Goldstein J, Nelson PS, Desprez P-Y, Campisi J. 2008. Senescence-associated secretory phenotypes reveal cell-nonautonomous functions of oncogenic RAS and the p53 tumor suppressor. PLoS Biol 6:2853–68.

9. Horn HF, Vousden KH. 2007. Coping with stress: multiple ways to activate p53. Oncogene 26:1306–1316.

10. Rufini a, Tucci P, Celardo I, Melino G. 2013. Senescence and aging: the critical roles of p53. Oncogene 32:5129–43.

11. Storer M, Mas A, Robert-Moreno A, Pecoraro M, Ortells MC, Di Giacomo V, Yosef R, Pilpel N, Krizhanovsky V, Sharpe J, Keyes WM. 2013. Senescence Is a Developmental Mechanism that Contributes to Embryonic Growth and Patterning. Cell 155:1119–1130.

12. Muñoz-Espín D, Cañamero M, Maraver A, Gómez-López G, Contreras J, Murillo-Cuesta S, Rodríguez-Baeza A, Varela-Nieto I, Ruberte J, Collado M, Serrano M. 2013. Programmed Cell Senescence during Mammalian Embryonic Development.

Cell 155:1104–1118.

13. Baz-martínez M, Silva-álvarez S Da, Rodríguez E, Guerra J. 2016. Cell senescence is an antiviral defense mechanism. Nat Publ Gr 1–11.

14. Demaria M, Ohtani N, Youssef SA, Rodier F, Toussaint W, Mitchell JR, Laberge R-M, Vijg J, Van Steeg H, Dollé MET, Hoeijmakers JHJ, de Bruin A, Hara E, Campisi J. 2014. An Essential Role for Senescent Cells in Optimal Wound Healing through Secretion of PDGF-AA. Dev Cell 31:722–733.

15. Dimri GP, Lee X, Basile G, Acosta M, Scott G, Roskelley C, Medrano EE, Linskens M, Rubelj I, Pereira-Smith O. 1995. A biomarker that identifies senescent human cells in culture and in aging skin in vivo. Proc Natl Acad Sci U S A 92:9363–7.

16. Herbig U, Ferreira M, Condel L, Carey D, Sedivy JM. 2006. Cellular Senescence in Aging Primates 1–2.

17. Ruhland MK, Loza AJ, Capietto A, Luo X, Knolhoff BL, Flanagan KC, Belt BA, Alspach E, Leahy K, Luo J, Schaffer A, Edwards JR, Longmore G, Faccio R, Denardo DG, Stewart SA. 2016. Stromal senescence establishes an immunosuppressive microenvironment that drives tumorigenesis. Nat Commun 7:1–18.

18. Baker DJ, Wijshake T, Tchkonia T, LeBrasseur NK, Childs BG, van de Sluis B, Kirkland JL, van Deursen JM. 2011. Clearance of p16Ink4a-positive senescent cells delays ageing-associated disorders. Nature 479:232–6.

19. Baker DJ, Childs BG, Durik M, Wijers ME, Sieben CJ, Zhong J, Saltness RA, Jeganathan KB, Verzosa GC, Pezeshki A, Khazaie K, Miller JD, Deursen JM Van. 2016. Naturally occurring p16INK4a-positive cells shorten healthy lifespan. Nature 530:184–189.

20. Baar MP, Brandt RMC, Putavet DA, Hoeijmakers JHJ, Campisi J, Keizer PLJ De, Pluijm I Van Der, Essers J, Cappellen WA Van, Ijcken WF Van, Houtsmuller AB. 2017. Targeted Apoptosis of Senescent Cells Restores Tissue Homeostasis in Response to Chemotoxicity Article Targeted Apoptosis of Senescent Cells Restores Tissue Homeostasis in Response to Chemotoxicity and Aging. Cell 169:132–140.e15.

21. Chang J, Wang Y, Shao L, Laberge R-M, Demaria M, Campisi J, Janakiraman K, Sharpless NE, Ding S, Feng W, Luo Y, Wang X, Nukhet A-B, Krager K, Ponnappan U, Martin H-J, Meng A, Zhou D. 2016. Clearance of senescent cells

by {ABT263} rejuvenates aged hematopoietic stem cells in mice. Nat Med 22:78–83.

22. Zhu Y, Tchkonia T, Fuhrmann-Stroissnigg H, Dai HM, Ling YY, Stout MB, Pirtskhalava T, Giorgadze N, Johnson KO, Giles CB, Wren JD, Niedernhofer LJ, Robbins PD, Kirkland JL. 2016. Identification of a novel senolytic agent, navitoclax, targeting the Bcl-2 family of anti-apoptotic factors. Aging Cell 15:428–435.

23. Roos CM, Zhang B, Palmer AK, Ogrodnik MB, Pirtskhalava T, Nassir M, Hagler M, Jurk D, Smith LA, Zhu Y, Schafer MJ, Kirkland JL, Miller JD. 2016. Chronic senolytic treatment alleviates established vasomotor dysfunction in aged or atherosclerotic mice 973–977.

24. Childs BG, Durik M, Baker DJ, van Deursen JM. 2015. Cellular senescence in aging and age-related disease: from mechanisms to therapy. Nat Med 21:1424–35.

25. Luo X, Fu Y, Loza AJ, Faccio R, Longmore GD, Stewart SA, Luo X, Fu Y, Loza AJ, Murali B, Leahy KM, Ruhland MK. 2016. Stromal-Initiated Changes in the Bone Promote Metastatic Niche Development Article Stromal-Initiated Changes in the Bone Promote Metastatic Niche Development. CellReports 14:82–92.

26. Fyhrquist F, Saijonmaa O, Strandberg T. 2013. The roles of senescence and telomere shortening in cardiovascular disease. NatRevCardiol 10:274–283.

27. Krtolica A, Parrinello S, Lockett S, Desprez PY, Campisi J. 2001. Senescent fibroblasts promote epithelial cell growth and tumorigenesis: a link between cancer and aging. Proc Natl Acad Sci U S A 98:12072–12077.

28. Pazolli E, Luo X, Brehm S, Carbery K, Chung J-J, Prior JL, Doherty J, Demehri S, Salavaggione L, Piwnica-Worms D, Stewart SA. 2009. Senescent stromal-derived osteopontin promotes preneoplastic cell growth. Cancer Res 69:1230–9.

29. Torres C, Königsberg M. 2016. Senescence associated secretory phenotype profile from primary lung mice fibroblasts depends on the senescence induction stimuli.

30. Salminen A, Kauppinen A, Kaarniranta K. 2012. Emerging role of NF-κB signaling in the induction of senescence-associated secretory phenotype (SASP). Cell Signal 24:835–45.

31. Alspach E, Fu Y, Stewart SA. 2013. Senescence and the pro-tumorigenic stroma.

Crit Rev Oncog 18:549–58.

32. Hanahan D, Weinberg RA. 2011. Hallmarks of cancer: The next generation. Cell 144:646–674.

33. Orimo A, Gupta PB, Sgroi DC, Arenzana-Seisdedos F, Delaunay T, Naeem R, Carey VJ, Richardson AL, Weinberg RA. 2005. Stromal fibroblasts present in invasive human breast carcinomas promote tumor growth and angiogenesis through elevated SDF-1/CXCL12 secretion. Cell 121:335–348.

34. Mintz B, Illmensee K. 1975. Normal genetically mosaic mice produced from malignant teratocarcinoma cells. Proc Natl Acad Sci U S A 72:3585–9.

35. Depinho RA. 2000. The age of cancer 408.

36. Jeyapalan JC, Ferreira M, Sedivy JM, Herbig U. 2007. Accumulation of senescent cells in mitotic tissue of aging primates. Mech Ageing Dev 128:36–44.

37. Laberge R, Awad P, Campisi J, Desprez P. 2012. Epithelial-Mesenchymal Transition Induced by Senescent Fibroblasts 39–44.

38. Rodier F, Coppé J-P, Patil CK, Hoeijmakers W a M, Muñoz DP, Raza SR, Freund A, Campeau E, Davalos AR, Campisi J. 2009. Persistent DNA damage signalling triggers senescence-associated inflammatory cytokine secretion. Nat Cell Biol 11:973–9.

39. Pazolli E, Alspach E, Milczarek A, Prior J, Piwnica-Worms D, Stewart SA. 2012. Chromatin remodeling underlies the senescence-associated secretory phenotype of tumor stromal fibroblasts that supports cancer progression. Cancer Res 72:2251–61.

40. Freund A, Patil CK, Campisi J. 2011. p38MAPK is a novel DNA damage response-independent regulator of the senescence-associated secretory phenotype. EMBO J 30:1536–48.

41. Kuilman T, Michaloglou C, Vredeveld LCW, Douma S, van Doorn R, Desmet CJ, Aarden L a, Mooi WJ, Peeper DS. 2008. Oncogene-induced senescence relayed by an interleukin-dependent inflammatory network. Cell 133:1019–31.

42. Chien Y, Scuoppo C, Wang X, Fang X, Balgley B, Bolden JE, Premsrirut P, Luo W, Chicas A, Lee CS, Kogan SC, Lowe SW. 2011. Control of the senescence-associated secretory phenotype by NF- k B promotes senescence and enhances chemosensitivity 2125–2136.

43. Orjalo A V, Bhaumik D, Gengler BK, Scott GK, Campisi J. 2009. Cell surface-bound IL-1alpha is an upstream regulator of the senescence-associated IL-6/IL-8 cytokine network. Proc Natl Acad Sci U S A 106:17031–6.

44. Laberge R-M, Sun Y, Orjalo A V, Patil CK, Freund A, Zhou L, Curran SC, Davalos AR, Wilson-Edell K a, Liu S, Limbad C, Demaria M, Li P, Hubbard GB, Ikeno Y, Javors M, Desprez P-Y, Benz CC, Kapahi P, Nelson PS, Campisi J. 2015. MTOR regulates the pro-tumorigenic senescence-associated secretory phenotype by promoting IL1A translation. Nat Cell Biol advance on.

45. Chen R-X, Xia Y-H, Xue T-C, Ye S-L. 2010. Transcription factor c-Myb promotes the invasion of hepatocellular carcinoma cells via increasing osteopontin expression. J Exp Clin cancer Res 29:172.

46. Chakraborty G, Jain S, Behera R, Ahmed M, Sharma P, Kumar V, Kundu GC. 2006. The multifaceted roles of osteopontin in cell signaling, tumor progression and angiogenesis. Curr Mol Med 6:819–830.

47. Reinholt FP, Hultenby K, Oldberg A, Heinegard D. 1990. Osteopontin-a possible anchor of osteoclasts to bone. Proc Natl Acad Sci 87:4473–4475.

48. Li Y, Xie Y, Cui D, Ma Y, Sui L, Zhu C, Kong H, Kong Y. 2015. Osteopontin promotes invasion, migration and epithelial-mesenchymal transition of human endometrial carcinoma cell HEC-1A through AKT and ERK1/2 signaling. Cell Physiol Biochem 37:1503–1512.

49. Anborgh PH, Mutrie JC, Tuck AB, Chambers AF. 2010. Role of the metastasis-promoting protein osteopontin in the tumour microenvironment. J Cell Mol Med 14:2037–44.

50. Weber CE, Li NY, Wai PY, Kuo PC. 2012. Epithelial-mesenchymal transition, TGF-β, and osteopontin in wound healing and tissue remodeling after injury. J Burn Care Res 33:311–8.

51. Finak G, Bertos N, Pepin F, Sadekova S, Souleimanova M, Zhao H, Chen H, Omeroglu G, Meterissian S, Omeroglu A, Hallett M, Park M. 2008. Stromal gene expression predicts clinical outcome in breast cancer. Nat Med 14:518–27.

52. Rudland P, Platt-Higgins A, El-Tanani M, de Silva Rudland S, Barraclough R, Winstanley J, Howitt R, West C. 2002. Prognostic significance of the metastasis-associated protein osteopontin in human breast cancer. Cancer Res 62:3417–3427.

53. Luo X, Ruhland MK, Pazolli E, Lind AC, Stewart SA. 2011. Osteopontin stimulates preneoplastic cellular proliferation through activation of the MAPK pathway. Mol Cancer Res 9:1018–29.

54. Yang L, Shang X, Zhao X, Lin Y, Liu J. 2012. Correlation study between OPN, CD44v6, MMP-9 and distant metastasis in laryngeal squamous cell carcinoma [Article in Chinese] Yang L1, Shang X, Zhao X, Lin Y, Liu J. Lin Chung Er Bi Yan Hou Tou Jing Wai Ke Za Zhi 26:989–92.

55. Ramji D, Foka P. 2002. CCAAT/enhancer-binding proteins: structure, function and regulation. Biochem J 575:561–575.

56. Zahnow CA. 2009. CCAAT/enhancer-binding protein beta: its role in breast cancer and associations with receptor tyrosine kinases. Expert Rev Mol Med 11:e12.

57. Agre P, Johnson PF, McKnight SL. 1989. Cognate DNA binding specificity retained after leucine zipper exchange between GCN4 and C/EBP. Science (80-) 246:922–6.

58. Descombes P, Schibler U. 1991. A liver-enriched transcriptional activator protein, LAP, and a transcriptional inhibitory protein, LIP, are translated from the same mRNA. Cell 67:569–579.

59. Chuang C-Y, Chang H, Lin P, Sun S-J, Chen P-H, Lin Y-Y, Sheu G-T, Ko J-L, Hsu S-L, Chang JT. 2012. Up-regulation of osteopontin expression by aryl hydrocarbon receptor via both ligand-dependent and ligand-independent pathways in lung cancer. Gene 492:262–9.

60. Suzuki K, Matsui Y, Higashimoto M, Kawaguchi Y, Seki S, Motomura H, Hori T, Yahara Y, Kanamori M, Kimura T. 2012. Myxoid Liposarcoma-Associated EWSR1-DDIT3 Selectively Represses Osteoblastic and Chondrocytic Transcription in Multipotent Mesenchymal Cells. PLoS One 7:e36682.

61. Tahirov TH, Sato K, Ichikawa-Iwata E, Sasaki M, Inoue-Bungo T, Shiina M, Kimura K, Takata S, Fujikawa A, Morii H, Kumasaka T, Yamamoto M, Ishii S, Ogata K. 2002. Mechanism of c-Myb-C/EBP beta cooperation from separated sites on a promoter. Cell 108:57–70.

62. Mink S, Kerber U, Klempnauer KH. 1996. Interaction of C/EBPbeta and v-Myb is required for synergistic activation of the mim-1 gene. Mol Cell Biol 16:1316–1325.

63. Ness SA, Kowenz-Leutz E, Casini T, Graf T, Leutz A. 1993. Myb and NF-M:

combinatorial activators of myeloid genes in heterologous cell types. Genes Dev 7:749–59.

64. Robert I, Sutter A, Quirin-Stricker C. 2002. Synergistic activation of the human choline acetyltransferase gene by c-Myb and C/EBPbeta. Brain Res Mol Brain Res 106:124–35.

65. Oh IH, Reddy EP. 1999. The myb gene family in cell growth, differentiation and apoptosis. Oncogene 18:3017–33.

66. Hall W, Bean C, Pollard M. 1941. Transmission of fowl leucosis through chick embryos and young chicks. Am J Vet Res 2:272–279.

67. Baluda M, Reddy E. 1994. Anatomy of an integrated avian myeloblastosis provirus: structure and function. Oncogene 9:2761–2774.

68. Lipsick J. 1996. One billion years of Myb. Oncogene 13:223–235.

69. Martin C, Paz-Ares J. 1997. MYB transcription factors in plants. Trends Genet.

70. Molvaersmyr A-K, Saether T, Gilfillan S, Lorenzo PI, Kvaløy H, Matre V, Gabrielsen OS. 2010. A SUMO-regulated activation function controls synergy of c-Myb through a repressor-activator switch leading to differential p300 recruitment. Nucleic Acids Res 38:4970–84.

71. Dahle O, Andersen TO, Nordgard O, Matre V, Del Sal G, Gabrielsen OS. 2003. Transactivation properties of c-Myb are critically dependent on two SUMO-1 acceptor sites that are conjugated in a PIASy enhanced manner. Eur J Biochem 270:1338–1348.

72. Miglarese MR, Richardson a F, Aziz N, Bender TP. 1996. Differential regulation of c-Myb-induced transcription activation by a phosphorylation site in the negative regulatory domain. J Biol Chem 271:22697–705.

73. Pani E, Menigatti M, Schubert S, Hess D, Gerrits B, Klempnauer K-H, Ferrari S. 2008. Pin1 interacts with c-Myb in a phosphorylation-dependent manner and regulates its transactivation activity. Biochim Biophys Acta 1783:1121–8.

74. Amaru Calzada A, Todoerti K, Donadoni L, Pellicioli A, Tuana G, Gatta R, Neri A, Finazzi G, Mantovani R, Rambaldi A, Introna M, Lombardi L, Golay J. 2012. The HDAC inhibitor Givinostat modulates the hematopoietic transcription factors NFE2 and C-MYB in JAK2(V617F) myeloproliferative neoplasm cells. Exp Hematol 40:634–45.e10.

75. Ramsay RG, Gonda TJ. 2008. MYB function in normal and cancer cells. Nat Rev Cancer 8:523–34.

76. Greig KT, Carotta S, Nutt SL. 2008. Critical roles for c-Myb in hematopoietic progenitor cells. Semin Immunol 20:247–56.

77. Gewirtz, AM and Calabretta B. 1988. A c-Myb antisense oligodeoxynucleotide inhibits normal human hematopoiesis. Science (80-) 1303–1306.

78. Mucenski ML, Mclain K, Kier A, Swerdlow SH, Schreiner CM, Miller TA, Pietryga DW, Scott WJ, Potter SS. 1991. A Functional c-myb Gene Is Required for Normal Murine Fetal Hepatic Hematopoiesis 65.

79. Greig KT, Graaf CA De, Murphy JM, Carpinelli MR, Heng S, Pang M, Frampton J, Kile BT, Hilton DJ, Nutt SL. 2017. Critical roles for c-Myb in lymphoid priming and early B-cell development 115:2796–2806.

80. Hu T, Simmons A, Yuan J, Bender TP, Alberola-ila J. 2010. The transcription factor c-Myb primes CD4 + CD8 + immature thymocytes for selection into the i NKT lineage. Nat Publ Gr 11:435–441.

81. Yuan J, Crittenden RB, Bender TP, Yuan J, Crittenden RB, Bender TP. 2010. c-Myb Promotes the Survival of CD4 + CD8 + Double-Positive Thymocytes through Upregulation of Bcl-xL. Jouirnal Immunol 2793–2804.

82. Garcia P, Clarke M, Vegiopoulos A, Berlanga O, Camelo A, Lorvellec M, Frampton J. 2009. Reduced c-Myb activity compromises HSCs and leads to a myeloproliferation with a novel stem cell basis. EMBO J 28:1492–1504.

83. Zhou Y, Ness SA. 2011. Myb proteins: angels and demons in normal and transformed cells. Front Biosci (Landmark Ed 16:1109–31.

84. Zorbas M, Sicurella C, Bertoncello I, Venter D, Ellis S, Mucenski ML, Ramsay RG. 1999. c-Myb is critical for murine colon development. Oncogene 18:5821–30.

85. Malaterre J, Carpinelli M, Ernst M, Alexander W, Cooke M, Sutton S, Dworkin S, Heath JK, Frampton J, McArthur G, Clevers H, Hilton D, Mantamadiotis T, Ramsay RG. 2007. c-Myb is required for progenitor cell homeostasis in colonic crypts. Proc Natl Acad Sci U S A 104:3829–3834.

86. Thompson MA, Rosenthal MA, Ellis SL, Expression DB-, Thompson MA, Rosenthal MA, Ellis SL, Friend AJ, Zorbas MI, Whitehead RH, Ramsay RG. 1998. c-Myb Down-Regulation Is Associated with Human Colon Cell Differentiation ,

Apoptosis , and Decreased Bcl-2 Expression c-Myb Down-Regulation Is Associated with Human Colon Cell Differentiation , 5168–5175.

87. Malaterre J, Mantamadiotis T, Dworkin S, Lightowler S, Yang Q, Ransome MI, Turnley AM, Nichols NR, Emambokus NR, Frampton J, Ramsay RG. 2008. c-Myb is required for neural progenitor cell proliferation and maintenance of the neural stem cell niche in adult brain. Stem Cells 26:173–181.

88. Karafiat V, Dvorakova M, Pajer P, Cermak V, Dvorak M. 2007. Melanocyte fate in neural crest is triggered by Myb proteins through activation of c-kit. Cell Mol Life Sci 64:2975–2984.

89. Chen R-X, Xia Y-H, Xue T-C, Ye S-L. 2010. Transcription factor c-Myb promotes the invasion of hepatocellular carcinoma cells via increasing osteopontin expression. J Exp Clin Cancer Res 29:172.

90. Schultz J, Lorenz P, Ibrahim SM, Kundt G, Gross G, Kunz M. 2009. The functional -443T/C osteopontin promoter polymorphism influences osteopontin gene expression in melanoma cells via binding of c-Myb transcription factor. Mol Carcinog 48:14–23.

91. Bein K, Husain M, Ware J, Mucenski ML, Rosenberg RD, Simons M. 1997. c-Myb function in fibroblasts. J Cell Physiol 173:319–26.

92. Nomura T, Sakai N, Sarai A, Sudo T, Kanei-Ishii C, Ramsay RG, Favier D, Gonda TJ, Ishii S. 1993. Negative autoregulation of c-myb activity by homodimer formation through the leucine zipper. J Biol Chem 268:21914–21923.

93. Ganter B, Chao ST, Lipsick JS. 1999. Transcriptional activation by the Myb proteins requires a specific local promoter structure. FEBS Lett 460:401–410.

94. Ness SA. 1999. Myb binding proteins: regulators and cohorts in transformation. Oncogene 18:3039–46.

95. Pattabiraman DR, Sun J, Dowhan DH, Ishii S, Gonda TJ. 2009. Mutations in multiple domains of c-Myb disrupt interaction with CBP/p300 and abrogate myeloid transforming ability. Mol Cancer Res 7:1477–86.

CHAPTER 2

c-Myb and C/EBPβ regulate OPN and other senescence-associated secretory phenotype factors

Kevin C. Flanagan, Elise Alspach, Ermira Pazolli, Shankar Parajuli, Laura L. Arthur, Roberto Tapia, and Sheila A. Stewart

INTRODUCTION

Age is a major risk factor in the development of cancer (1). In addition to the accumulation of epithelial cell mutations, age-dependent changes in the stromal compartment play an important role in tumor promotion (2–7). One of these changes is the accumulation of senescent stromal cells that possess the ability to stimulate preneoplastic and neoplastic cell growth. First described as an *in vitro* phenomenon caused by repeated cell divisions, senescence can also be caused by a number of genotoxic stresses including telomere shortening or dysfunction, DNA double strand breaks, oxidative stress, tumor suppressor expression, and oncogene activation (8). Senescent cells are associated with a flattened morphology, the presence of heterochromatic foci (SAHFs), positive senescence-associated β-galactosidase staining, and an altered gene expression and secretion profile termed the senescence-associated secretory phenotype (SASP; ref. 8–12). Significantly, senescence is now known to occur both *in vitro* and *in vivo* (9, 13) where it impacts a diverse number of biologic processes including cancer.

Senescence acts as a potent tumor suppressive mechanism in a cell autonomous setting by preventing the proliferation of cells with activated oncogenes or excessive DNA damage. However, as individuals age, senescent cells accumulate within tissues where they are postulated to contribute to aging phenotypes (9, 10). Aged mice cleared of $p16^{Ink4a}$-positive senescent cells have reduced incidences of several age-related pathologies (2, 14). Further, senolytic drugs that target senescent cells can ameliorate many age-related maladies, underscoring the importance of these cells in age related

diseases (15–17). Additionally, the largest risk factor for cancer is age, and there is significant evidence that accumulating senescent cells paradoxically contribute to cancer development and progression in a cell non-autonomous fashion. As with other age-related diseases, elimination of senescent cells reduces spontaneous tumor rates in naturally aged mice (14, 17). The SASP can promote growth and transformation of epithelial cells in numerous models, suggesting that secretion of the SASP by accumulating senescent cells may contribute to age-related tumorigenesis (3, 4, 7, 11, 12, 18–20).

The SASP consists of numerous secreted factors including cytokines, mitogens, and extracellular matrix remodelers that are upregulated at the mRNA and protein levels (7, 12). The regulation of SASP expression is complex and incompletely understood but recent work has revealed that both the cell type and senescence inducer can significantly impact the mechanisms that regulate SASP expression as well as the specific SASP factors expressed (21). The expression of many factors, including the canonical SASP factors IL-6 and IL-8, requires p38MAPK, ATM, and NF-κB for transcriptional activation (5, 8, 12). Additionally, p38MAPK regulates many SASP factors via post-transcriptional stabilization of their mRNA (Chapter 3, ref. 6). However, not all SASP factors are regulated by these same pathways. For instance, while p38MAPK is an important regulator of the SASP, one study found that it regulated only 25 of 37 factors studied at the protein level while we previously reported that it regulates only 50 of 248 factors at the mRNA level in our model (5, 6).

One such factor is osteopontin (OPN), a pro-tumorigenic protein which has numerous physiological and pathological roles, including regulating bone turnover, cell adhesion and migration, and inflammation (22–25). OPN is a secreted matrix protein that is upregulated in response to wounds, acts to recruit immune cells, can suppress apoptosis, and is upregulated and diagnostically relevant in a number of cancer types (24, 26–28). OPN is also robustly upregulated in response to senescence. Previously we showed that senescent BJ skin fibroblasts lose the ability to promote preneoplastic cell growth when they are depleted of OPN. Furthermore, recombinant OPN induces preneoplastic cell growth in the absence of senescent cells (7, 29). While the importance of senescent fibroblast-derived OPN is underscored by its ability to promote preneoplastic cell growth, the regulation of OPN in response to senescence is not understood. SASP regulators ATM and NF-κB are not required for OPN induction in response to senescence (30). Other SASP regulators, such as C/EBPβ, have not been studied in conjunction with OPN. Indeed, there are no known regulators of OPN in response to senescence. Because of senescent-derived OPN's ability to promote preneoplastic cell proliferation, it is important to understand how OPN is regulated in this context. Additionally, elucidating the regulation of OPN may provide insights into the regulation of other SASP factors that are regulated in a similar manner.

To identify regulators of OPN, we used an OPN promoter reporter to identify a senescence response element (SRE) that was required for activation of the OPN promoter in response to senescence. Using Transfac® to analyze the SRE for transcription factor binding motifs, we identified a number of putative regulators of OPN

in senescence, including C/EBPβ and c-Myb. C/EBPβ is a transcription factor known to regulate IL-6 and IL-8 in response to senescence (31). Likewise, it has been shown to regulate OPN in a lung cancer cell line (32). c-Myb is a proto-oncogene important for hematopoietic development (33). Additionally, c-Myb is a known regulator of OPN in hepatocellular carcinoma and melanoma models (24, 34). However, c-Myb is poorly characterized in fibroblasts and has not been studied in mammalian cell senescence. Further, c-Myb and C/EBPβ can collaborate to activate transcription of a number of genes, including mim-1 and ChAT (35–37). Therefore, we hypothesized that c-Myb and C/EBPβ regulate OPN and other SASP factors.

METHODS

Cell lines and treatments

Human foreskin BJ fibroblasts and 293T cells were cultured as previously described (7). HaCAT preneoplastic keratinocyte cells stably expressing click beetle red (CBR) luciferase (HaCAT-CBR) and HEK 293T cells were grown in DMEM containing 10% heat-inactivated FBS and 1% penicillin/streptomycin (Sigma; ref. 7). All cells were cultured at 37°C in 5% carbon dioxide and 5% oxygen.

Cells were treated with 0.1 U/mL bleomycin sulfate (Sigma) for 24 hours. Cell pellets were collected 96 hours after the start of bleomycin treatment and RNA was isolated using TRI Reagent (Life Technologies) and Ambion RNA Isolation kit (ThermoFisher).

Plasmids

OPN promoter luciferase constructs consisted of a fragment of the OPN promoter driving expression of luciferase in the pGL3 vector (38). Fragments used were OPN80 (nucleotide [nt] -80 to nt +86), OPN108 (nt -108 to nt +86), OPN135 (nt -135 to nt +86), OPN190 (nt -190 to nt +86), and OPN400 (nt -400 to nt +86). The nt reported correspond to those upstream (-) or downstream (+) of the transcriptional start site. The OPN-LUC promoter constructs were a gift from the Paul C. Kuo Lab (38). OPN190-LUC mutant c-Myb binding site was created using QuikChange II Site-Directed Mutagenesis (Agilent) and by following manufacturer's protocol. The c-Myb binding site was changed from 5'-ttaactgtagatt-3' to 5'-tt*gcta*gtagac*t*-3'. pCMV-FLAG-LAP2 (Addgene plasmid #15738) and pBabe-puro LIP (Addgene plasmid #15713) were gifts from Joan Massague (39). pCDNA3.1-Myb was a gift of Dr. Robert Rosenberg. pWZL hygro H-Ras V12 was a gift from Scott Lowe (Addgene plasmid # 18749, ref. 37). shMyb_2 (pSIREN-RetroQ-MYB-shRNA) was a gift from Judy Lieberman (Addgene plasmid # 25790; ref. 37). All other shRNA constructs were obtained from the Children's Discovery Institute's viral vector-based RNAi core at Washington University in St. Louis and were supplied in the pLKO.1-puro backbone. The sequences are as follows: shLUC (5'-TCACAGAATCGTCGTATGCAG-3'), shCEBP_1 (5'-CGACTTCCTCTCCGACCTCTT-3'), shCEBP_2 (5'-GCACAGCGACGAGTACAAGAT-3'), shMYB_2 (5'-CCAGATTGTAAATGCTCATTT-3').

SA-βgal

Senescence-associated-β-galactosidase staining was carried out as previously described (7).

Growth Assay

50,000 untreated or bleomycin-treated BJ fibroblasts expressing the indicated short hairpins were plated 96 hours after the start of treatment as previously described. Cell number was counted daily for four days using a hemocytometer. Significance was determined using a 2-way ANOVA with Bonferroni post-test.

Western Blot

Cell pellets were lysed in buffer containing 50 mM Tris pH 8.0, 5 mM EDTA, 0.5% NP-40, and 100 mM sodium chloride for 20 minutes at 4°C. Protein concentration was quantified using the Bradford Protein Assay (Bio-Rad). Membranes were blocked for one hour in 5% milk in TBS-T. The primary antibodies used were mouse monoclonal anti-FLAG M2 (Sigma; catalog number F1804) diluted 1:1000; rabbit polyclonal anti-C/EBPβ (Santa Cruz sc-150) diluted 1:2500; rabbit polyclonal anti-c-Myb rabbit polyclonal (Santa Cruz sc-517) diluted 1:250; and anti-γ-actin (Novus; catalog number NB600-533) diluted 1:5000. All secondary antibodies from the appropriate species were horseradish peroxidase–conjugated (The Jackson Laboratory) and diluted at 1:10,000. All antibodies were diluted in 2% BSA (Sigma-Aldrich) in TBS-T or 1% milk in TBS-T.

Viral transduction

Viral transduction was performed as previously described (7). All constructs were stably expressed using viral transduction unless otherwise noted.

Luciferase Reporter Assay

BJ fibroblasts were transiently co-transfected with pGL3-Renilla and pGL3-OPN constructs using Lipofectamine 2000 (Thermo Fisher Scientific) and promoter activity was determined using Promega Dual Luciferase Reporter Assay (Promega) by following manufacturer's protocol.

Chromatin Immunoprecipitation

Cells were transiently transfected with pcDNA-c-Myb WT (Myb), pGL3-OPN190 (OPN190), pGL3-OPN190 mutant c-Myb binding site (OPN190 Mut), or pCMV-Flag-LAP2 in 15 cm plates using 7 µg DNA and the TransIT® LT1 Reagent transfection system (Mirus). Cells were fixed 48 hours later using 1% formaldehyde in PBS for 20 minutes. Fixation was quenched with 125 mM glycine for 5 minutes with gentle rotation, cells were washed with PBS and collected by scraping and centrifugation at 200xg for 5 minutes at 4°C. Cells were lysed in 2 mL lysis buffer (1% SDS, 10 mM EDTA, 50 mM Tris pH 8.1) containing protease inhibitors (pepstatin, 1 µg/mL; aprotinin, 1 µg/mL; leupeptin, 1 µg/mL; PMSF, 100 µM) for 15 minutes. The lysate was sonicated at 50 Amps with 30 s on, 30 s off for 6 rounds to achieve DNA fragments approximately 200-500 bp in length as measured by electrophoresis. One mg protein was used for each immunoprecipitation. Lysate was diluted fivefold into ChIP dilution buffer (0.01% SDS, 1.1% Triton X-100, 1.2 mM EDTA, 16.7 mM Tris-HCl pH 8.1, 167 mM NaCl) and incubated at 4°C overnight with 5 µg appropriate antibody with vertical rotation. Antibodies used: anti-Myb (Santa Cruz sc-517); anti-C/EBPβ (Santa Cruz sc-150);

Rabbit IgG (Cell Signaling 2729); anti-Flag M2 (Sigma F1804); mouse IgG1 (for Flag ChIPs, Cell Signaling 5415).

Quantitative PCR

cDNA synthesis and quantitative PCR was performed using manufacturer's instructions (SYBR Green, Life Technologies and Taqman, Applied Biosystems). Primers used: GAPDH (F: GCATGGCCTTCGGTGTCC, R: AATGCCAGCCCCAGCGTCAAA), IL-6 (F: ACATCCTCGACGGCATCTCA, R: TCACCAGGCAAGTCTCCTCA), IL-8 (F: GCTCTGTGTGAAGGTGCAGT, R: TGCACCCAGTTTTCCTTGGG), OPN (F: TTGCAGCCTTCTCAGCCAA, R: AAGCAAATCACTGCAATTCTC), c-Myb (IDT PrimeTime® Std qPCR assay #Hs.PT.58.264008, Probe: 5'-56-FAM/CCTTCCGAC/ZEN/GCATTGTAGAATTCCAGT/3IABkFQ/-3', F: 5'-CTCCTGCAGATAACCTTCCTG-3', R: 5'-GCAGAAATCGCAAAGCTACTG-3'), C/EBPβ (Taqman assay # Hs00270923_s1), OPN TSS (Taqman assay # AJRR84Z), OPN190 (F:CTTTATGTTTTTGGCGTCTTCCA, R: CTAGCAAAATAGGCTGTCCC), IL-6 promoter (F: 5'-GCCATGCTAAAGGACGTCACA-3', R: 5'-GGGCTGATTGGAAACCTTATTAAGA-3'), IL-8 promoter (F: 5'-AAGTGTGATGACTCAGGTTTGC-3', R: 5'-GCACCCTCATCTTTTCATTATG- 3'), MMP1 (IDT PrimeTime® Std qPCR assay #Hs.PT.58.38692586, Probe: 5'-56-FAM/TCCGTGTAG/ZEN/CACATTCTGTCCCTG/3IABkFQ/-3', F: 5'-GCCAAAGGAGCTGTAGATGTC -3', R: 5'-GACAGAGATGAAGTCCGGTTT -3'), CXCL5 (IDT PrimeTime® std qPCR assay #Hs.PT.58.41058007.g, Probe: 5'-/56/FAM/CGGGGAGGG/ZEN/CAGGGAAGATG/3IABkFQ/-3', F: 5'-

GAACAGGCTTTACATTCAGACAG-3', R: 5'-GGGTTAGAGGATTGCAGAAGA-3'), IL1β (IDT PrimeTime® std qPCR assay #Hs.PT.58.1518186, Probe: 5'-/56-FAM/AGAAGTACC/ZEN/TGAGCTCGCCAGTGA/3IABkFQ/-3', F: 5'-GAACAAGTCATCCTCATTGCC-3', R: 5'-CAGCCAATCTTCATTGCTCAAG-3').

Microarray

Microarray analysis was performed by the Genome Technology Access Center at Washington University. Cells expressing shLUC were senesced using bleomycin or Ras expression. Further analysis was restricted to genes that were either significantly up- or down-regulated in both bleomycin and Ras groups. Fold changes in bleomycin relative to untreated groups were then compared between the shLUC, shCEBP_2, and shMYB_1 groups. Two biological replicates for each group were analyzed. Statistical analysis was done using linear model fitting and the R package limma using an adjusted p-value<0.05 as the cutoff for significance (42, 43). GO Term Enrichment Analysis was performed using the Gene Ontology Consortium PANTHER software version 11.1 (released 2016-10-24) and the PANTHER Overrepresentation Test (released 2016-07-15). The PANTHER protein class annotation was used and our datasets were compared to the Homo Sapiens reference list with Bonferroni correction for multiple comparisons (44).

Coculture

Coculture experiments were performed as previously described with the following modifications (7). A total of 1.3×10^4 fibroblasts were plated in black-walled 96-well

plates (Fisher Scientific). Cells were incubated in starve medium (DMEM + 1% penicillin/streptomycin) for 3 days before the addition of HaCAT-CBR cells. HaCAT-CBR cells were cultured in starve medium for 24 hours before plating on fibroblasts. A total of 1.0×10^3 HaCAT-CBR cells were plated on fibroblasts and incubated for six days. On day six, live-cell bioluminescence imaging was performed on an IVIS 50 (PerkinElmer; Living Image 4.3, 1 min exposure, bin8, FOV12cm, f/stop1, open filter). D-luciferin (150mg/ml; Gold Biotechnology, St. Louis, MO) was added to black-walled plates 10 min prior to imaging.

Statistical analysis

Data is presented as the mean ± SEM. Student's t-test was used to determine significance when comparing two groups. When comparing three or more groups, one-way ANOVA with Dunnett's post-test was used, except where noted. In all cases, a p-value less than 0.05 was considered significant.

RESULTS

The OPN promoter contains a senescence response element

Given the pro-tumorigenic nature of OPN and its unique regulation among studied SASP factors, we sought to determine the mechanism of OPN regulation during senescence. To do so, we used promoter reporter constructs composed of regions of the OPN promoter driving transcription of luciferase to identify sequences in the OPN promoter required for transcriptional activation during senescence (38). To carry out these analyses, BJ fibroblasts were transfected with the reporter constructs and induced

to senesce by treatment with bleomycin for 24 hours. Four days after the start of bleomycin treatment, when cells displayed a senescent phenotype as demonstrated by a flattened morphology and staining positive for senescence-associated β-galactosidase (SA-βgal; **Fig. 2.1A**), we assessed luciferase activity. We used regions of the OPN promoter spanning from the +86 nucleotide to the upstream site indicated (**Fig. 2.1B**). While the +86 to -135 nucleotide region of the promoter had only ~two-fold increase in luciferase activity in bleomycin treated cells relative to non-senescent cells, the region spanning from +86 to -190 nucleotide had 4.9-fold increased expression in senescent compared to non-senescent fibroblasts. The increased induction of expression observed in response to senescence when the -135 to -190 nucleotide region was present suggested that this region, which we termed the senescence response element (OPN-SRE), contains important senescence-associated transcription factor binding motifs (**Fig. 2.1C**).

Transfac® analysis of the OPN-SRE promoter region revealed numerous putative binding sites for a variety of transcription factors, including HNF1, ZBTB16, HMGA1, SOX, FOXH1, C/EBPβ, and c-Myb. Preliminary data suggested that many of these factors were not required for OPN induction in response to senescence (data not shown). Therefore, we focused on the transcription factors C/EBPβ and c-Myb. C/EBPβ regulates the induction of numerous SASP factors including IL-6 and IL-8 in response to oncogene induced senescence (31). In contrast, while c-Myb transcriptionally activates OPN in several epithelial cell models (24, 34), its roles in fibroblasts and in senescence are poorly studied. However, c-Myb and C/EBPβ can

interact and have been shown to co-activate transcription of several genes in other settings (45–47). Given these data, we examined C/EBPβ and c-Myb as possible regulators of OPN in response to senescence.

C/EBPβ is required for robust OPN expression in response to senescence

C/EBPβ regulates the induction of several SASP factors including IL-6 and IL-8 in response to oncogene induced senescence (31, 48) and has been implicated in control of OPN expression in other systems (32, 49, 50). To test whether C/EBPβ was required for the induction of OPN in response to senescence, we depleted BJ fibroblasts of C/EBPβ using two independent shRNAs (**Fig. 2.2A**). Upon the induction of senescence, C/EBPβ-depleted cells displayed reduced OPN expression relative to fibroblasts expressing a control short hairpin. Indeed, shC/EBPβ cells had 42% and 77% reduced OPN induction (shCEBP_1 and shCEBP_2, respectively) compared to shLUC expressing cells (**Fig. 2.2B**). In agreement with previous studies (31), we found that C/EBPβ depletion also reduced IL-6 (39% and 78%, shCEBP_1 and shCEBP_2, respectively) and IL-8 (78% and 97%, shCEBP_1 and shCEBP_2, respectively) induction in response to senescence. Interestingly, depletion of C/EBPβ did not affect senescence induction in our system as measured by SA-βgal and cell growth measurement (**Fig. 2.2C-D**).

To confirm C/EBPβ's role in regulating OPN, we inhibited C/EBPβ in BJ fibroblasts by stably expressing a dominant negative form of C/EBPβ, LIP. C/EBPβ has three isoforms: LAP1, LAP2, and LIP (51). LAP1 and LAP2 are transcriptional activators

while LIP, which contains the DNA binding domain but lacks the transactivation domain, is an inhibitory isoform that acts as a dominant negative to the activating isoforms. Compared to empty vector controls (Vector), OPN induction was reduced by 59% and IL-6 induction by 75% in LIP-expressing cells (DN-CEBP) in response to senescence (**Fig. 2.2E**). Importantly, inhibition of C/EBPβ did not affect senescence induction as measured by SA-β-gal (**Fig. 2F**). Thus, C/EBPβ is required for OPN, IL-6, and IL-8 induction in response to senescence, but depletion or inhibition does not prevent the induction of senescence in our system. C/EBPβ, therefore, represents a common factor of the previously distinct regulatory pathways of OPN and SASP factors such as IL-6 and IL-8.

C/EBPβ binds to the OPN promoter

The promoters of OPN, IL-6 and IL-8 all contain C/EBPβ binding sites. To test whether C/EBPβ directly binds the OPN promoter, we used chromatin immunoprecipitation (ChIP) in non-senescent and bleomycin-treated 293T cells. In response to bleomycin, there was robust induction of senescence as measured by SA-βgal staining (**Fig. 2.3A**). Because the upregulation of many SASP factors is transcription-dependent early after a senescence-inducing treatment but less dependent on transcription once senescence is fully established, we collected cells 48 h after the start of bleomycin treatment when transcription was robust (6). Immunoprecipitation with an anti-C/EBPβ antibody that recognizes all three C/EBPβ isoforms revealed binding of C/EBPβ to the IL-6 and IL-8 promoters as has been previously shown (**Fig. 2.3B**; ref. 28). In addition, there was significant binding to the OPN promoter in both non-senescent (0.05% input) and

senescent (0.07% input) cells. Interestingly, binding of exogenous Flag-tagged LAP2, the full length activating isoform of C/EBPβ, to the OPN, IL-6, and IL-8 promoters increased in response to senescence (**Fig. 2.3C)**. We observed this effect despite measuring greater Flag-LAP2 expression in non-senescent cells than in senescent cells (**Fig. 2.3E**).

c-Myb is required for robust OPN expression in senescent cells

Having established C/EBPβ as a regulator of OPN, we asked whether there were additional regulators in response to senescence. Thus, we returned to our promoter analysis to identify additional regulators of OPN. In addition to the C/EBPβ binding site, the SRE of the OPN promoter contains a putative c-Myb binding sequence. C-Myb is a proto-oncogene transcription factor but has never been implicated in mammalian senescence. Furthermore, while c-Myb is not well studied in fibroblasts, it has been shown to regulate fibrosis and many factors upregulated in fibrosis are also upregulated in senescence (52, 53), raising the possibility that it may play a role in regulating SASP factor expression. Importantly, c-Myb and C/EBPβ can interact and co-activate transcription in other contexts, suggesting they may act in a similar manner in response to senescence (45–47).

To establish a role for c-Myb in the regulation of OPN during senescence, human fibroblasts were depleted of c-Myb using two independent short hairpins. Using bleomycin to induce senescence (**Fig. 2.4A**), we measured OPN mRNA expression by qRT-PCR. Using two hairpins to deplete c-Myb, we observed a 37% and 45%

(shMYB_1 and shMYB_2, respectively) reduction in c-Myb protein levels relative to γ-actin (**Fig. 2.4B**), which resulted in a 64% and 77% decrease in OPN mRNA induction relative to shLUC control (**Fig. 2.4C).** Importantly, depletion of c-Myb did not inhibit senescence-induction, as measured by SA-βgal and cell growth assays, indicating that c-Myb is necessary for OPN induction but not senescence induction (**Fig. 2.4A,D**),

C-Myb has not previously been reported to regulate the SASP. Therefore, we asked whether c-Myb regulates other SASP factors in addition to OPN. Knockdown of c-Myb resulted in significantly reduced IL-6 (90% and 78%, shMYB_1 and shMYB_2, respectively) and IL-8 (89% and 84%, shMYB_1 and shMYB_2, respectively) mRNA expression in response to senescence (**Fig. 2.4C**), indicating that c-Myb regulates multiple SASP factors and suggesting that it may broadly regulate C/EBPβ-dependent SASP factors.

c-Myb regulates OPN via direct binding and activation of the OPN promoter

To test whether c-Myb directly regulates OPN transcription, we used chromatin immunoprecipitation (ChIP) in 293T cells ectopically expressing c-Myb. ChIP analysis of c-Myb revealed that it is significantly bound to the OPN promoter relative to IgG control in both non-senescent (0.007 percent input Myb relative to 0.003 IgG) and senescent (0.014 percent input relative to 0.002 IgG; **Fig. 2.5A**) cells. Additionally, c-Myb also bound the IL-6 and IL-8 promoters at similar levels, indicating that c-Myb directly regulates SASP factors other than OPN. Further, in senescent cells c-Myb significantly bound the WT OPN190-luciferase promoter reporter construct compared to

IgG controls (0.34 c-Myb percent input relative to 0.18 IgG; **Fig. 2.5B**). However, mutation of the putative c-Myb binding site on the OPN190 reporter (OPN190-MUT MBS) eliminated c-Myb binding (0.10 Myb percent input relative to 0.08 IgG), indicating that c-Myb binds specifically to this site. While WT OPN190 promoter activity is activated 4.3-fold following bleomycin treatment, OPN190-MUT MBS is not activated (1.3-fold; **Fig. 2.5C**), indicating that c-Myb binding to the OPN promoter is required for the transcriptional induction of OPN following senescence induction.

c-Myb and C/EBPβ regulate overlapping subsets of the SASP

While it has been snown that C/EBPβ regulates the SASP, c-Myb has not previously been implicated as a SASP regulator. To determine whether c-Myb regulates additional SASP factors beyond OPN, IL-6, and IL-8, we performed a microarray comparing transcript levels in non-senescent and senescent BJ fibroblasts expressing either a control short hairpin (shLUC) or a hairpin targeting either c-Myb or C/EBPβ (shMyb_1 or shCEBP_2, respectively). We restricted our analysis to 834 SASP genes, those which were significantly upregulated both by bleomycin-induced senescence and Ras-induced senescence (**Supplemental Table 2.1**). We compared the gene fold-upregulation in bleomycin-treated cells relative to untreated cells in the shLUC, shMYB_1, and shCEBP_2 groups. Comparing the fold-upregulation between groups, we found that 127/834 genes were C/EBPβ-dependent (**Fig. 2.6A, Supplemental Table 2.2**). Importantly, 59/834 genes were c-Myb-dependent (**Supplemental Table 2.3**). Interestingly, 47/59 c-Myb-dependent genes were also C/EBPβ-dependent, suggesting c-Myb largely regulates C/EBPβ-dependent genes. We performed GO Term

enrichment analysis on the SASP, C/EBPβ-dependent, and c-Myb-dependent gene sets. There were no significant enrichments among these gene sets relative to each other. However, the SASP was enriched for expected terms such as chemokine, cytokine, and extracellular matrix glycoprotein relative to the genome. Further, both C/EBPβ and c-Myb were similarly enriched for the terms chemokine, cytokine, and serine protease inhibitor.

In accordance with our qPCR findings, IL-6 and IL-8 are among the C/EBPβ- and c-Myb-dependent genes (**Fig. 2.6B**). However, while OPN induction was reduced in shC/EBPβ and shMyb cells, this reduction was not significant. This difference was significant when measured by qPCR (**Fig. 2.4C**), suggesting that the microarray data lacks sufficient power to find significance for genes with smaller changes. Therefore, our analysis likely underestimates the number of genes regulated by both C/EBPβ and c-Myb.

In addition to the genes we had already studied, we used qPCR to validate CXCL5, IL1β, and MMP1, three genes which were significantly dependent on both C/EBPβ and c-Myb in our microarray data. All three genes recapitulated the microarray results (**Fig. 2.6C**). These data suggest that c-Myb is an important regulator of many C/EBPβ-dependent SASP genes in addition to OPN, IL-6, and IL-8.

c-Myb and C/EBPβ knockdown inhibits preneoplastic cell growth promotion by senescent fibroblasts

Senescent fibroblasts promote the growth of neoplastic and preneoplastic epithelial cells in coculture and xenograft models via secretion of SASP factors (7, 29). Depletion of OPN in senescent BJ skin fibroblasts is sufficient to eliminate the growth promotion that senescent BJ fibroblasts provide to HaCAT preneoplastic keratinocytes. Because c-Myb and C/EBPβ regulate OPN and other SASP factors, we tested whether depletion of c-Myb and C/EBPβ would reduce the growth advantage provided by senescent cells using this same skin carcinoma coculture model.

HaCAT cells stably expressing click beetle red luciferase were plated on top of a confluent monolayer of either non-senescent or senescent fibroblasts in serum-free media and allowed to grow for six days. Recapitulating previous work, senescent fibroblasts dramatically increased HaCAT cell growth as measured by live cell imaging (7, 29). However, this growth was significantly lower for HaCAT cells cocultured with either shC/EBPβ or shMyb expressing fibroblasts (**Fig. 2.7A**), indicating the importance of C/EBPβ and c-Myb in regulating the SASP and its downstream pro-tumorigenic effects.

DISCUSSION

The SASP plays important roles in wound healing and pathology, including the promotion of tumor development. Thus, understanding the complex regulation of the SASP will provide opportunities for therapeutic intervention. Many regulators of the SASP have been identified. However, it is clear that not all SASP factors are regulated by the same pathways. The SASP factor OPN is a potent pro-tumorigenic factor and is

involved in numerous other physiological and pathological pathways such as bone turnover and the development of kidney stones (23, 54). Previous work by our laboratory found that OPN is not dependent on the canonical SASP regulators ATM and NF-κB (30), illustrating that SASP factors are not subject to a single regulatory program.

We have identified C/EBPβ and c-Myb as critical regulators of the pro-tumorigenic SASP factor OPN. Depletion of C/EBPβ using shRNA and dominant negative inhibition significantly decreased OPN induction in response to senescence (**Fig. 2.2B,E**). As has been previously reported, C/EBPβ is also required for the induction of IL-6 and IL-8 (31). However, in contrast to that study which used an oncogene-induced senescence model, we did not observe a decrease in senescence induction in response to C/EBPβ depletion or inhibition (**Fig. 2.2A,D,F**). While the cause of this difference is not clear, it may be due to differences in cell type, senescence-induction, or the level of C/EBPβ depletion. Nonetheless, the robust senescence induction observed, together with our ChIP data (**Fig. 2.3B-C),** indicate that OPN is directly regulated by C/EBPβ and is not simply induced indirectly by the senescence program.

While C/EBPβ has previously been reported as an important SASP regulator, very little has been published about the mechanism of C/EBPβ activation of SASP genes. We observed that although there is no significant change in total C/EBPβ binding to the OPN, IL-6, or IL-8 promoters, binding of an exogenously expressed, activating form of C/EBPβ, Flag-LAP2, significantly increases in response to senescence (**Fig. 2.3C, Fig.**

2.7B). These data suggest that C/EBPβ regulation of SASP factor transcription may be more complex than simple binding, but require changes in specific isoform binding.

Our data establish that c-Myb is a novel regulator of components of the SASP. Depletion of c-Myb using shRNA significantly decreased the induction of OPN, IL-6, and IL-8 in response to senescence (**Fig. 2.4C**). An additional 57 putative target factors were identified via microarray (**Fig. 2.6A**), and three of these putative targets (MMP1, CXCL5, and IL1B) were validated with qRT-PCR (**Fig. 2.6C**). The regulation of at least some of these genes is direct, as c-Myb binds directly to the OPN, IL-6, and IL-8 promoters in both non-senescent and senescent cells (**Fig. 2.5A**). Interestingly, there is an increase in promoter occupancy in senescent cells relative to non-senescent, which, while non-significant, raises the possibility that c-Myb may increase binding to the promoters of some SASP factors in response to senescence. Mutation of the c-Myb binding site on the OPN promoter disrupts this binding and abrogates promoter activation in response to bleomycin (**Fig. 2.5B-C**). Together these data indicate that c-Myb is critical for the induction of not only OPN, but a larger subset of the SASP. Although c-Myb has not been extensively studied in fibroblasts, one of its known roles is regulating fibrosis (52, 53). Here we show that c-Myb regulates SASP factors, including matrix proteins OPN and MMP1, suggesting that c-Myb plays an important role in regulating the extracellular matrix in multiple physiological contexts.

C/EBPβ and c-Myb commonly act as co-activators of transcription (35–37). Our data indicate that both transcription factors are required for the induction of OPN. In addition,

via microarray analysis, we identified 47 additional SASP genes which are dependent on both C/EBPβ and c-Myb (**Fig. 2.6A**). Only 12 c-Myb-dependent factors were not also C/EBPβ-dependent, indicating that c-Myb generally regulates C/EBPβ-dependent factors. We hypothesize that C/EBPβ and c-Myb interact to activate a cohort of SASP factors, but more work is needed to investigate whether these mechanisms studied in other contexts are also at play in senescent cells.

While OPN upregulation in senescence is independent of ATM and NF-κB, it does require C/EBPβ and c-Myb for expression. C/EBPβ and c-Myb also regulate IL-6, IL-8, and other NF-κB-dependent genes, suggesting that there are not simply distinct SASP master regulatory pathways, but multiple SASP regulators which act together and separately in a complex network to regulate the individual factors that are collectively the SASP. More work is needed to understand the interplay among the various regulatory pathways and which factors they regulate.

ACKNOWLEDGMENTS

We thank Paul C. Kuo for the OPN-LUC promoter constructs, Joan Massague for the pCMV-FLAG-LAP2 and pBabe-puro-LIP plasmids, Judy Lieberman for pSIREN-RetroQ-MYB-shRNA, and Robert Rosenberg for the pcDNA3.1-Myb plasmid. Other shRNA constructs were obtained from the Children's Discovery Institute's viral vector-based RNAi core at Washington University in St. Louis. We thank the Genome Technology Access Center in the Department of Genetics at Washington University School of Medicine for help with genomic analysis. The Center is partially supported by NCI

Cancer Center Support Grant #P30 CA91842 to the Siteman Cancer Center and by ICTS/CTSA Grant# UL1TR000448 from the National Center for Research Resources (NCRR), a component of the National Institutes of Health (NIH), and NIH Roadmap for Medical Research. This publication is solely the responsibility of the authors and does not necessarily represent the official view of NCRR or NIH. We thank Lynne Marsala for live cell imaging (supported by NIH P50 CA094056), Hayley Moore, Daniel Teasley, Bhavna Murali, Hui Huang, Talon Trecek, and members of the ICCE Institute at Washington University School of Medicine for experimental support and discussion. Financial Support**:** NIH 5 R01 CA130919 (SAS), NIH Cellular Biochemical and Molecular Sciences Pre-doctoral Training Grant T32 GM007067 (KCF, EA and LLA), NIH F31 CA189669 (KCF), American Cancer Society Research Scholar Award (SAS). The work was supported in part by the Siteman Investment Program (supported by The Foundation for Barnes-Jewish Hospital Cancer Frontier Fund (FBJH CFF 3773); Barnard Trust; Fashion Footwear Charitable Foundation of New York, Inc.; and, the National Cancer Institute Cancer Center Support Grant P30CA091842, Eberlein, PI) (SAS). Luminescent imaging was supported by NIH P50 CA094056.

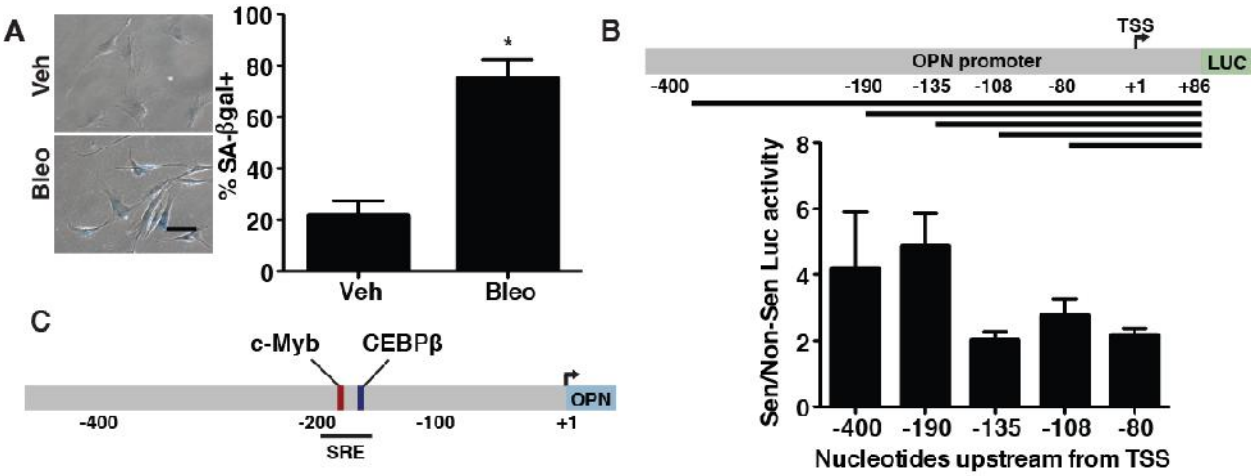

Figure 2.1: The senescence-responsive region of the OPN promoter contains c-Myb and C/EBPβ binding sites

A) Treatment of BJ fibroblasts with bleomycin induces a significant increase in senescence as indicated by increased senescence-associated β-galactosidase staining, n=3, *p<0.05. Scale bar=100 μm **B)** Schematic of expression of luciferase reporter constructs that were driven by fragments of the OPN promoter spanning from nucleotide +86 to the indicated number of bases upstream from the transcription start site (TSS; top). BJ fibroblasts expressing the indicated promoter reporter constructs were treated with vehicle or bleomycin to induce senescence. Relative luciferase activity in senescent relative to non-senescent fibroblasts indicates a senescence-responsive element (SRE) between -135 and -190 bases upstream of the TSS (bottom), n=3. **C)** Schematic of OPN promoter. The SRE includes putative binding sites for the transcription factors c-Myb and C/EBPβ.

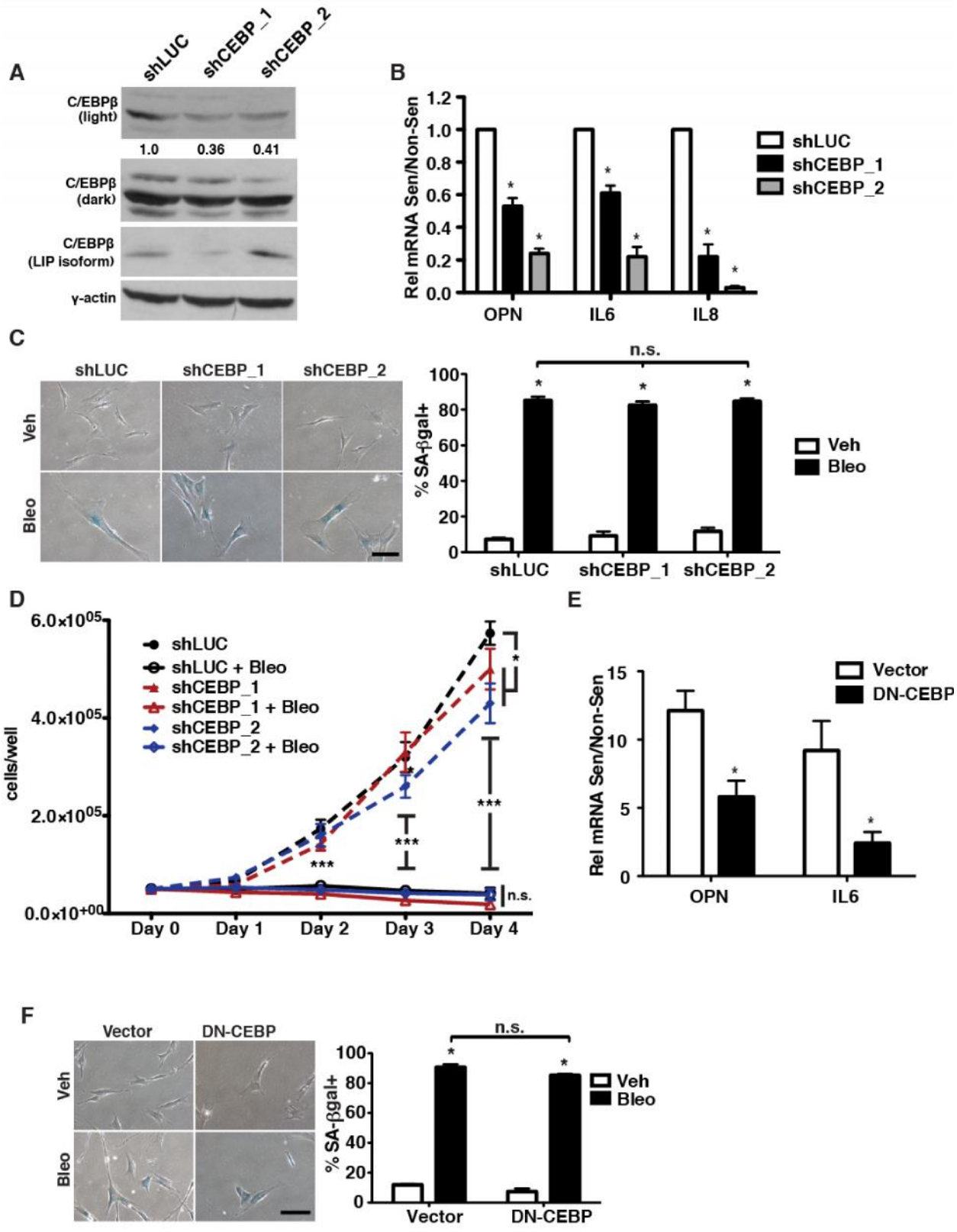

Figure 2.2: C/EBPβ is required for OPN induction in response to senescence

A) C/EBPβ protein was measured in control or shCEBP-expressing cells via Western blot. shCEBP_1 had 64% reduced levels of activating C/EBPβ isoforms (LAP1&2) while shCEBP_2 had 59% reduced activating C/EBPβ isoforms, n=3. **B)** OPN, IL-6, and IL-8 mRNA expression were decreased in senescent shCEBP_1 and shCEBP_2 BJs relative to control (shLUC), n=3, *p<0.05. **C)** Senescence-associated β-galactosidase (SA-βgal) staining was used to measure senescence induction in BJ fibroblasts expressing one of two independent shRNAs targeting C/EBPβ (shCEBP_1, shCEBP_2) or a control hairpin (shLUC) and treated with bleomycin (Bleo, left). There is no significant difference in percent SA-βgal+ cells among any of the hairpins (right), n=3, n.s.=non-significant, *p<0.05. Scale bar=100 μm **D)** Cell proliferation over four days in non-senescent or bleomycin-treated fibroblasts was not affected by depletion of C/EBPβ, n=3, *p<0.05. **E)** Expression of OPN and IL-6 are significantly reduced in senescent cells expressing dominant negative C/EBPβ (DN-CEBP) relative to empty vector control, n=4, *p<0.05 **F)** SA-βgal staining indicates no change in senescence induction following bleomycin treatment in vector compared to DN-CEBP fibroblasts, n=3, n.s.=non-significant, *p<0.05, ***p<0.001. Scale bar=100 μm.

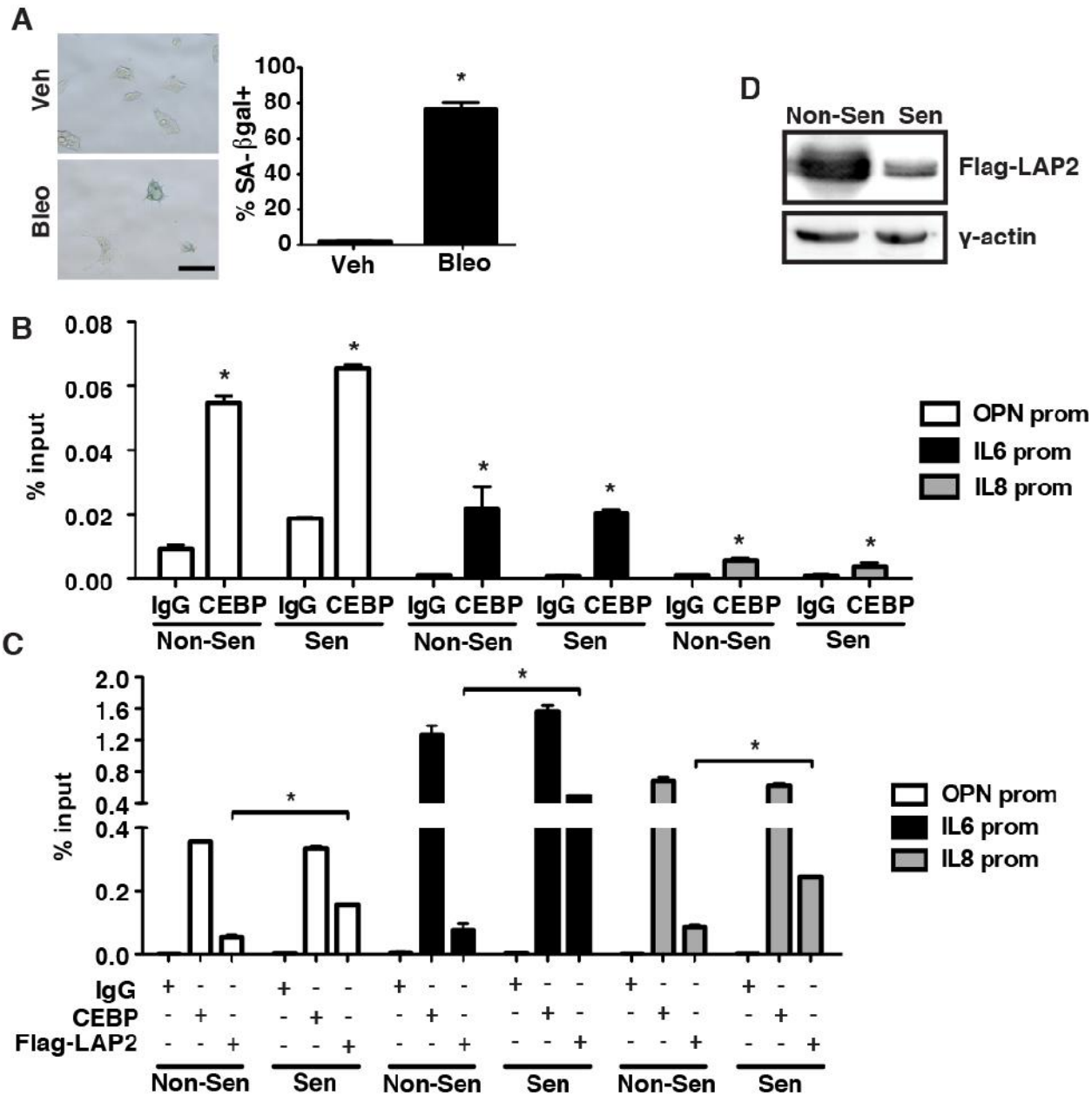

Figure 2.3: C/EBPβ isoform binds SASP promoters in senescent cells

A) Treatment of 293T HEK cells with bleomycin induces a significant increase in senescence as indicated by increased senescence-associated β-galactosidase staining, n=3, *p<0.05. Scale bar=100 μm. **B)** Chromatin immunoprecipitation (ChIP) using a C/EBPβ antibody which recognizes all three C/EBPβ isoforms or a non-specific control

(IgG) indicates that C/EBPβ binds to the OPN, IL-6, and IL-8 promoters in both vehicle and bleomycin-treated 293Ts, representative experiment, n=3, *p<0.05. **C)** ChIP in 293Ts transfected with a Flag-tagged full length C/EBPβ isoform (Flag-LAP2). An antibody recognizing all three C/EBPβ isoforms (CEBP) or an anti-Flag antibody was used to detect binding of the total C/EBPβ relative to exogenous Flag-LAP2 to the OPN, IL-6 and IL-8 promoters in vehicle (Non-Sen) and bleomycin-treated (Sen) 293Ts. While there was little change in total C/EBPβ bound to the OPN, IL-6, or IL-8 promoters, Flag-LAP2 binding to all three promoters was significantly increased in senescent cells, representative experiment, n=3, *p<0.05. **D)** Western blotting using an anti-Flag antibody indicated that Flag-LAP2 expression is significantly higher in non-senescent 293Ts than senescent 293Ts, n=3.

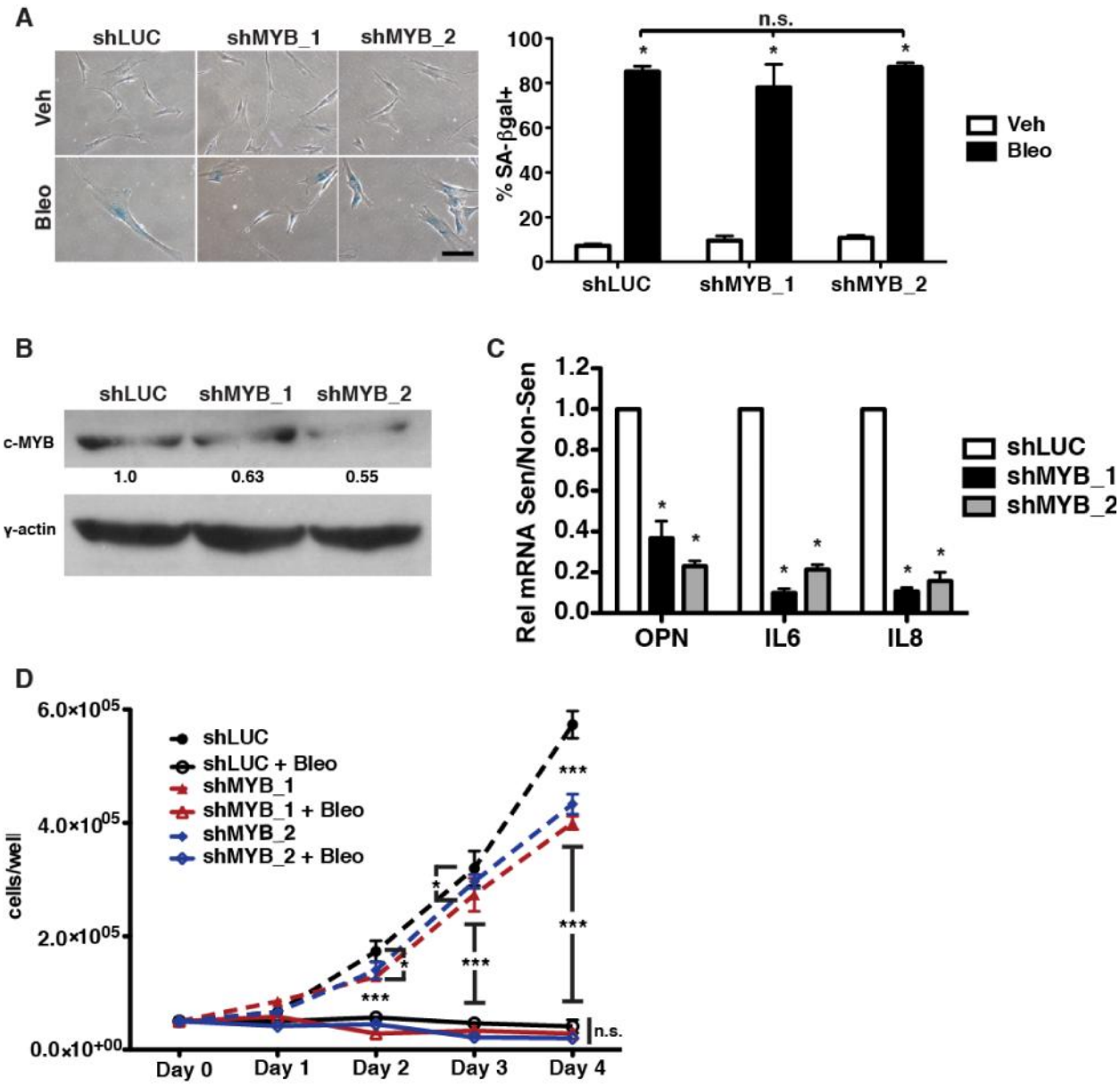

Figure 2.4: c-Myb regulates OPN, IL-6, and IL-8 in response to senescence

A) Senescence-associated β-galactosidase (SA-βgal) staining was used to measure senescence induction in bleomycin-treated BJ fibroblasts expressing one of two independent shRNAs targeting c-Myb (shMYB_1, shMYB_2) or a control hairpin (shLUC; left). There is no significant difference in percent SA-βgal+ cells among any of the hairpins (right), n=3, n.s.=non-significant, *p<0.05. Scale bar=100 μm **B)** c-Myb protein was measured in control or shMYB-expressing cells via Western blot. shMYB_1

had 37% reduced levels of c-MYB while shMYB_2 had 45% reduced c-Myb, n=3. **C)** OPN, IL-6, and IL-8 mRNA expression were decreased in senescent shMYB_1 and shMYB_2 BJs relative to control (shLUC), n=3, *p<0.05. **D)** Cell proliferation over four days in non-senescent or bleomycin-treated fibroblasts was not affected by depletion of c-Myb, n=3 *p<0.05, ***p<0.001.

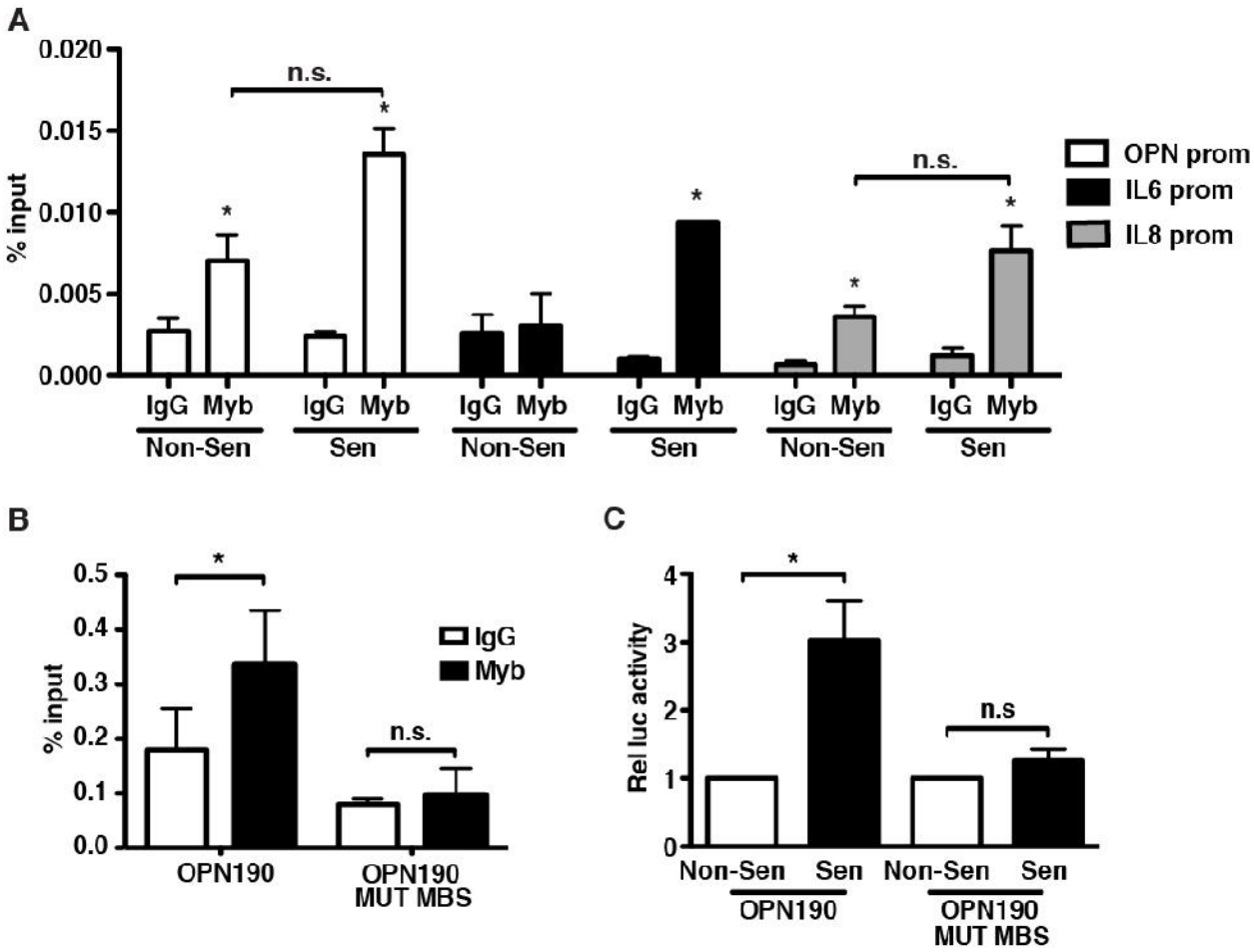

Figure 2.5: OPN induction in senescent cells requires c-Myb binding to the OPN promoter

A) Chromatin immunoprecipitation was used to measure c-Myb binding to the OPN, IL-6, and IL-8 promoters in 293T cells expressing exogenous c-Myb cDNA. C-Myb significantly binds to all three endogenous promoters, representative experiment, n=3, n.s.=non-significant, *p<0.05. **B)** c-Myb binds the OPN190 promoter reporter construct relative to IgG control. Mutation of the c-Myb binding site eliminates binding to the OPN190 construct, n=3, n.s.=non-significant, *p<0.05. **C)** Luciferase activity is increased in senescent BJ fibroblasts expressing the WT OPN190 construct relative to non-senescent cells, but not in fibroblasts expressing the mutant c-Myb binding site

OPN190 construct (OPN190MUT MBS), n=4, n.s.=non-significant, *p<0.05.

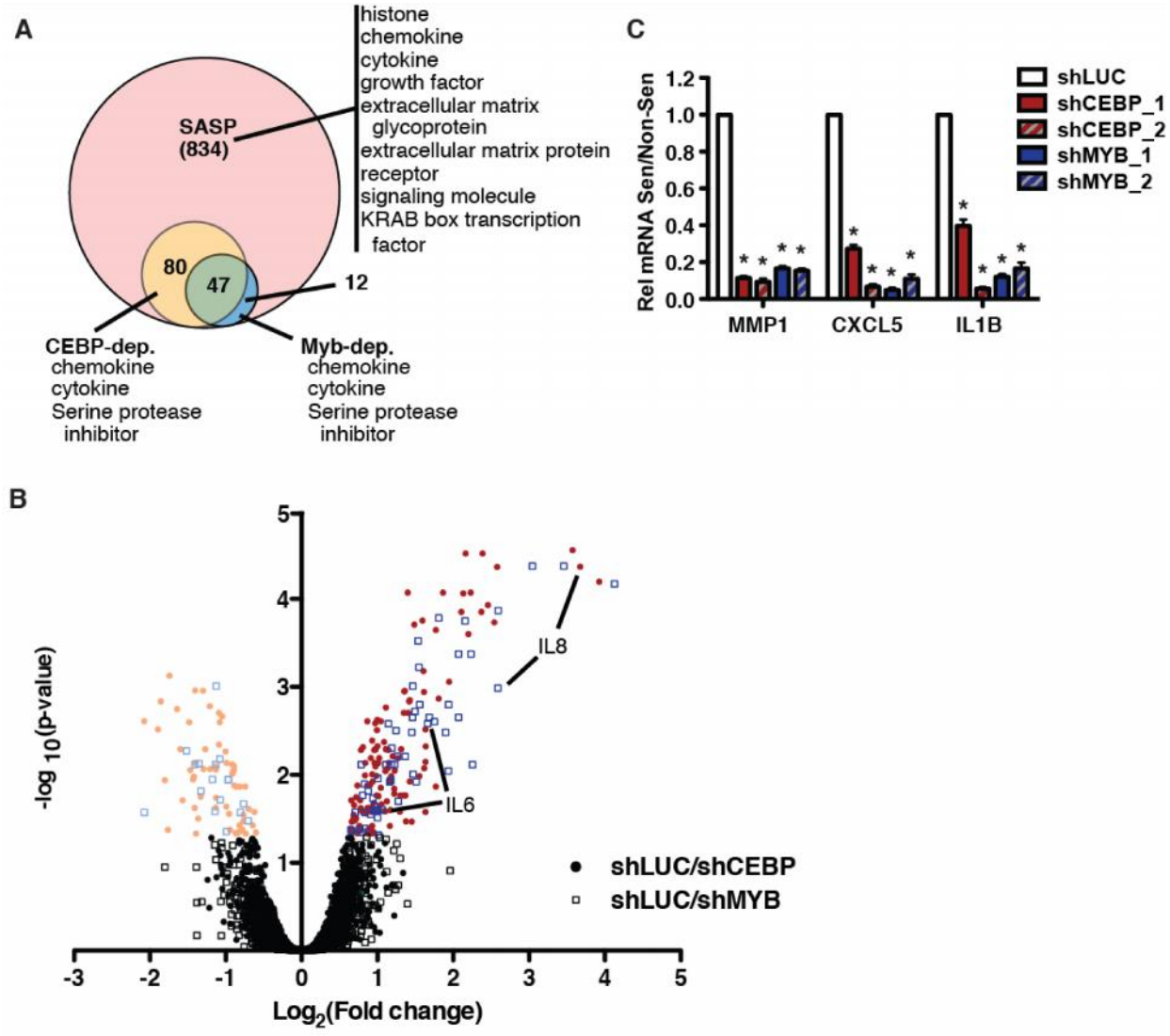

Figure 2.6: c-Myb and C/EBPβ regulate a subset of the SASP

A) A microarray was performed to compare gene expression and induction in response to senescence among control, shCEBP_2 and shMYB_1 expressing fibroblasts. 834 genes were identified as SASP factors. Of these, 127 were solely C/EBPβ dependent, 12 were solely c-Myb dependent, and 47 were dependent on both transcription factors. GO Term enrichment analysis was performed. Genes were considered dependent if their induction in response to senescence was significantly reduced in the experimental

hairpin condition relative to control, $p<0.05$. **B)** The $\log_2$ fold change in induction (bleomycin over non-senescent) of shLUC relative to shCEBP_2 or shMYB_1 is plotted relative to the negative $\log_{10}$ of the p-value. Genes with significantly higher (bright colors, right) or lower (pale colors, left) induction in shLUC relative to shCEBP (circles) or shMYB (open boxes) are indicated. **C)** The C/EBPβ- and c-Myb-dependent SASP factors MMP1, CXLC5, and IL1B were validated using qRT-PCR. Depletion of C/EBPβ or c-Myb with two different hairpins each significantly reduced induction of these SASP factors.

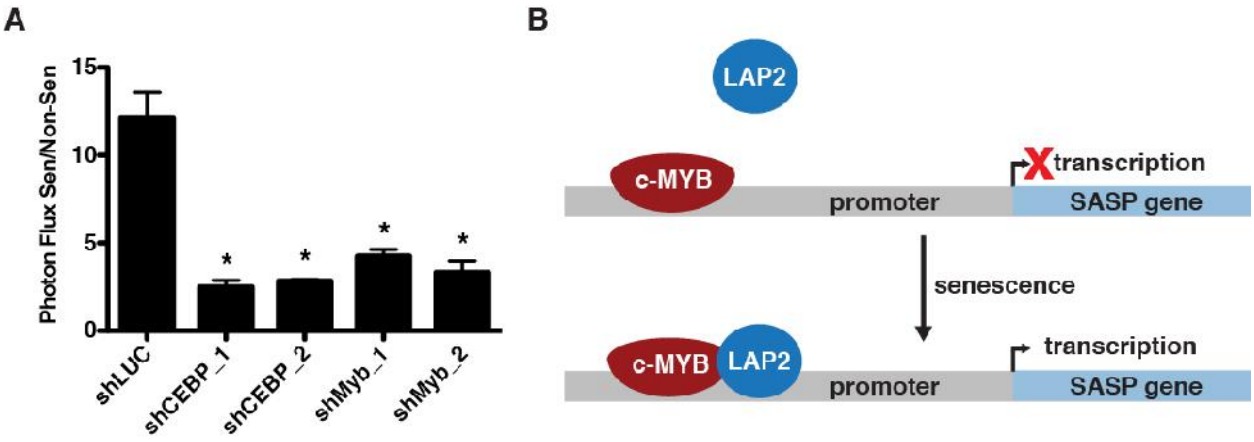

Figure 2.7: Depletion of c-Myb or C/EBPβ inhibits preneoplastic cell growth promotion by senescent fibroblasts

A) HaCAT keratinocytes expressing CBR luciferase were cocultured with non-senescent or senescent BJs expressing either a control shRNA (shLUC) or shRNAs targeting C/EBPβ (shCEBP_1 and shCEBP_2) or c-Myb (shMYB_1 and shMYB_2). HaCAT proliferation was measured using bioluminescent imaging after six days of coculture, shown as fold growth when cocultured with senescent fibroblasts relative to non-senescent fibroblasts. Depletion of either C/EBPβ or c-Myb in senescent BJs significantly reduces the ability to promote HaCAT cell growth, n=3, *$p<0.05$. **B)** Schematic showing the proposed model of regulation of OPN and other SASP factors by c-Myb and C/EBPβ. In response to senescence, the activating isoform of C/EBPβ, LAP2, increases occupancy on the SASP promoter, inducing transcription.

Supplemental Table 2.1: Microarray SASP genes

Gene Symbol	Bleo Upreg	Ras Upreg	Gene Symbol	Bleo Upreg	Ras Upreg	Gene Symbol	Bleo Upreg	Ras Upreg
CXCL5	59.6	28.5	ENC1	4.3	3.3	LOC105374171	4.7	2.7
CXCL8	26.8	27.6	SAT1	5.1	3.3	RRM2B	2.2	2.7
SERPINB4	98.9	25.0	PAPPA	1.5	3.3	IRAK2	4.6	2.7
IL1B	22.1	14.2	TREM1	1.4	3.3	EHF	7.8	2.7
CLDN1	14.2	13.2	CXCL3	2.7	3.3	VTRNA1-3	1.9	2.6
IL24	6.5	11.0	CCL20	1.9	3.3	HIST1H4H	2.7	2.6
IL13RA2	38.9	7.9	CD24	1.5	3.3	TSPAN13	7.2	2.6
CXCL1	3.1	7.6	STC1	5.8	3.2	TNFRSF10A	2.0	2.6
EREG	16.0	6.9	CDCP1	12.4	3.2	STAT4	1.9	2.6
IL1A	29.4	6.6	LRRC15	7.5	3.2	APLP1	1.3	2.5
GDF15	3.9	6.5	PSTPIP2	1.9	3.2	NEFM	4.0	2.5
SERPINB2	9.3	6.2	P3H2	2.9	3.2	HIST1H2BN	2.0	2.5
C3	2.0	6.1	CSF2	21.5	3.2	CDKN1A	1.4	2.5
LOC105369848	20.4	6.1	NFKBIZ	3.7	3.1	AOX1	1.4	2.5
MMP3	9.5	5.8	CYFIP2	2.2	3.1	GADD45A	1.7	2.5
ESM1	9.0	5.7	PI3	3.1	3.1	SOD2	1.7	2.5
CTSS	7.5	5.4	LOC105374003	43.9	3.0	PHLDA1	4.7	2.5
LOC541472	2.6	5.4	C10orf55	17.5	3.0	LOC105369808	2.3	2.5
SLC16A6	40.9	5.2	THSD1	1.6	3.0	AKR1B1	2.0	2.5
RRAD	4.9	4.8	CES2	1.4	3.0	LOC105369893	29.2	2.4
ITGA2	12.5	4.7	IFI30	1.7	3.0	HSD11B1	1.6	2.4
TFPI2	6.1	4.7	PAG1	3.6	3.0	DUSP6	9.1	2.4
C15orf48	5.1	4.5	LCE1F	416.1	2.9	TMEM132A	2.4	2.4
ACPP	29.8	4.4	TNFAIP3	2.9	2.9	PMAIP1	7.0	2.4
KCTD4	14.9	4.4	DUSP4	9.2	2.9	ANOS1	19.2	2.4
MIR222	1.9	4.3	WDR63	2.0	2.9	RAB27B	2.3	2.4
CSF3	8.2	4.2	STEAP1	5.2	2.9	CYP3A7	2.4	2.4
IL6	1.9	4.1	MMP1	4.3	2.9	LOC105376374	9.6	2.4
SPP1	4.9	4.0	PTGS2	2.0	2.9	RNF152	4.7	2.3
HIST1H2BG	5.5	3.9	PTPN22	2.7	2.9	SERPINB3	5.6	2.3
C1QTNF1	1.4	3.9	SEC11C	3.4	2.9	TIGAR	2.0	2.3
AMPD3	6.6	3.9	LRRN3	1.7	2.8	42797	2.6	2.3
TMEM158	6.6	3.8	CHST7	2.6	2.8	SEMA3A	5.7	2.3
LIF	4.4	3.8	LPXN	4.7	2.8	MLLT11	6.3	2.3
TM4SF1	11.5	3.8	PLAU	15.0	2.8	TMEM68	1.5	2.3
LINC01021	1.5	3.7	DLGAP1-AS2	2.3	2.8	INA	3.0	2.3
SLC22A4	2.7	3.7	ERN1	3.3	2.8	FJX1	3.0	2.3
KRTAP2-3	2.0	3.7	COL10A1	36.4	2.7	SHC4	2.0	2.3
ULBP1	4.0	3.7	IRAK3	1.6	2.7	EVI2A	1.4	2.2
KRTAP3-1	2.9	3.6	DTNA	2.3	2.7	IL11	6.0	2.2
ACER2	1.5	3.5	POU2F2	5.7	2.7	PARM1	1.6	2.2
LINC01291	2.2	3.4	MAMDC2	1.5	2.7	STEAP2	4.0	2.2
PRLR	2.1	3.3	HIST1H2BC	3.2	2.7	LCE2A	39.8	2.2

Supplemental Table 2.1: Microarray SASP genes

Gene Symbol	Bleo Upreg	Ras Upreg	Gene Symbol	Bleo Upreg	Ras Upreg	Gene Symbol	Bleo Upreg	Ras Upreg
EPG5	1.9	2.2	DOCK5	1.9	2.0	LOC105379676	1.9	1.8
ZC3H12C	4.1	2.2	NCEH1	2.0	2.0	CPEB4	1.9	1.8
DYRK3	2.2	2.2	LOC105376236	1.5	2.0	LOC105376694	5.0	1.8
ADRB2	1.8	2.2	ATP13A3	2.4	2.0	TP53I3	1.5	1.8
NRG1	4.4	2.2	SVIL	3.4	2.0	STYK1	2.0	1.8
DHRS7	2.3	2.1	PIM2	2.0	2.0	C16orf52	2.2	1.8
LOC105369340	2.0	2.1	HBEGF	1.4	2.0	LOC101926893	1.9	1.8
POPDC3	5.9	2.1	ANPEP	3.8	2.0	TMEM154	6.9	1.8
GM2A	1.8	2.1	PLD1	1.4	2.0	CCND1	2.1	1.8
RHBDF2	2.5	2.1	NT5E	3.4	2.0	PNP	3.4	1.8
HIST2H2BE	2.2	2.1	ABCA1	3.2	2.0	MYDGF	1.4	1.8
RNF19B	1.7	2.1	TNFRSF10D	3.3	2.0	TRIB1	3.4	1.8
GK	2.9	2.1	SUSD6	1.5	2.0	FBXO22	1.5	1.8
MAP3K5	3.4	2.1	DUSP5	4.8	2.0	HIPK2	1.9	1.8
EPHA2	2.1	2.1	PGF	1.5	2.0	EML2	1.7	1.8
BCL2L1	2.0	2.1	PLAT	2.1	2.0	CYB5R2	2.0	1.8
ITGA6	4.6	2.1	OGFRL1	2.3	1.9	SQRDL	1.7	1.8
PID1	3.1	2.1	FBXO22-AS1	2.0	1.9	LRP8	3.0	1.8
LOC105376626	7.5	2.1	ODC1	3.5	1.9	LUCAT1	1.7	1.8
IER3	2.9	2.1	TNFRSF10B	1.4	1.9	GXYLT1	1.4	1.8
CASP3	3.6	2.1	MIR4482	2.5	1.9	IGF2R	2.5	1.8
ABL2	2.6	2.1	DNER	2.0	1.9	TPCN1	1.7	1.8
DGKA	1.4	2.1	BCL2A1	4.4	1.9	LOC105379695	2.3	1.8
PCDH9	4.2	2.1	NOMO1	1.5	1.9	SGTB	1.7	1.8
FOLR3	1.8	2.1	MMP16	2.4	1.9	ERO1B	1.6	1.8
GDNF	2.2	2.1	SNORD66	2.9	1.9	RASSF8	2.4	1.8
ARHGEF28	5.0	2.1	ABLIM3	3.6	1.9	SLC8A1-AS1	2.0	1.8
ANGPTL4	1.3	2.1	LOC100507006	1.7	1.9	HSPH1	2.0	1.8
SMURF2	3.2	2.1	SLC39A14	1.7	1.9	CYB5R1	1.5	1.8
C8orf4	1.8	2.1	TM7SF3	1.5	1.9	FBXO32	1.9	1.8
OR51A4	1.6	2.0	SLC9A1	2.3	1.9	NEFL	9.2	1.8
ZC3H12A	2.2	2.0	ITGA3	2.5	1.9	KYNU	4.0	1.8
DLL4	4.6	2.0	LOC105373723	1.6	1.9	ATG4A	2.2	1.8
RAP1GAP2	2.0	2.0	LAPTM5	2.0	1.9	EDA2R	1.3	1.8
ATP6V0A1	2.7	2.0	SERPINB7	1.8	1.9	RETSAT	1.4	1.8
FAM180A	1.8	2.0	TAF13	3.0	1.9	AIM1	2.0	1.8
LOC105374433	1.6	2.0	SIPA1L3	3.3	1.9	TMEM38B	2.8	1.7
PLK3	2.5	2.0	ABTB2	1.4	1.9	CYLD	1.7	1.7
SNORA14B	2.7	2.0	PTCHD4	1.5	1.9	LOC105369568	3.9	1.7
THEMIS2	3.0	2.0	DAZL	7.1	1.9	MIR146A	9.4	1.7
HERC5	1.8	2.0	METTL6	1.8	1.9	RPSAP52	1.6	1.7
FBXL19-AS1	1.4	2.0	PRKX	1.6	1.8	SLC20A1	4.6	1.7
NPC1	2.0	2.0	MT1L	4.9	1.8	NMNAT2	1.6	1.7

Supplemental Table 2.1: Microarray SASP genes

Gene Symbol	Bleo Upreg	Ras Upreg	Gene Symbol	Bleo Upreg	Ras Upreg	Gene Symbol	Bleo Upreg	Ras Upreg
PLAUR	2.4	1.7	NFKBIA	1.4	1.7	ELK3	1.6	1.6
MIR4451	2.2	1.7	C17orf89	1.3	1.7	MRPL39	1.5	1.6
INHBA	6.1	1.7	PGPEP1	1.5	1.7	UHRF1BP1L	1.6	1.6
ARHGAP22	3.6	1.7	GPR183	3.5	1.7	NSF	1.6	1.6
PLA2G4C	2.0	1.7	PLEK2	15.7	1.7	MAP2K3	2.0	1.6
HAGH	1.3	1.7	ORMDL2	1.8	1.6	AEN	1.5	1.6
TNIP1	1.7	1.7	RAB3B	1.4	1.6	EPT1	2.1	1.6
GRAMD1B	1.9	1.7	CITED4	4.0	1.6	OSGIN2	2.4	1.6
EMC7	1.5	1.7	DNAJB9	1.6	1.6	GPR4	6.7	1.6
MMP12	13.1	1.7	EVC	1.3	1.6	TMEM63B	1.3	1.6
ADGRE2	3.5	1.7	RRS1	1.7	1.6	MYCT1	1.7	1.6
LOC105374745	3.8	1.7	GLA	2.6	1.6	FEZ1	1.6	1.6
DCBLD2	5.3	1.7	LOC644135	2.2	1.6	OSTM1	1.7	1.6
MAFF	2.0	1.7	UXS1	1.5	1.6	ETV4	3.1	1.6
HAS2	3.3	1.7	HK2	1.7	1.6	PNPO	1.5	1.6
GSTO1	2.4	1.7	UCN2	3.7	1.6	HERC4	1.4	1.6
LINC01002	2.0	1.7	CDA	1.7	1.6	ZNF267	1.6	1.6
WDFY2	2.1	1.7	WTAPP1	2.7	1.6	HMGA2	2.5	1.6
TSSC2	1.6	1.7	NOMO2	1.4	1.6	WDR66	1.6	1.6
RND3	1.3	1.7	STK4	1.6	1.6	EAF1	1.8	1.6
CPED1	2.3	1.7	CABYR	1.4	1.6	SDC1	1.5	1.6
MYOCD	1.6	1.7	YRDC	2.3	1.6	NOG	3.3	1.6
SLC11A2	1.3	1.7	MTHFD2L	1.9	1.6	PSME4	1.8	1.6
PLCB4	1.4	1.7	ETV1	4.3	1.6	C2orf81	2.2	1.6
LAMC2	2.9	1.7	MAP4K3	1.5	1.6	NFKB2	1.6	1.6
ADAM23	1.6	1.7	ATP2B1	2.5	1.6	TOP1	2.2	1.6
ABCA13	1.5	1.7	PTP4A1	1.6	1.6	ITPRIP	2.6	1.6
ASB5	3.3	1.7	TNFRSF21	16.8	1.6	ZPR1	2.1	1.6
POMGNT1	1.7	1.7	MICA	2.0	1.6	LOC105377023	1.3	1.6
C9orf72	2.4	1.7	LOC101927121	1.7	1.6	CHMP5	1.8	1.6
MYO6	1.4	1.7	DAGLB	1.4	1.6	FCRLB	1.6	1.6
SRA1	1.9	1.7	NOMO3	1.4	1.6	PPP1R15A	1.8	1.6
PROCR	2.1	1.7	PSMD2	2.3	1.6	LOC101928820	2.1	1.6
CDIP1	1.5	1.7	DYNC1H1	2.0	1.6	LOC105369844	3.3	1.6
DPP4	1.5	1.7	ZNF468	1.3	1.6	RABGGTA	1.4	1.6
SERPINB10	1.4	1.7	KCTD1	1.3	1.6	PDGFC	1.4	1.6
CD274	6.9	1.7	SLC31A2	1.6	1.6	GSAP	2.4	1.6
AGTRAP	1.3	1.7	SRXN1	1.8	1.6	WDR43	1.4	1.6
DCUN1D3	2.0	1.7	SLC4A7	1.4	1.6	MCTP1	7.7	1.5
SESN2	1.4	1.7	ZCCHC6	2.1	1.6	ZNF432	1.4	1.5
MAP7	1.4	1.7	RALA	3.4	1.6	ADIRF	1.7	1.5
LOC101929470	1.8	1.7	E2F7	10.3	1.6	KIF3B	1.6	1.5
NEDD4L	1.8	1.7	KIF21A	1.8	1.6	FAM214B	2.1	1.5

Supplemental Table 2.1: Microarray SASP genes

Gene Symbol	Bleo Upreg	Ras Upreg	Gene Symbol	Bleo Upreg	Ras Upreg	Gene Symbol	Bleo Upreg	Ras Upreg
UCHL3	2.0	1.5	EGFR	1.4	1.5	LOC105379272	1.6	1.5
EIF5A2	1.4	1.5	GFM2	1.9	1.5	NEU1	1.7	1.5
SOWAHC	1.6	1.5	42798	1.3	1.5	SQSTM1	1.5	1.5
ITPR3	1.7	1.5	AK5	1.9	1.5	MAPKBP1	1.4	1.5
BCAP31	1.6	1.5	LOC105369204	1.5	1.5	GDF11	1.3	1.5
RPLP0P2	12.1	1.5	UBA6	2.1	1.5	SLFN5	1.6	1.5
SRPX2	1.6	1.5	NCLN	1.7	1.5	LIG4	1.6	1.5
C6orf1	1.3	1.5	CLCA4	1.4	1.5	SMOX	1.7	1.5
MCC	1.5	1.5	POLR3A	2.3	1.5	PITPNC1	4.2	1.5
HYOU1	2.0	1.5	HSPA13	1.5	1.5	TLDC1	1.4	1.5
GLRX	2.0	1.5	UBASH3B	1.6	1.5	C15orf54	2.6	1.5
PPP3CC	1.4	1.5	ETNK1	1.9	1.5	NCR3LG1	1.4	1.5
PI4K2A	1.6	1.5	FUCA2	1.3	1.5	TNFAIP1	1.2	1.5
MYO5A	2.5	1.5	DOCK4	12.8	1.5	NIPA1	1.3	1.5
LINC00589	1.5	1.5	NAV3	3.6	1.5	PRMT5	1.5	1.5
CREM	1.6	1.5	SPRY2	5.1	1.5	UHMK1	1.7	1.5
MAFK	1.5	1.5	RIPK2	2.1	1.5	SATB2	2.6	1.5
FXR2	1.7	1.5	CNST	1.4	1.5	DAP3	1.6	1.5
TNFAIP2	1.3	1.5	LURAP1L	1.3	1.5	C3orf52	2.1	1.5
PAK2	1.4	1.5	PPFIBP1	1.5	1.5	FLJ42627	1.4	1.5
ELL	1.9	1.5	ITPR2	2.0	1.5	METTL8	1.4	1.5
ANKRD31	1.5	1.5	PTPN1	1.9	1.5	PDIA4	1.7	1.5
LOC105369313	2.8	1.5	UBE2M	1.9	1.5	TBC1D9	1.7	1.5
LINC01204	2.1	1.5	ZNF276	1.5	1.5	DEDD2	1.4	1.5
FOSL1	1.7	1.5	FAM210B	3.5	1.5	FHOD3	2.5	1.5
LOC101928461	1.9	1.5	NKX3-1	1.3	1.5	G6PC	1.3	1.5
STEAP3	5.0	1.5	EDEM3	1.9	1.5	PFN2	1.3	1.5
SCARB1	2.1	1.5	NR1D1	1.5	1.5	ZNF622	2.1	1.5
PARD6B	2.2	1.5	PWARSN	2.2	1.5	C18orf8	1.4	1.5
CORO2A	1.6	1.5	ABHD5	1.7	1.5	TAB3	1.5	1.5
SLC35G2	1.5	1.5	MYO10	2.6	1.5	MAFG	1.6	1.5
TCEB3	1.5	1.5	PEX19	1.2	1.5	ASB1	1.6	1.5
STX3	1.5	1.5	LOC100505622	1.5	1.5	FAM214A	1.5	1.4
DGKE	2.1	1.5	MAP1A	1.8	1.5	PNO1	2.0	1.4
ARID3A	1.7	1.5	ABHD3	1.7	1.5	ARFGEF2	1.4	1.4
TRMT6	2.3	1.5	PPP2R1B	1.5	1.5	MXD1	1.5	1.4
DNAJB11	1.4	1.5	NFKBIB	1.7	1.5	SLC22A1	1.4	1.4
MKLN1-AS	1.3	1.5	ATF3	1.4	1.5	TSPYL1	1.6	1.4
ATP6AP1	1.2	1.5	BHMT2	2.9	1.5	MSC	2.1	1.4
DDA1	2.0	1.5	GPR3	2.8	1.5	TOR1AIP2	1.4	1.4
NDUFAB1	2.0	1.5	SCAMP3	1.3	1.5	PIP4K2C	1.5	1.4
GSS	1.9	1.5	LOC105376382	5.9	1.5	MSI2	2.3	1.4
DNAJC3	1.3	1.5	NEK10	1.6	1.5	MFSD2A	1.6	1.4

Supplemental Table 2.1: Microarray SASP genes

Gene Symbol	Bleo Upreg	Ras Upreg	Gene Symbol	Bleo Upreg	Ras Upreg	Gene Symbol	Bleo Upreg	Ras Upreg
PTPRF	1.3	1.4	PSMD14	2.0	1.4	PSMD3	1.6	1.4
COQ10B	2.1	1.4	LOC105372190	2.0	1.4	ERRFI1	4.6	1.4
PSMC5	1.5	1.4	SUCO	1.6	1.4	DPP9	1.9	1.4
CHMP1B	1.6	1.4	PKIA	6.4	1.4	NLRP1	1.7	1.4
PSMC4	1.8	1.4	SLC39A2	1.5	1.4	FMNL2	3.8	1.4
NFKBIE	1.3	1.4	LAMA1	1.5	1.4	GTPBP4	1.9	1.4
MYEF2	1.4	1.4	MMP14	2.0	1.4	TANC1	1.3	1.4
FRMD5	1.7	1.4	LOC105374556	2.7	1.4	PIKFYVE	1.5	1.4
MORN4	1.5	1.4	UNC13B	1.6	1.4	BTBD9	1.3	1.4
BVES	2.6	1.4	SENP5	1.6	1.4	G0S2	3.1	1.4
LOC101928225	1.5	1.4	LRP10	1.2	1.4	SDF2L1	1.9	1.4
PAQR5	1.5	1.4	GABARAPL2	1.7	1.4	CCNH	1.3	1.4
NFE2L1	1.3	1.4	HMGXB3	2.5	1.4	DBNDD1	1.7	1.4
LOC105373813	1.4	1.4	URB1-AS1	1.5	1.4	HS3ST3B1	2.3	1.4
WIPI1	1.5	1.4	TRIM25	1.5	1.4	SAMD8	1.8	1.4
PTRH2	1.9	1.4	CEP170B	1.2	1.4	UBALD2	2.2	1.4
TUSC2	1.5	1.4	SREK1IP1	1.5	1.4	HTT	2.1	1.4
KLHL32	1.4	1.4	SPRY4	4.3	1.4	ATP1B3	1.4	1.4
CEP104	1.3	1.4	TRIM23	1.3	1.4	CLDN12	1.3	1.4
CCBE1	2.4	1.4	PLEKHB2	2.1	1.4	STXBP1	2.0	1.4
GGT3P	1.6	1.4	EMP1	1.9	1.4	OXSR1	1.6	1.4
TERF2IP	1.6	1.4	SLC35D1	1.4	1.4	RNF181	1.4	1.4
SLC37A2	2.5	1.4	SPATA17	1.6	1.4	GDPD1	2.5	1.4
ASCC3	1.4	1.4	SERINC2	2.7	1.4	EFTUD1	1.6	1.4
SEC23B	2.2	1.4	UBXN8	1.5	1.4	FGFR1OP	1.4	1.4
ELOVL4	2.0	1.4	SEC61A2	1.7	1.4	HSPA5	1.7	1.4
MCL1	2.0	1.4	FADS1	1.7	1.4	ZFAND2A	1.5	1.4
HIVEP2	1.3	1.4	AMN1	2.3	1.4	SDE2	1.9	1.4
CMTM4	1.4	1.4	UST	2.1	1.4	KLHL21	1.3	1.4
MTOR	1.8	1.4	IGDCC4	1.6	1.4	QSOX2	1.8	1.4
ZNF121	1.6	1.4	ECE1	1.6	1.4	IDS	1.5	1.4
ACSL4	1.5	1.4	FMN1	2.0	1.4	WNK4	1.4	1.4
ADGRA3	1.6	1.4	SMTN	1.5	1.4	ZMYND8	1.8	1.4
RGAG4	1.6	1.4	NRIP3	4.9	1.4	TMEM8A	1.4	1.4
FIBCD1	1.9	1.4	DENND2A	2.7	1.4	SECISBP2	1.4	1.4
ATG2A	1.5	1.4	DKK2	2.5	1.4	MAP4K4	1.5	1.4
PDLIM4	1.9	1.4	GALNT15	1.7	1.4	PPTC7	1.6	1.4
MIR2909	1.5	1.4	SNORD116-12	1.4	1.4	ITPKC	1.3	1.4
TMEM131	1.8	1.4	IL4R	1.6	1.4	PISD	1.4	1.4
PPIF	3.4	1.4	LARP4	1.4	1.4	TFRC	1.6	1.4
EMC1	1.4	1.4	SBNO1	1.7	1.4	SELPLG	1.3	1.4
ASAP2	2.0	1.4	EDEM1	2.4	1.4	TMCO1	1.4	1.4
GTF2F2	1.5	1.4	HMGA1	2.0	1.4	WWC3	1.4	1.4

Supplemental Table 2.1: Microarray SASP genes

Gene Symbol	Bleo Upreg	Ras Upreg	Gene Symbol	Bleo Upreg	Ras Upreg	Gene Symbol	Bleo Upreg	Ras Upreg
ZDHHC5	1.3	1.4	SLC17A5	1.4	1.4	PSMB7	1.5	1.3
ATP6V1E1	1.6	1.4	UFD1L	1.6	1.3	HSPA9	1.7	1.3
CRADD	2.1	1.4	CCL5	1.4	1.3	TMED5	1.5	1.3
TOMM34	2.4	1.4	ORAOV1	1.7	1.3	FAM96B	1.7	1.3
TMEM33	2.1	1.4	BAZ2A	1.4	1.3	KIAA1217	1.3	1.3
MTF1	1.4	1.4	SLC33A1	1.7	1.3	TMED9	1.3	1.3
GCC2	1.2	1.4	RPRD1A	1.7	1.3	WSB2	1.3	1.3
ANKRD52	1.7	1.4	CHMP4C	1.4	1.3	ACO1	1.5	1.3
LINC00884	1.2	1.4	BNC1	6.7	1.3	PTCHD3	1.4	1.3
PLCXD1	2.5	1.4	UGGT1	1.4	1.3	ZBTB21	2.0	1.3
BAZ1A	1.6	1.4	MAST4	1.4	1.3	ATP6V1D	1.6	1.3
CD109	1.3	1.4	CCND2	1.4	1.3	LOC105370145	1.3	1.3
GFPT1	1.7	1.4	SLC2A6	2.0	1.3	PINK1	1.5	1.3
NEDD4	1.4	1.4	TSTA3	1.2	1.3	SLC4A4	2.8	1.3
GSG1	1.4	1.4	ERLEC1	1.3	1.3	IPPK	1.5	1.3
UAP1	1.4	1.4	CD44	1.7	1.3	FAM129B	1.4	1.3
LYST	1.8	1.4	YIPF6	1.4	1.3	XPC	1.4	1.3
FKBP4	2.0	1.4	STYXL1	1.5	1.3	H2AFJ	1.3	1.3
BBS7	1.5	1.4	CUBN	1.9	1.3	ATP2C1	1.3	1.3
PIEZO1	1.3	1.4	KDSR	1.2	1.3	LHFPL2	1.8	1.3
RAB3IP	1.3	1.4	SMURF1	1.5	1.3	ABHD2	1.5	1.3
FBXO28	2.2	1.4	SRP54	1.6	1.3	CLCN3	1.4	1.3
JARID2	1.8	1.4	PWAR5	2.6	1.3	BAK1	1.6	1.3
RICTOR	1.5	1.4	ORAI1	1.5	1.3	SMCR8	1.5	1.3
AVL9	1.8	1.4	SPTY2D1	1.5	1.3	MOXD1	1.6	1.3
AUP1	1.4	1.4	COX7A2	1.5	1.3	GSK3B	1.4	1.3
TMEM2	1.8	1.4	TFAP2C	2.0	1.3	MBOAT7	1.3	1.3
MT2A	1.5	1.4	CDC37	1.6	1.3	CPNE3	2.3	1.3
ARSG	1.8	1.4	CISD1	1.6	1.3	LGALSL	1.5	1.3
NXPE3	1.3	1.4	TRIM37	1.4	1.3	CSRNP1	2.4	1.3
ISOC1	3.1	1.4	FAM91A1	1.7	1.3	PRDM4	1.3	1.3
PRKCD	1.6	1.4	HIST1H2AC	1.3	1.3	FLJ32255	1.4	1.3
RUSC2	1.4	1.4	TOR4A	1.4	1.3	TXNRD1	2.3	1.3
BTN2A2	1.9	1.4	SERP1	1.3	1.3	CANT1	1.4	1.3
TSPAN14	2.9	1.4	AFF1	1.5	1.3	SPIRE1	1.7	1.3
GTF2B	1.5	1.4	DESI1	1.8	1.3	SFXN4	1.3	1.3
HDAC9	1.5	1.4	PFKFB3	2.0	1.3	MCFD2	1.2	1.3
VEPH1	3.0	1.4	PLOD2	1.5	1.3	SEC14L2	1.3	1.3
JADE2	1.3	1.4	ARHGAP18	2.0	1.3	PDHX	1.4	1.3
METTL13	1.3	1.4	KLHL18	1.7	1.3	LRRC36	1.3	1.3
DNAJC5	1.4	1.4	AKIRIN1	1.8	1.3	UBR4	1.5	1.3
SLC3A2	1.5	1.4	EIF1AY	1.6	1.3	SYNRG	1.4	1.3
RCL1	1.5	1.4	EPB41L4B	1.5	1.3	UROD	1.4	1.3

Supplemental Table 2.1: Microarray SASP genes

Gene Symbol	Bleo Upreg	Ras Upreg	Gene Symbol	Bleo Upreg	Ras Upreg	Gene Symbol	Bleo Upreg	Ras Upreg
SYNE1	1.2	1.3	TMBIM1	1.2	1.3	MICALL1	1.2	1.3
LOC102723721	1.4	1.3	GRPEL1	2.0	1.3	RASA2	1.3	1.3
PCNXL4	1.4	1.3	MLLT4	1.4	1.3	ADIPOR1	1.3	1.3
ACO2	1.4	1.3	ATP6V1H	1.9	1.3	SLAIN2	1.5	1.3
SIK3	1.3	1.3	C2CD2L	1.8	1.3	SLC22A5	1.2	1.3
PHYH	1.4	1.3	PHLDA2	3.4	1.3	CCT3	1.7	1.3
PIN1	1.3	1.3	PVR	2.0	1.3	P4HA2	1.3	1.3
GAPVD1	1.6	1.3	SLC19A2	1.4	1.3	TRAF3IP2	1.3	1.3
MYBBP1A	1.6	1.3	CES1P1	1.3	1.3	TRMT1	1.7	1.3
RPTOR	1.3	1.3	PITRM1	1.3	1.3	DIS3	1.5	1.3
PLAA	1.4	1.3	DYRK1B	1.3	1.3	UCK2	1.7	1.3
KCNMA1	1.7	1.3	QPCTL	2.0	1.3	ALAS1	1.6	1.3
PSEN2	1.3	1.3	UEVLD	1.3	1.3	CCNDBP1	1.2	1.3
DUSP1	1.4	1.3	VEGFC	2.5	1.3	ICOSLG	1.3	1.2
CPEB1	1.9	1.3	B4GALT7	1.2	1.3	PTAR1	1.7	1.2
TMEM120B	1.4	1.3	VCP	1.4	1.3	SLC30A7	1.7	1.2
SERPINE1	2.1	1.3	BECN1	1.2	1.3	GHITM	1.5	1.2
KLC1	1.4	1.3	FXYD5	1.4	1.3	NRDC	1.4	1.2
COQ6	1.3	1.3	EIF4E	1.8	1.3			
TMEM57	1.4	1.3	LOC727896	1.7	1.3			
ALG2	1.4	1.3	USP36	1.4	1.3			

Supplemental Table 2.2: C/EBPβ-dependent SASP factors

CXCL5	HMGA1	RGCC
EREG	MAP3K5	ERRFI1
SERPINB2	AKR1B1	SLC8A1-AS1
CXCL8	ITGA6	LOC105369848
IL13RA2	ODC1	CDKN3
SERPINB4	LINC01291	OGFRL1
CXCL1	PLAT	NCEH1
MMP1	CPED1	EMP1
LPXN	SMURF2	COL10A1
TMEM158	TREM1	SHCBP1
IL24	HAS2	TOP2A
TM4SF1	PHLDA1	ELK3
ESM1	FJX1	SHC4
LOC105376382	CXCL3	TMEM132A
IL1B	CEP55	PAQR5
STC1	PLAU	ARHGAP18
TFPI2	ANPEP	RPSAP52
LOC105376374	TNFAIP3	IL6
CTSS	DUSP6	C10orf55
ACPP	FHOD3	AOX1
C3	CDK1	IL11
PTGS2	IRAK3	PRLR
CDCP1	PID1	TRIM55
CSF2	ITGA2	PLEK2
SLC22A4	SEMA3A	SERPINB3
MMP3	VEPH1	ETV4
CYB5R2	LIF	ANOS1
PI3	IL1A	RASSF8
RNF152	DLL4	PDIA4
NFKBIZ	AIM1	SLC39A14
DENND2A	APCDD1	WDFY2
SOD2	SPC24	HSD11B1
FAM180A	PLK1	OR51A4
CSF3	NT5E	RIPK2
ANLN	FOSL1	LCE1F
C2orf81	CLDN1	LMNB1
LCE2A	AMPD3	MARCH3
DTNA	CCL20	AK5
KIF2C	LOC105374171	APLP1

Supplemental Table 2.2: C/EBPβ-dependent SASP factors

UAP1	SLC35G2	ENC1
INA	NEDD4L	FCRLB
DUSP4	CASP3	
SLC16A6	PDLIM4	

Supplemental Table 2.3: c-Myb-dependent SASP factors

CXCL5	STEAP2
IL24	NFKBIZ
SERPINB4	LCE2A
ACPP	CCL20
SERPINB2	LIF
CXCL1	MMP1
STC1	TREM1
TM4SF1	TNFRSF21
IL13RA2	GALNT15
C3	RNF152
EHF	ATP13A3
CXCL8	SAT1
CSF3	ARHGEF28
PI3	AOX1
CTSS	SHC3
CXCL3	CPED1
COL10A1	LPXN
EREG	GM2A
CSF2	IL11
IL6	MAP3K5
DTNA	
PTGS2	
IL1B	
TMEM158	
SLC16A6	
TFPI2	
CDCP1	
LOC541472	
C1QTNF1	
SLC22A4	
TMEM132A	
SOD2	
OR51A4	
LOC105376374	
FHOD3	
P3H2	
LCE1F	
AMPD3	
ANPEP	

REFERENCES

1. Depinho RA. 2000. The age of cancer 408.

2. Baker DJ, Wijshake T, Tchkonia T, LeBrasseur NK, Childs BG, van de Sluis B, Kirkland JL, van Deursen JM. 2011. Clearance of p16Ink4a-positive senescent cells delays ageing-associated disorders. Nature 479:232–6.

3. Krtolica A, Parrinello S, Lockett S, Desprez PY, Campisi J. 2001. Senescent fibroblasts promote epithelial cell growth and tumorigenesis: a link between cancer and aging. Proc Natl Acad Sci U S A 98:12072–12077.

4. Liu D, Hornsby PJ. 2007. Senescent human fibroblasts increase the early growth of xenograft tumors via matrix metalloproteinase secretion. Cancer Res 67:3117–26.

5. Freund A, Patil CK, Campisi J. 2011. p38MAPK is a novel DNA damage response-independent regulator of the senescence-associated secretory phenotype. EMBO J 30:1536–48.

6. Alspach E, Flanagan KC, Luo X, Ruhland MK, Huang H, Pazolli E, Donlin MJ, Marsh T, Piwnica-Worms D, Monahan J, Novack D V., McAllister SS, Stewart S a. 2014. p38MAPK Plays a Crucial Role in Stromal-Mediated Tumorigenesis. Cancer Discov 4:716–729.

7. Pazolli E, Luo X, Brehm S, Carbery K, Chung J-J, Prior JL, Doherty J, Demehri S, Salavaggione L, Piwnica-Worms D, Stewart SA. 2009. Senescent stromal-derived osteopontin promotes preneoplastic cell growth. Cancer Res 69:1230–9.

8. Campisi J. 2005. Senescent cells, tumor suppression, and organismal aging: good citizens, bad neighbors. Cell 120:513–22.

9. Pazolli E, Stewart SA. 2008. Senescence: the good the bad and the dysfunctional. Curr Opin Genet Dev 18:42–7.

10. Coppé J-P, Desprez P-Y, Krtolica A, Campisi J. 2010. The senescence-associated secretory phenotype: the dark side of tumor suppression. Annu Rev Pathol 5:99–118.

11. Coppé J-P, Kauser K, Campisi J, Beauséjour CM. 2006. Secretion of vascular endothelial growth factor by primary human fibroblasts at senescence. J Biol Chem 281:29568–74.

12. Coppé J-P, Patil CK, Rodier F, Sun Y, Muñoz DP, Goldstein J, Nelson PS, Desprez P-Y, Campisi J. 2008. Senescence-associated secretory phenotypes reveal cell-nonautonomous functions of oncogenic RAS and the p53 tumor suppressor. PLoS Biol 6:2853–68.

13. Hayflick L. 1965. The limited in vitro lifetime of human diploid cell strains. Exp Cell Res 37:614–36.

14. Baker DJ, Childs BG, Durik M, Wijers ME, Sieben CJ, Zhong J, Saltness RA, Jeganathan KB, Verzosa GC, Pezeshki A, Khazaie K, Miller JD, Deursen JM Van. 2016. Naturally occurring p16INK4a-positive cells shorten healthy lifespan. Nature 530:184–189.

15. Roos CM, Zhang B, Palmer AK, Ogrodnik MB, Pirtskhalava T, Nassir M, Hagler M, Jurk D, Smith LA, Zhu Y, Schafer MJ, Kirkland JL, Miller JD. 2016. Chronic senolytic treatment alleviates established vasomotor dysfunction in aged or atherosclerotic mice 973–977.

16. Chang J, Wang Y, Shao L, Laberge R-M, Demaria M, Campisi J, Janakiraman K, Sharpless NE, Ding S, Feng W, Luo Y, Wang X, Nukhet A-B, Krager K, Ponnappan U, Martin H-J, Meng A, Zhou D. 2016. Clearance of senescent cells by {ABT263} rejuvenates aged hematopoietic stem cells in mice. Nat Med 22:78–83.

17. Baar MP, Brandt RMC, Putavet DA, Hoeijmakers JHJ, Campisi J, Keizer PLJ De, Pluijm I Van Der, Essers J, Cappellen WA Van, Ijcken WF Van, Houtsmuller AB. 2017. Targeted Apoptosis of Senescent Cells Restores Tissue Homeostasis in Response to Chemotoxicity Article Targeted Apoptosis of Senescent Cells Restores Tissue Homeostasis in Response to Chemotoxicity and Aging. Cell 169:132–140.e15.

18. Ruhland MK, Loza AJ, Capietto A, Luo X, Knolhoff BL, Flanagan KC, Belt BA, Alspach E, Leahy K, Luo J, Schaffer A, Edwards JR, Longmore G, Faccio R, Denardo DG, Stewart SA. 2016. Stromal senescence establishes an immunosuppressive microenvironment that drives tumorigenesis. Nat Commun 7:1–18.

19. Luo X, Fu Y, Loza AJ, Faccio R, Longmore GD, Stewart SA, Luo X, Fu Y, Loza AJ, Murali B, Leahy KM, Ruhland MK. 2016. Stromal-Initiated Changes in the Bone Promote Metastatic Niche Development Article Stromal-Initiated Changes in the Bone Promote Metastatic Niche Development. CellReports 14:82–92.

20. Bavik C, Coleman I, Dean JP, Knudsen B, Plymate S, Nelson PS. 2006. The Gene Expression Program of Prostate Fibroblast Senescence Modulates Neoplastic Epithelial Cell Proliferation through Paracrine Mechanisms 794–802.

21. Torres C, Königsberg M. 2016. Senescence associated secretory phenotype profile from primary lung mice fibroblasts depends on the senescence induction stimuli.

22. Weber CE, Li NY, Wai PY, Kuo PC. 2012. Epithelial-mesenchymal transition, TGF-β, and osteopontin in wound healing and tissue remodeling after injury. J Burn Care Res 33:311–8.

23. Reinholt FP, Hultenby K, Oldberg A, Heinegard D. 1990. Osteopontin-a possible anchor of osteoclasts to bone. Proc Natl Acad Sci 87:4473–4475.

24. Chen R-X, Xia Y-H, Xue T-C, Ye S-L. 2010. Transcription factor c-Myb promotes the invasion of hepatocellular carcinoma cells via increasing osteopontin expression. J Exp Clin Cancer Res 29:172.

25. Chakraborty G, Jain S, Behera R, Ahmed M, Sharma P, Kumar V, Kundu GC. 2006. The multifaceted roles of osteopontin in cell signaling, tumor progression and angiogenesis. Curr Mol Med 6:819–830.

26. Anborgh PH, Mutrie JC, Tuck AB, Chambers AF. 2010. Role of the metastasis-promoting protein osteopontin in the tumour microenvironment. J Cell Mol Med 14:2037–44.

27. Finak G, Bertos N, Pepin F, Sadekova S, Souleimanova M, Zhao H, Chen H, Omeroglu G, Meterissian S, Omeroglu A, Hallett M, Park M. 2008. Stromal gene expression predicts clinical outcome in breast cancer. Nat Med 14:518–27.

28. Rudland P, Platt-Higgins A, El-Tanani M, de Silva Rudland S, Barraclough R, Winstanley J, Howitt R, West C. 2002. Prognostic significance of the metastasis-associated protein osteopontin in human breast cancer. Cancer Res 62:3417–3427.

29. Luo X, Ruhland MK, Pazolli E, Lind AC, Stewart SA. 2011. Osteopontin stimulates preneoplastic cellular proliferation through activation of the MAPK pathway. Mol Cancer Res 9:1018–29.

30. Pazolli E, Alspach E, Milczarek A, Prior J, Piwnica-Worms D, Stewart SA. 2012. Chromatin remodeling underlies the senescence-associated secretory phenotype of tumor stromal fibroblasts that supports cancer progression. Cancer Res

72:2251–61.

31. Kuilman T, Michaloglou C, Vredeveld LCW, Douma S, van Doorn R, Desmet CJ, Aarden L a, Mooi WJ, Peeper DS. 2008. Oncogene-induced senescence relayed by an interleukin-dependent inflammatory network. Cell 133:1019–31.

32. Chuang C-Y, Chang H, Lin P, Sun S-J, Chen P-H, Lin Y-Y, Sheu G-T, Ko J-L, Hsu S-L, Chang JT. 2012. Up-regulation of osteopontin expression by aryl hydrocarbon receptor via both ligand-dependent and ligand-independent pathways in lung cancer. Gene 492:262–9.

33. Greig KT, Carotta S, Nutt SL. 2008. Critical roles for c-Myb in hematopoietic progenitor cells. Semin Immunol 20:247–56.

34. Schultz J, Lorenz P, Ibrahim SM, Kundt G, Gross G, Kunz M. 2009. The functional -443T/C osteopontin promoter polymorphism influences osteopontin gene expression in melanoma cells via binding of c-Myb transcription factor. Mol Carcinog 48:14–23.

35. Mink S, Kerber U, Klempnauer KH. 1996. Interaction of C/EBPbeta and v-Myb is required for synergistic activation of the mim-1 gene. Mol Cell Biol 16:1316–1325.

36. Ness SA, Kowenz-Leutz E, Casini T, Graf T, Leutz A. 1993. Myb and NF-M: combinatorial activators of myeloid genes in heterologous cell types. Genes Dev 7:749–59.

37. Robert I, Sutter A, Quirin-Stricker C. 2002. Synergistic activation of the human choline acetyltransferase gene by c-Myb and C/EBPbeta. Brain Res Mol Brain Res 106:124–35.

38. Takami Y, Russell MB, Gao C, Mi Z, Guo H, Mantyh CR, Kuo PC. 2007. Sp1 regulates osteopontin expression in SW480 human colon adenocarcinoma cells. Surgery 142:163–9.

39. Gomis RR, Alarco C, Nadal C, Poznak C Van, Massague J. 2006. C / EBP b at the core of the TGF b cytostatic response and its evasion in metastatic breast cancer cells 203–214.

40. Serrano M, Lin AW, Mccurrach ME, Beach D, Lowe SW. 1997. Oncogenic ras Provokes Premature Cell Senescence Associated with Accumulation of p53 and p16 INK4a 88:593–602.

41. Navarro F, Gutman D, Meire E, Ca M, Rigoutsos I, Bentwich Z, Lieberman J.

2016. miR-34a contributes to megakaryocytic differentiation of K562 cells independently of p53 114:2181–2193.

42. Ritchie ME, Phipson B, Wu D, Hu Y, Law CW, Shi W, Smyth GK. 2015. limma powers differential expression analyses for RNA-sequencing and microarray studies. Nucleic Acids Res 43:e47.

43. Benjamini Y, Hochberg Y. 1995. Controlling the False Discovery Rate : A Practical and Powerful Approach to Multiple Testing. J R Stat Soc 57:289–300.

44. Mi H, Huang X, Muruganujan A, Tang H, Mills C, Kang D, Thomas PD. 2017. PANTHER version 11 : expanded annotation data from Gene Ontology and Reactome pathways , and data analysis tool enhancements 45:183–189.

45. Tahirov TH, Sato K, Ichikawa-Iwata E, Sasaki M, Inoue-Bungo T, Shiina M, Kimura K, Takata S, Fujikawa A, Morii H, Kumasaka T, Yamamoto M, Ishii S, Ogata K. 2002. Mechanism of c-Myb-C/EBP beta cooperation from separated sites on a promoter. Cell 108:57–70.

46. Burk O, Mink S, Ringwald M, Klempnauer KH. 1993. Synergistic activation of the chicken mim-1 gene by v-myb and C/EBP transcription factors. EMBO J 12:2027–38.

47. Ness S, Kowenz-Leutz E, Casini T, Graf T, Leutz A. 1993. Myb and NF-M: combinatorial activators of myeloid genes in heterologous cell types. Genes Dev 7:749–759.

48. Huggins CJ, Malik R, Lee S, Salotti J, Thomas S, Martin N, Quiñones O a, Alvord WG, Olanich ME, Keller JR, Johnson PF. 2013. C/EBPγ suppresses senescence and inflammatory gene expression by heterodimerizing with C/EBPβ. Mol Cell Biol 33:3242–58.

49. Suzuki K, Matsui Y, Higashimoto M, Kawaguchi Y, Seki S, Motomura H, Hori T, Yahara Y, Kanamori M, Kimura T. 2012. Myxoid Liposarcoma-Associated EWSR1-DDIT3 Selectively Represses Osteoblastic and Chondrocytic Transcription in Multipotent Mesenchymal Cells. PLoS One 7:e36682.

50. Christakos S, Dhawan P, Benn B, Porta A, Hediger M, Oh GT, Jeung E-B, Zhong Y, Ajibade D, Dhawan K, Joshi S. 2007. Vitamin D: molecular mechanism of action. Ann N Y Acad Sci 1116:340–8.

51. Descombes P, Schibler U. 1991. A liver-enriched transcriptional activator protein, LAP, and a transcriptional inhibitory protein, LIP, are translated from the same

mRNA. Cell 67:569–579.

52. Lee KS, Buck M, Houglum K, Chojkier M. 1995. Activation of Hepatic Stellate Cells by TGFa and Collagen Type I Is Mediated by Oxidative Stress Through c-myb Expression 96:2461–2468.

53. Piccinini G, Luchetti MM, Caniglia ML, Carossino AM, Montroni M, Introna M, Gabrielli A. 1996. c-myb Proto-Oncogene Is Expressed by Quiescent Scleroderma Fibroblasts and, Unlike B-myb Gene, Does Not Correlate With Proliferation. J Invest Dermatol 106:1281–1286.

54. Kohri K, Yasui T, Okada A. 2012. Biomolecular mechanism of urinary stone formation involving osteopontin 623–637.

CHAPTER 3

p38MAPK plays a crucial role in stromal mediated tumorigenesis

Elise Alspach, Kevin C. Flanagan, Xianmin Luo, Megan K. Ruhland, Hui Huang, Ermira Pazolli, Maureen J. Donlin, Timothy Marsh, David Piwnica-Worms, Joseph Monahan, Deborah V. Novack, Sandra S. McAllister, and Sheila A. Stewart

Kevin C. Flanagan was a contributing author to this work.

This chapter was originally published in 2014 in *Cancer Discovery*

INTRODUCTION

The critical role the tumor microenvironment (TME) plays in disease is underscored by findings that changes within stromal cells can predict clinical outcome (1-3). For this reason, many groups have focused on how various stromal cell types impact tumorigenesis. For example, activated fibroblasts isolated from carcinomas (cancer-associated fibroblasts or CAFs) promote preneoplastic cell growth and increase tumor cell migration, invasion, and angiogenesis (4). Likewise, senescent fibroblasts, which are also found in human tissue (5), support tumorigenesis through the promotion of growth, invasion, and angiogenesis (6-8). Intriguingly, both senescent fibroblasts and CAFs express a plethora of pro-tumorigenic factors and in senescent cells this is referred to as the senescence-associated secretory phenotype (SASP) (6, 9).

There is significant overlap between the pro-tumorigenic factors expressed in CAFs and senescent cells. Expression array analyses of human fibroblasts treated with granulin, which renders a CAF-like phenotype (10), and fibroblasts isolated from human tumors reveal that both populations express SASP factors ((11, 12) and reviewed in (13)). In addition, CAFs isolated by laser capture micro-dissection (LCM) or via cell surface marker expression similarly display SASP factor expression (1-4, 14). Finally, cells that fail to enter senescence following exposure to a senescence-inducing stress robustly express SASP factors (15, 16), indicating that entrance into senescence is not a prerequisite for SASP expression. Together, these observations raise the possibility that the mechanisms that govern SASP expression are conserved in many tumor-promoting fibroblasts and are not dependent upon the induction of senescence. Thus,

identifying mechanisms that activate and sustain SASP expression will have a profound impact on our understanding of the development of a pro-tumorigenic TME and the identification of novel therapeutic targets.

Despite the profound impact the pro-tumorigenic SASP has on tumor cell growth and progression, the mechanisms that lead to its activation and maintenance remain poorly understood. The majority of regulatory pathways elucidated thus far have focused on SASP factor transcription, specifically by NFκB and C/EBPβ (15-19). NFκB's transcriptional activation of the SASP is dependent on the mitogen-activated protein kinase p38 (p38MAPK) and the DNA-damage response protein ATM (19). However, in other systems p38MAPK facilitates expression of cytokines including IL6 by impacting post-transcriptional mRNA stability, possibly through the RNA binding-protein AUF1 (20-22). Post-transcriptional regulation of the SASP by p38MAPK has yet to be investigated.

Given the importance of the SASP on stromal-supported tumorigenesis, we investigated the impact of p38MAPK on SASP-mediated tumor promotion. We demonstrate that inhibition of p38MAPK activity abrogates the tumor promoting capacity of senescent fibroblasts. Furthermore, inhibiting p38MAPK in CAFs inhibits their tumor promoting abilities, demonstrating for the first time that regulatory mechanisms elucidated in senescent stroma are applicable in CAFs. Finally, we elucidate a p38MAPK-dependent post-transcriptional SASP regulatory pathway that modulates RNA-binding protein activity.

METHODS

Cell lines and treatments

BJ human foreskin fibroblasts were obtained from Dr. Robert Weinberg (Massachusetts Institute of Technology, Cambridge, MA) and were cultured as previously described (23). IMR90 human lung fibroblasts were purchased from ATCC (Manassas, VA) and were cultured in Dulbecco's Modified Eagle's Medium (DMEM) supplemented with 10% FBS (Sigma, St. Louis, MO) and 1% penicillin/streptomycin. Patient-derived breast cancer-associated fibroblasts were purchased from Asterand (Detroit, MI) and cultured in DMEM supplemented with 10% FBS, 1 μg/mL hydrocortisone, 5 μg/mL transferrin, 5 μg/mL insulin, and 1% penicillin/streptomycin. Fibroblasts were treated with bleomycin sulfate (100 μg/mL, Sigma, St. Louis, MO) for 24 hours, followed by incubation in normal culture medium for the time points indicated. Fibroblasts were treated with actinomycin D (10 μg/mL, Sigma, St. Louis, MO) for 24 hours, SB203580 (10 μM, Millipore, Billerica, MA) for 48 hours, or CDD-111 (also referred to as SP-006, 1 μM, Confluence Life Sciences, St. Louis, MO) for 48 hours unless indicated otherwise. SB203580 and CDD-111 were replenished daily. Fibroblasts were treated with 2 fresh changes of 4 mM sodium butyrate (NaB, Sigma, St. Louis, MO) for 72 or 120 hours. RNA was isolated using TRI Reagent (Life Technologies, Carlsbad, CA) at the time points indicated. HaCaT preneoplastic keratinocyte cells (obtained from Dr. Norbert E. Fusenig, German Cancer Research Center, Heidelberg, Germany) stably expressing click beetle red (CBR) luciferase (HaCat-CBR) (16) were grown in DMEM supplemented with 10% heat-inactivated FBS and 1% penicillin/streptomycin (Sigma, St. Louis, MO).

BPH1 preneoplastic prostate epithelial cells (obtained from Dr. Robert Weinberg, Massachusetts Institute of Technology, Cambridge, MA) stably expressing CBR luciferase (BPH1-CBR) were growth in DMEM supplemented with 10% non-heat inactivated FBS and 1% penicillin/streptomycin. All cells were cultured at 37 °C in 5% carbon dioxide and 5% oxygen. No cell lines used were authenticated.

Plasmids

The luciferase reporter construct fused to the 3' UTR of IL6 (lucIL6) was a gift from Dr. Nicholas Davidson (Washington University School of Medicine, St. Louis, MO) and was subcloned into the *Eco*RI site of pBABE-hygro. Luciferase reporter constructs fused to the 3' UTR of GMCSF or GAPDH were purchased from Switch Gear Genomics (Menlo Park, CA) and were subcloned in to pBABE-hygro using the *Sna*bI and *Sal*I restriction sites. Short hairpin RNA sequences targeting human AUF1 (shAUF1A: 5'-AGAGTGGTTATGGGAAGGTAT-3', shAUF1B: 5'-AGTAAGAACGAGGAGGATGAA-3'), p38 (5'-GCCGTATAGGATGTCAGACAA-3') and Hsp27 (5-CCCGGACGAGCTGACGGTCAA-3') were obtained from the Children's Discovery Institute's viral vector-based RNAi core at Washington University in St. Louis, and were supplied in the pLKO.1-puro backbone. Luciferase reporter assays were performed using a plasmid containing an NFκB-responsive promoter driving expression of firefly luciferase (NFκB-luc) and a plasmid encoding *Renilla* luciferase driven by the thymidine kinase promoter, obtained from Dr. David Piwnica-Worms (Washington University School of Medicine, St. Louis, MO).

Senescence-associated β-galactosidase (SA-β-gal) staining

SA-β-gal staining was carried out as described previously (23).

Quantitative PCR

cDNA synthesis and quantitative PCR was performed using previously published protocols and manufacturers' instructions (42) (SYBR Green, Life Technologies, Carlsbad, CA). Primers for GAPDH (F: 5'-GCATGGCCTTCGGTGTCC-3', R: 5'-AATGCCAGCCCCAGCGTCAAA-3'), IL6 (F: 5'-ACATCCTCGACGGCATCTCA-3', R: 5'-TCACCAGGCAAGTCTCCTCA-3'), IL8 (F: 5'-GCTCTGTGTGAAGGTGCAGT-3', R: 5'-TGCACCCAGTTTTCCTTGGG-3'), MMP3 (F: 5'-GTTTTGGCCCATGCCTATGCCCC-3', R: 5'-GGAGTCAGGGGGAGGTCCATAGAGG-3'), CCL20 (F: 5'-CTGCGGCGAATCAGAAGCAGC-3', R: 5'-CCTTCATTGGCCAGCTGCCGT-3'), lucIL6 (F: 5'-CGGGCGCGGTCGGTAAAGTT-3', R: 5'-AAACAACAACGGCGGCGGGA-3'), and lucGMCSF and lucGAP (F: 5'-GAGAAACATGCGGAGAACGC-3', R: 5'-AGCATGCACGATAGCCTTGA-3') were purchased from IDT. GMCSF cDNA was amplified using a Taqman probe/primer set (catalog number Hs00929873_m1, Life Technologies, Carlsbad, CA).

ELISA

Conditioned medium was generated by incubating cells for 24 hours in serum-free medium. Following collection, secreted IL6 protein levels were measured using the human IL6 Quantikine ELISA kit (catalog number D6050, R&D Systems, Minneapolis, MN).

Western blot analysis

Cell pellets were lysed in buffer containing 50 mM Tris pH 8.0, 5 mM EDTA, 0.5% NP40 and 100 mM sodium chloride for 20 minutes at 4 °C. Protein concentration was quantified using the Bradford Protein Assay (Bio-Rad, Berkeley, CA). The primary antibodies used were: polyclonal AUF1 (Millipore, Billerica, MA, catalog number 07260MI) at 1:3000, polyclonal p-p38 (PhosphoSolutions, Aurora, CO, catalog number p190-1802) at 1:1000, polyclonal p38 (Cell Signaling, Boston, MA, catalog number 9218) at 1:1000, monoclonal β-catenin (BD Biosciences, San Jose, CA, catalog number 610153) at 1:5000, and monoclonal α-tubulin (Abcam, Cambridge, MA, product number ab6160) at 1:1000. All secondary antibodies from the appropriate species were horseradish peroxidase-conjugated (Jackson Laboratories, Bar Harbor, ME) and diluted 1:10000.

Virus Production

Virus was produced as described previously (23).

RNA-binding protein immunoprecipitation (RIP)

Cell pellets from $7x10^7$ BJ fibroblasts were lysed in the same buffer used for western blot analysis. Protein concentration was analyzed using the Bradford Protein Assay (Bio-Rad, Berkeley, CA). Three mg of protein was used for each immunoprecipitation. The following primary antibody was used: 30 µg of polyclonal AUF1 (Millipore, Billerica, MA, catalog number 07260MI). Equivalent amounts of normal IgG antibody (Cell Signaling, Boston, MA) were used to control for specific immunoprecipitation. Cell

lysates were pre-cleared with 20 µL protein A Dynabeads (Life Technologies, Carlsbad, CA) for 30 minutes at 4 °C prior to immunoprecipitation. 100 µL Protein A Dynabeads were used for each immunoprecipitation. Beads were washed 3 times in 0.1 M monosodium phosphate and then incubated in 0.1 M monosodium phosphate with the appropriate antibody for at least 1 hour at room temperature. Beads were then washed 3 times in Buffer A (1x PBS, 0.1% SDS, 0.3% sodium deoxycholate, 0.3% NP40), followed by incubation for 30 minutes at room temperature in NT2 buffer (50 mM Tris pH 7.4, 150 mM sodium chloride, 1 mM magnesium chloride). Antibody-bound beads were then added to pre-cleared cell lysates, and immunoprecipitated overnight at 4 °C. 100 µL of cell lysate was removed from the IgG immunoprecipitation to be used for input controls. Immunoprecipitated beads were washed 2 times with each of the following buffers: Buffer A, Buffer B (5x PBS, 0.1% SDS, 0.5% sodium deoxycholate, 0.5% NP40) and Buffer C (50 mM Tris pH 7.4, 10 mM magnesium chloride, 0.5% NP40). Beads were then resuspended in NT2 containing 0.1% SDS, 80 U RNase OUT (Life Technologies, Carlsbad, CA), and 30 µg Proteinase K and incubated at 55 °C for 30 minutes. RNA was isolated from the beads by adding 1 mL of TRI Reagent (Life Technologies, Carlsbad, CA). Following cDNA synthesis, mRNA levels of SASP factors were analyzed by qPCR using the primers and procedures described above.

Luciferase reporter assay

BJ fibroblasts were transiently transfected with plasmids encoding NFκB-luc and *Renilla* luciferase. *Renilla* luciferase expression was used to standardize for transfection efficiency. Transfection was performed using manufacturer's protocol for the

Lipofectamine 2000 reagent (Life Technologies, Carlsbad, CA). Luciferase activities were measured 48 hours post-transfection using live cell imaging as described (43).

Co-culture

Co-culture experiments were performed as previously described with the following modifications (23). 1.3×10^4 fibroblasts were plated in black-walled 96 well plates (Fisher Scientific, Pittsburgh, PA). Cells were incubated in starve medium (DMEM + 1% penicllin/streptomycin) for 3 days before the addition of HaCat-CBR cells. SB203580 was refreshed daily until HaCaT-CBR plating. HaCat-CBR cells were cultured in starve medium for 24 hours prior to plating on fibroblasts. 1.0×10^3 HaCat-CBR cells were plated on fibroblasts and incubated for the indicated length of time. At the times indicated, D-luciferin (Biosynth, Naperville, IL) was added to a final concentration of 150 µg/mL. After ten minutes, plates were imaged using an IVIS 100 camera (PerkinElmer, Downers Grove, IL) using the following settings: exposure=10 s–5 min, field of view=15, binning=16, f/stop=1, open filter.

Xenografts

$1x10^6$ BPH1-CBR preneoplastic prostate epithelial cells were co-injected with $1x10^6$ BJ human foreskin fibroblasts. Cells were injected subcutaneously in a 50:50 mixture of DMEM:growth factor-reduced Matrigel (BD Biosciences, San Jose, CA) into the rear flanks of female NcR nude mice (Taconic, Germantown, NY). *In vivo* bioluminescence imaging was performed on the days indicated on an IVIS 100 (PerkinElmer, Downers Grove, IL; Living Image 3.2, 1–60 s exposures, binning 4, 8 or, 16, FOV 15 cm, f/stop 1,

open filter) following IP injection of D-luciferin (150 mg/kg; Biosynth, Naperville, IL). For analysis, total photon flux (photons/sec) was measured from a fixed region of interest over the xenografts using Living Image 2.6 (PerkinElmer, Downers Grove, IL).

RNA Sequence Analysis

Total RNA was isolated using TRI Reagent (Life Technologies, Carlsbad, CA) and the RiboPure RNA isolation kit (Life Technologies, Carlsbad, CA) following the manufacturer's instructions. Ribosomal RNA was removed by poly-A selection using oligo-dT beads. mRNA was then fragmented and reverse transcribed to yield double stranded cDNA using random hexamers. cDNA was blunt ended, had an A base added to the 3' ends, and then had Illumina sequencing adapters ligated to the ends. Ligated fragments were then amplified for 12 cycles using primers incorporating unique index tags. Fragments were sequenced on an Illumina HiSeq-2000 (San Diego, CA) using single reads extending 50 bases. Raw data was de-multiplexed and aligned to the reference genome using TopHat. Transcript abundances were then estimated from the alignment files using Cufflinks. EdgeR was used for differential expression analysis.

Generation of CAFs

Primary breast tissue was collected without patient identifiers in compliance with a protocol approved by the Brigham and Women's Hospital (Institutional Review Board 93-085). Fibroblasts were isolated (10, 11) and immortalized through expression of hTERT-GFP (44) as previously described.

To generate cancer-associated fibroblasts (CAFs), $3x10^6$ human mammary fibroblasts were co-injected with $1x10^6$ MCF7-Ras tumor cells subcutaneously into nude mice. After tumors reached 1 cm, mice were euthanized and CAFs were re-isolated by digesting tissues in 1 mg/ml collagenase A for 1-4 hours at 37 °C with continuous rotation. Resulting cell suspensions were dispersed with an 18-gauge needle, washed 2 times with resuspension buffer (2% heat-inactivated fetal calf serum in sterile Hank's Balanced Salt Solution (HBSS)), and filtered through 70 m nylon mesh. GFP+ CAFs were then isolated by fluorescence-activated cell sorting and maintained under their standard culture conditions. CAFs were confirmed to be human by staining with human specific mitochondrial DNA (data not shown).

Oral dosage of p38MAPK inhibitor

The p38MAPK small molecule inhibitor CDD-111 (Confluence Life Sciences, Inc, St. Louis, MO) was compounded at 516 ppm with Purina Rodent Chow #5001 (St. Louis, MO) to generate a daily exposure of 80 mg/kg/day. Female NcR nude mice (Taconic, Germantown, NY) were fed ad libitum.

LPS challenge and TNFα ELISA

Female NcR nude mice (Taconic, Germantown, NY) were fed ad libitum for 3 days. 100 ng lipopolysaccharide (LPS) (Sigma, St. Louis, MO) was then administered by IP injection. Serum was collected 1 hour after LPS dosage. TNFα levels were analyzed by ELISA (R&D Systems, Minneapolis, MN)

Staining of xenograft tumors

Following excision, tumors were fixed in 10% formalin and embedded in paraffin for sectioning. Standard H&E technique was used for all sections. Serial sections were stained for Ki67 (1:50, catalog number 550609, BD Bioscience, San Jose, CA), p16 (1:100, catalog number sc-1661, Santa Cruz Biotechnology, Dallas, TX) and vimentin (1:700, catalog number ab45939, Abcam, Cambridge, MA).

Statistical Analysis

Data is presented as the mean ± SEM. Statistical significance was determined using the Student's *t* test, with a p value < 0.05 considered significant. Percent mRNA remaining was calculated as the fold mRNA in ActD-treated SIPS cells over untreated SIPS cells. Overrepresented gene ontology terms in the expression data were identified using a Fisher's exact test, with a significance threshold of $p < 0.05$ as implemented in GOstat (45).

RESULTS

p38MAPK activity controls the pro-tumorigenic properties of the SASP

SASP factors promote preneoplastic cell growth (6-8, 23, 24) and p38MAPK contributes significantly to the initiation of SASP factor expression (25). To confirm this, senescent fibroblasts (fibroblasts staining positive for senescence-associated β-gal, **Supplemental Fig. 3.1A**) were treated with a highly specific small-molecule inhibitor of p38MAPK (SB203580) (26). Hsp27 is a direct downstream target of p38MAPK. Therefore, to confirm that our treatment inhibited the kinase activity of p38MAPK, we measured

Hsp27 phosphorylation by Western blot analysis. We found that SB203580 treatment led to a reduction in Hsp27 phosphorylation, indicating successful inhibition of p38MAPK activity (**Fig. 3.1A**). As expected, SB203580 treatment of senescent fibroblasts resulted in a significant reduction in the expression of SASP factors IL6, IL8, and GMCSF (**Fig. 3.1B**). To determine if p38MAPK activity was responsible for the tumor-promoting activities of senescent cells, we performed co-culture experiments with normal human fibroblasts induced to senesce by treatment with bleomycin (referred to throughout as stress-induced premature senescence, SIPS) and preneoplastic HaCaT keratinocyte cells expressing click beetle red (CBR) luciferase (HaCaT-CBR) (23). Prior to the addition of HaCAT-CBR cells, fibroblasts were treated with vehicle or SB203580 as indicated in **Fig. 3.1C**. Senescent fibroblasts treated with vehicle increased the growth of HaCaT-CBR cells compared to HaCaT-CBR cells cultured with young fibroblasts (**Fig. 3.1D**), recapitulating our previously published observations (15, 23). However, while inhibition of p38MAPK had no effect on HaCAT-CBR cells grown in the absence of fibroblasts (**Supplemental Fig. 3.1B**), we found that p38MAPK inhibition reduced the pro-tumorigenic activity of senescent fibroblasts by significantly reducing HaCaT-CBR cell growth (**Fig. 3.1D**).

Given the potent impact of p38MAPK inhibition in co-culture experiments, we next examined the impact of p38MAPK depletion on preneoplastic cell growth in xenograft experiments. P38MAPK was depleted from senescent fibroblasts (**Fig. 3.1E**), resulting in a significant reduction in the level of p38MAPK-dependent SASP factor IL8 (**Fig. 3.1F**). To assess the impact of p38MAPK loss *in vivo*, young, senescent, or p38MAPK-

depleted senescent fibroblasts were admixed with the preneoplastic epithelial cell line BPH1 expressing CBR luciferase (BPH1-CBR) and injected subcutaneously into nude mice. Tumor growth was analyzed by bioluminescence imaging. As expected, senescent fibroblasts increased BPH1-CBR cell growth relative to young fibroblasts (**Fig. 3.1G**). However, depletion of p38MAPK and subsequent reduction in p38MAPK-dependent SASP factor expression reduced tumor growth to the level observed when BPH1-CBR cells were co-injected with young fibroblasts (**Fig. 3.1G**). These results indicate that expression of p38MAPK-dependent SASP factors within the TME plays a pivotal role in preneoplastic cell growth *in vivo*.

The pro-tumorigenic SASP is subject to post-transcriptional regulation

We next sought to elucidate the mechanism by which p38MAPK regulates pro-tumorigenic SASP factor expression. Previous work demonstrated that p38MAPK modulates NFκB-driven transcription of SASP factors including IL6 and IL8 (19). To determine that the effects of p38MAPK inhibition were transcriptionally based, senescent fibroblasts were treated with the transcription inhibitor actinomycin D (ActD) at several time points following bleomycin treatment. SASP factor expression was significantly inhibited when cells were treated with ActD 24 hours after bleomycin treatment (**Fig. 3.2A**), a time point at which SASP factor mRNA was increased (**Supplemental Fig. 3.2A**), but cells were not yet senescent (**Supplemental Fig. 3.1A**). These results indicate that at this time point SASP factor expression is dependent on transcription. Surprisingly, at 96 hours after bleomycin treatment, when cells displayed morphological features characteristic of senescence including staining positive for SA-β-

gal (**Supplemental Fig. 3.1A**), treatment with ActD failed to reduce SASP factor mRNA levels (**Fig. 3.2A**). These changes in mRNA were also reflected at the protein level. Indeed, we found that IL6 protein levels in conditioned medium collected from cells treated with ActD at 24 hours fell drastically compared to untreated cells. In contrast, when cells were treated with ActD at 96 hours, IL6 protein levels remained high (**Fig. 3.2B**). Given p38MAPK inhibition at the later time point significantly reduced SASP expression (**Fig. 3.1B**), these findings raised the possibility that p38MAPK impacts SASP factor mRNA stability rather than NFκB-driven transcriptional activation upon the acquisition of senescence. To confirm that p38MAPK had no effect on NFκB-driven transcription at the later time point, normal human fibroblasts were transduced with an NFκB transcription reporter plasmid driving expression of luciferase (NFκB-luc). Transduced cells were treated with bleomycin, and 72 hours later senescent cells were treated with the p38MAPK inhibitor SB203580 for an additional 48 hours. As expected, when SB203580 treatment was initiated 72 hours after bleomycin treatment, there was no significant effect on NFκB transcriptional activity (**Fig. 3.2C).** These results indicate that after the establishment of senescence, p38MAPK has a profound effect on SASP factor mRNA stability.

To address whether SASP factor mRNA stability was affected in cells undergoing replicative senescence or other types of stress-induced senescence, normal human fibroblasts were induced to senesce through telomere dysfunction (replicative senescence, RS) or treatment with the histone deacetylase inhibitor sodium butyrate (NaB). Cells undergoing RS or NaB-induced senescence robustly induced expression

of SASP factors, including IL6 and IL8 (**Supplemental Fig. 3.2B and Supplemental Fig. 3.2C, respectively**). Further, we found that SASP factor mRNAs were significantly stabilized in cells that had undergone RS or NaB-induced senescence (**Fig. 3.2D and Supplemental Fig. 3.2D, respectively**). Significantly, SASP factor mRNA stabilization was not limited to skin fibroblasts; when IMR90 human lung fibroblasts were treated with bleomycin, they displayed a similar increase in SASP factor mRNA stability 96 hours post-bleomycin treatment (**Supplemental Fig. 3.2E**). Together, these data indicate that SASP factor mRNAs are stabilized by a post-transcriptional regulatory program that is active in fibroblasts from diverse tissues, regardless of the mechanism through which senescence is induced.

p38MAPK post-transcriptionally regulates the SASP

Our results indicate that p38MAPK inhibition reduces SASP expression and TME-dependent promotion of tumorigenesis but does not affect the activity of the primary transcriptional regulator of the SASP, NFκB, following induction of senescence. Interestingly, p38MAPK post-transcriptionally regulates IL6 and IL8 in other contexts (20, 21). Thus, we investigated p38MAPK's role in stabilizing SASP factor mRNA. We first examined whether p38MAPK was active throughout the time course under investigation. To assess p38MAPK activation, lysates were prepared from cells 24 or 96 hours after bleomycin treatment and examined for phosphorylated p38MAPK (p-p38) by Western blot analysis. In agreement with previous findings (19), we observed that phosphorylated p38MAPK increased from 24 to 96 hours following bleomycin treatment (**Supplemental Fig. 3.2F**). These kinetics were consistent with SASP factor mRNA

stabilization, suggesting that p38MAPK activation regulates SASP factor mRNA stability.

To elucidate p38MAPK's role in regulating SASP factor mRNA stabilization, normal human fibroblasts depleted of p38MAPK (shp38) were treated with ActD 24 or 96 hours after bleomycin treatment (**Fig. 3.2E**). When treated with ActD 24 hours after bleomycin treatment, cells expressing shSCR or shp38 displayed decreased SASP mRNA stability, indicating that p38MAPK does not post-transcriptionally regulate SASP mRNAs at this time point. As expected, both IL6 and IL8 mRNA stability increased when shSCR control cells were treated with ActD 96 hours after bleomycin treatment, although not to the same extent as that observed in non-transduced fibroblasts. In contrast, when shp38 cells were treated with ActD 96 hours post-bleomycin treatment, they displayed significantly reduced IL6 and IL8 mRNA stability when compared to cells expressing the control hairpin (shSCR) (**Fig. 3.2E**). Similar results were obtained with a second independent shRNA targeting p38MAPK (data not shown).

The 3' UTRs of SASP factor transcripts control mRNA stabilization in stromal cells

We next examined the mechanisms by which SASP factor mRNA was stabilized. The 3' untranslated region (UTR) of many mRNAs contains protein binding motifs that alter mRNA stability under diverse biological stimuli (27). To determine whether the 3' UTRs of SASP factor mRNAs govern post-transcriptional regulation, we utilized a luciferase reporter cDNA fused to the 3' UTR of IL6 (lucIL6) or GMCSF (lucGMCSF). A luciferase

reporter cDNA fused to the 3' UTR of GAPDH (lucGAP) was used as a control. Normal human fibroblasts were stably transduced with the luciferase reporter constructs and luciferase mRNA levels were monitored in response to ActD at the time points indicated (**Fig. 3.3A**). Similar to our observations with the endogenous IL6 and GMCSF transcripts, we observed that the stability of the lucIL6 and lucGMCSF transcripts increased significantly when treated with ActD 96 hours compared to 24 hours after bleomycin treatment (**Fig. 3.3A**). As expected, there was no significant change in the stability of the lucGAP transcript (**Fig. 3.3A**), indicating that 3' UTR-dependent mRNA stabilization was specific for SASP factor mRNA and did not extend to all mRNAs in response to senescence. These results indicate that the 3' UTR of SASP factor transcripts mediates increases in mRNA stability.

AUF1 directly binds to SASP factor mRNA and modulates their stabilization

AUF1 is a protein that binds the 3' UTRs of many mRNAs including IL6, IL8, and GMCSF and reduces their stability (28-30). Furthermore, p38MAPK is known to impact AUF1 activity in other settings (22), although a link between AUF1 and p38MAPK in the post-transcriptional regulation of IL6 and IL8 has not been demonstrated. To examine AUF1 binding to SASP factor mRNA in response to senescence, we utilized RNA-binding protein immunoprecipitation (RIP) to examine AUF1 binding to SASP factor mRNAs in response to senescence. Cell lysates were collected 24 and 96 hours after bleomycin treatment and subjected to immunoprecipitation with either an AUF1-specific antibody or a nonspecific IgG; mRNA levels were normalized to the levels of each transcript measured in the input fractions. We observed that AUF1 occupancy on IL6

and IL8 mRNAs significantly decreased from 24 to 96 hours after bleomycin treatment (**Fig. 3.3B**), corresponding with the increase in mRNA stability observed in **Fig. 3.2**. We observed similar results for GMCSF and CCL20 mRNA, indicating that this mechanism impacts many SASP factor mRNAs (**Fig. 3.3B**). This observation suggests that decreased AUF1 binding leads to increased mRNA stability once senescence is established.

We next sought to determine whether AUF1 was required to destabilize SASP mRNAs. To address this question, we stably transduced normal human fibroblasts with two independent short-hairpin RNA (shRNA) constructs targeting AUF1 (shAUF1a and shAUF1b) (**Fig. 3.3C**). AUF1-depleted cells were treated with bleomycin and 24 hours later treated with ActD, a time at which AUF1 is bound to SASP factor mRNAs displaying reduced stability (**Fig. 3.3B**). In contrast to control cells, we found that AUF1 depletion significantly increased the stability of IL6 and IL8 mRNA at the early time point when these mRNAs are normally unstable (**Fig. 3.3D**). These data demonstrate that before senescence is established, AUF1 destabilizes SASP mRNAs by binding to their 3' UTRs.

To address whether the impact of p38MAPK on SASP mRNA stabilization was due to modulation of AUF1–SASP mRNA binding, we carried out RIP analysis. Following bleomycin treatment, normal human fibroblasts were treated with SB203580 or vehicle control as described in **Fig. 3.3E**. In contrast to control cells in which AUF1 occupancy decreased at the late time point, there was no decrease in AUF1 occupancy on IL8

mRNA in p38MAPK-inhibited cells collected 96 hours after bleomycin treatment (**Fig. 3.3E**). Similar results were obtained for IL6 (data not shown). These observations indicate that p38MAPK activation is required to release AUF1 from SASP factor mRNA. Further, these studies suggest that loss of SASP factor mRNA stabilization in p38MAPK inhibited cells (**Fig. 3.2**) is the result of a failure to remove AUF1 from SASP factor transcripts.

p38MAPK-dependent factors are expressed in the TME of breast cancer lesions

The TME plays a pivotal role in tumor progression, and recent expression analyses indicate that TME-specific expression changes are predictive of clinical outcome (1-3). Both senescent fibroblasts and CAFs express pro-tumorigenic SASP factors, raising the intriguing possibility that the regulatory mechanisms that control SASP expression in senescent cells also operate in cancer-associated stroma. Given the importance of p38MAPK in SASP factor expression**,** we carried out a meta-analysis to establish a list of p38MAPK-regulated genes in senescent fibroblasts and evaluated their expression in the TME of human breast cancers (**Fig. 3.4A**). We performed RNA sequence analysis (RNA-seq) of young, senescent, and p38MAPK-inhibited senescent human fibroblasts and observed that IL6 and IL8 expression was p38MAPK-dependent. Along with previously identified factors, we found that 50 additional SASP factors were p38MAPK-dependent, including GMCSF, GCSF, IL1α, IL1β, CXCL1, CXCL2, CXCL5, CCL20, MMP1, and MMP7 (**Supplemental Table 3.1, Fig. 3.4A**). A subset of these factors was validated by qRT-PCR (**Supplemental Fig. 3.3A**). Gene ontology (GO) process analysis performed on the p38MAPK-dependent factors demonstrated that genes

related to the regulation of inflammation, chemotaxis, cell adhesion, angiogenesis, and proliferation were significantly enriched in this gene set (**Fig. 3.4B**).

We next compared our p38MAPK-dependent SASP list to factors significantly over-expressed in the TME of breast cancer (BC) lesions. We examined three data sets generated from microarray analyses of normal stroma versus cancer-associated stroma that had been obtained by laser capture micro-dissection of breast tissue (1-3) (**Fig. 3.4A**). Of the 50 p38MAPK-dependent factors identified in senescent fibroblasts, we found that 29 were expressed in the stroma of the Finak breast cancer dataset (1), including CXCL2 and IL24. Seventeen factors were expressed in the TME of the Ma breast cancer data set (2), including IL1β. Finally, 7 factors overlapped with the Karnoub breast cancer data set (3), including CCL20 (**Supplemental Table 3.1)**. Furthermore, CCL20, CXCL5, IL11, IL1β, IRAK3, MMP1, MPP7, and SOD2 were expressed in the BC-associated stromal compartment of at least two studies (**Fig. 3.4C**). Of note, CCL20, CXCL5, IL11, IL1β, and MMP1 are factors with known pro-tumorigenic activities (31-35). We observed that BC-associated stromal genes compose a large percentage of the total number of p38MAPK-dependent SASP factors involved in the regulation of inflammation, chemotaxis, angiogenesis, and cell adhesion based on GO process analyses (**Fig. 3.4B**). Given that these factors are associated with disease progression, our findings raise the possibility that anti-p38MAPK therapy could significantly impact tumor progression in humans.

Inhibition of p38MAPK abrogates the pro-tumorigenic activities of CAFs

Expression of p38MAPK-dependent factors within the stroma of breast cancer lesions raised the possibility that they contribute to the tumor promoting activities of CAFs. Therefore, we examined whether inhibition of p38MAPK would abrogate the tumor-promoting activities of CAFs as it did for senescent fibroblasts. To generate CAFs, we obtained normal human mammary fibroblasts from reduction mammoplasty (NMF), admixed them with MCF7-Ras breast carcinoma cells and injected the cell mixture into immunocompromised mice and allowed tumors to grow. Human CAFs were isolated from these tumors and we assessed their tumor-promoting potential by co-culturing them with preneoplastic HaCaT skin keratinocytes expressing CBR luciferase (HaCaT-CBR). As expected, CAFs significantly stimulated HaCaT-CBR cell growth compared to HaCaT-CBR cells cultured with parental NMF fibroblasts (**Fig. 3.4D**). To investigate the importance of p38MAPK-dependent CAF factors, we inhibited p38MAPK in CAFs with SB203580 and assessed their ability to promote preneoplastic cell growth. Similar to what we observed when senescent fibroblasts were treated with the p38MAPK inhibitor SB203580 (**Fig. 3.1C**), CAFs treated with SB203580 failed to promote HaCaT-CBR cell growth (**Fig. 3.4D**). These results indicate that p38MAPK regulates the tumor-promoting activity of CAFs. Together with our meta-analysis and expression of p38MAPK-dependent genes in the stromal compartment of human breast cancer lesions, these observations suggest that p38MAPK plays a central role in sustaining the expression of tumor-promoting factors. Thus, stromal p38MAPK represents a novel therapeutic target for senescent and non-senescent cancer-associated stromal compartments in breast cancer.

p38MAPK inhibition compromises the tumor-promoting capacity of the microenvironment

The critical importance of SASP factor expression in our tumor models and our work to uncover the mechanisms that sustain SASP factor expression identified p38MAPK as a central player in SASP expression in senescent cells as well as in CAFs. Given our findings that p38MAPK-dependent factors are expressed in human breast cancer lesions, we evaluated the feasibility of targeting p38MAPK in a preventative and therapeutic setting. Several p38MAPK inhibitors have entered phase II clinical trails for rheumatoid arthritis and thus have proven safe in a nonlethal disease (36, 37). We obtained a p38MAPK inhibitor (CDD-111, also referred to as SD-0006 (38), Confluence Life Sciences) and compounded it into mouse chow. CDD-111 was chosen because it can be orally administered and shows high specificity for the p38MAPK α subunit (38). Indeed, extensive analysis of CDD-111 revealed that it is selective for p38MAPK α over fifty other kinases including p38MAPK β, γ, and δ. Furthermore, the IC_{50} for inhibiting tumor necrosis factor-α (TNFα) release *in vitro* and *in vivo* was less than 200 nM (38). Treatment of senescent cells with CDD-111 *in vitro* revealed that it effectively reduced SASP expression as evidenced by a significant reduction in IL6 and IL8 levels (data not shown).

To establish the impact of orally administered CDD-111 on p38MAPK activity in our system, mice were placed on CDD-111 (p38i) or control chow for three days, challenged with LPS, and serum TNFα levels were measured. We found that mice receiving oral p38i failed to mount a robust TNFα response following an LPS challenge

compared to animals receiving control chow (**Supplemental Fig. 3.3B**). We also verified that p38i inhibited SASP expression *in vivo*. Senescent normal human fibroblasts were injected subcutaneously into the rear flanks of nude mice maintained on control or p38i chow. Ten days after injection the cells were removed, RNA was isolated, and the levels of human IL8 were analyzed by qRT-PCR. Senescent fibroblasts isolated from mice on p38i had significantly less IL8 mRNA than senescent fibroblasts isolated from mice on control chow (**Fig. 3E**), demonstrating that CDD-111 inhibited SASP expression *in vivo*.

We next evaluated the p38MAPK inhibitor's efficacy in a xenograft setting. BPH1-CBR cells admixed with young or senescent fibroblasts were subcutaneously injected into mice maintained on control or p38i chow (**Fig. 3.4F**). Bioluminescence analysis of tumor growth revealed that p38i significantly reduced the growth of BPH1-CBR cells co-injected with senescent fibroblasts (**Fig. 3.4G & H**). Analysis of cellular proliferation (Ki67 staining) revealed that senescent fibroblasts significantly increased BPH1 cell proliferation compared to when BPH1 cells were co-injected with young fibroblasts (**Fig. 3.5A**). Importantly, the increase BPH1 proliferation that was noted in the presence of senescent fibroblasts was markedly reduced when mice were maintained on p38i versus control chow (**Fig. 3.5A**). These data demonstrate that the reduced tumor size observed in response to p38i administration was a result of decreased epithelial cell proliferation. Importantly, the difference in epithelial cell proliferation between tumors containing senescent stroma from p38i- and control-fed mice was not due to differences in stromal composition between these tumor types, as staining for a senescence

marker, p16, and a fibroblast marker, vimentin, demonstrated that 1) senescent fibroblasts persisted throughout the time course of the experiment regardless of p38MAPK inhibition and 2) the stromal composition of treated and untreated tumors was similar. Vascularity and myeloid infiltration were also investigated in these tumors. No significant differences in either vascularity or leukocyte infiltration were noted (data not shown). Administration of CDD-111 to mice injected with BPH1 cells admixed with young fibroblasts also resulted in a decrease in epithelial cell growth, although not to the same extent as that observed in tumors containing senescent fibroblasts. Oral administration of CDD-111 had no significant impact on BPH1-CBR cells injected alone (data not shown).

To address the effectiveness of p38MAPK inhibition in a therapeutic setting, mice were injected with BPH1-CBR cells admixed with senescent fibroblasts and tumors were allowed to grow for one week until the average tumor volume reached 74 mm^3. Mice were then administered control or p38i chow and bioluminescence imaging was used to monitor tumor growth. Significantly, tumor growth was arrested in mice receiving p38i. In contrast, tumors in mice receiving control chow continued to show significant growth (**Fig. 3.5B**).

To investigate the applicability of orally administered p38i in CAF-containing microenvironments, we obtained primary CAFs (pCAFs) from a lesion removed from a patient with invasive breast cancer. We subcutaneously injected BPH1 cells alone or BPH1 cells admixed with pCAFs into nude mice fed either control or p38i chow as

described for the experiments in **Fig. 3.4F**. As expected, there was no difference in BPH1 cell growth whether mice were fed control or p38i chow (**Fig. 3.5C**). Importantly, in mice receiving control chow, BPH1 cells admixed with pCAFs grew significantly more than BPH1 cells injected alone, verifying that our patient-derived fibroblasts were *bona fide* CAFs (**Fig. 3.5C**). pCAF-mediated BPH1 growth was significantly inhibited in mice receiving p38i (**Fig. 3.5C**), similar to what was observed with senescent fibroblast-mediated BPH1 growth (**Fig. 3.4G and H**). These findings, combined with those from p38MAPK inhibition of senescent-fibroblast driven tumors, suggest that p38MAPK is a viable, stromal specific therapeutic target that may show efficacy in diverse tumor microenvironments and diverse tumor types

DISCUSSION

The regulation of SASP expression is complex, involving the DNA damage response (16), HDAC1 activity (15), and transcriptional regulation by NFκB and C/EBPβ (17-19). p38MAPK perhaps best exemplifies the complexity of SASP regulation. Previous reports have shown that p38MAPK impacts NFκB-driven transcriptional control of SASP expression immediately following exposure to a senescence-inducing signal (19). In our system, p38MAPK inhibition had no effect on NFκB transcriptional activity when it was initiated after cells acquired the senescent phenotype as evidenced by SA-β-gal staining. However, p38MAPK inhibition did have a significant impact on SASP factor mRNA stability. Our data are consistent with p38MAPK playing a dual role in SASP factor expression. We hypothesize that SASP factor expression is achieved through

early rounds of transcription followed by post-transcriptional mRNA stabilization, both of which require distinct p38MAPK functions.

Inhibiting the SASP represents a novel stromal-specific therapeutic cancer modality that could be beneficial at multiple stages of tumorigenesis. We have demonstrated that senescent cells are present in the microenvironment before the formation of preneoplastic lesions and that SASP factors promote preneoplastic cell growth (15, 23). The SASP also promotes more aggressive malignancies by increasing angiogenesis and invasion (9, 39). Finally, the SASP is hypothesized to promote later events in cancer progression including metastasis and recurrence through its promotion of cancer stem cell formation and chemo-resistant niches (7, 40, 41). Together, these findings suggest that inhibition of the SASP will prevent the development and/or progression of malignancies. p38MAPK could provide an ideal target as it impacts both the transcriptional and post-transcriptional regulation of SASP (19) and may be particularly effective because it can inhibit SASP expression after the stabilization of SASP mRNAs has already occurred.

Our findings that oral administration of a p38MAPK inhibitor dramatically inhibits SASP-mediated tumor growth driven by senescent fibroblasts and CAFs indicates for the first time that the tumor-promoting capabilities of senescent and cancer-associated fibroblasts are mediated through similar signaling pathways. Furthermore, these findings suggest that p38MAPK is an important therapeutic target with wide applicability in a variety of tumor-promoting microenvironments. This is strengthened by our in silico

analysis of the stromal compartment of breast cancer lesions, which we show express many p38MAPK-dependent genes. These data are intriguing in light of the fact that p38MAPK inhibitors have moved into phase II and III clinical trials for inflammatory diseases including rheumatoid arthritis, Crohn's disease, and psoriasis, demonstrating their tolerability in patients (36, 37). Given our findings, we suggest that p38MAPK inhibitors warrant investigation for use as anti-neoplastic therapy.

ACKNOWLEDGMENTS

The authors thank Dr. Nicholas Davidson for the lucIL6 construct and advice on the RIP protocol; Julie Prior and The BRIGHT Institute at Washington University School of Medicine for live animal imaging and advice, and Amey Barakat for technical assistance with mitochondrial DNA staining. RNAi constructs for this project were obtained through the Broad Institute and funded in part by the Children's Discovery Institute of Washington University in St. Louis. The authors also thank the Genome Technology Access Center in the Department of Genetics at Washington University School of Medicine for help with genomic analysis. The Center is supported by NCI Cancer Center Support Grant P30 CA91842 to the Siteman Cancer Center and by ICTS/CTSA Grant UL1RR024992 from the National Center for Research Resources (NCRR). The authors further thank Dr. John Edwards for assistance in RNA-seq analyses; Mr. Daniel Teasley, Drs. Michelle Hurchla, Katherine Weilbaecher, Gregory Longmore, Andrey Shaw, and Kendall Blumer for critical reading of the article; Dr. Craig Allred for advice on human expression; and Mr. Adnan Elhammali for assistance with GO processes analysis. Financial support: This study was financially supported by NIH 5 R01

CA130919 (to S.A. Stewart), NIH Cellular Biochemical and Molecular Sciences Predoctoral Training Grant T32 GM007067 (to E. Alspach and K.C. Flanagan), an American Cancer Society Research Scholar Award (to S.A. Stewart and S.S. McAllister), and NIH RO1 CA166284-01 (to S.S. McAllister). Molecular imaging was funded by NIH P50 CA94056 (to D. Piwnica-Worms). Histologic analysis was supported by NIH P30 AR057235 to the Washington University Musculoskeletal Research Center (to D.V. Novack). The RNAi constructs were obtained from the Viral-vector–based RNAi Core at Washington University, which is supported by a grant from the Children's Discovery Institute and Broad Institute.

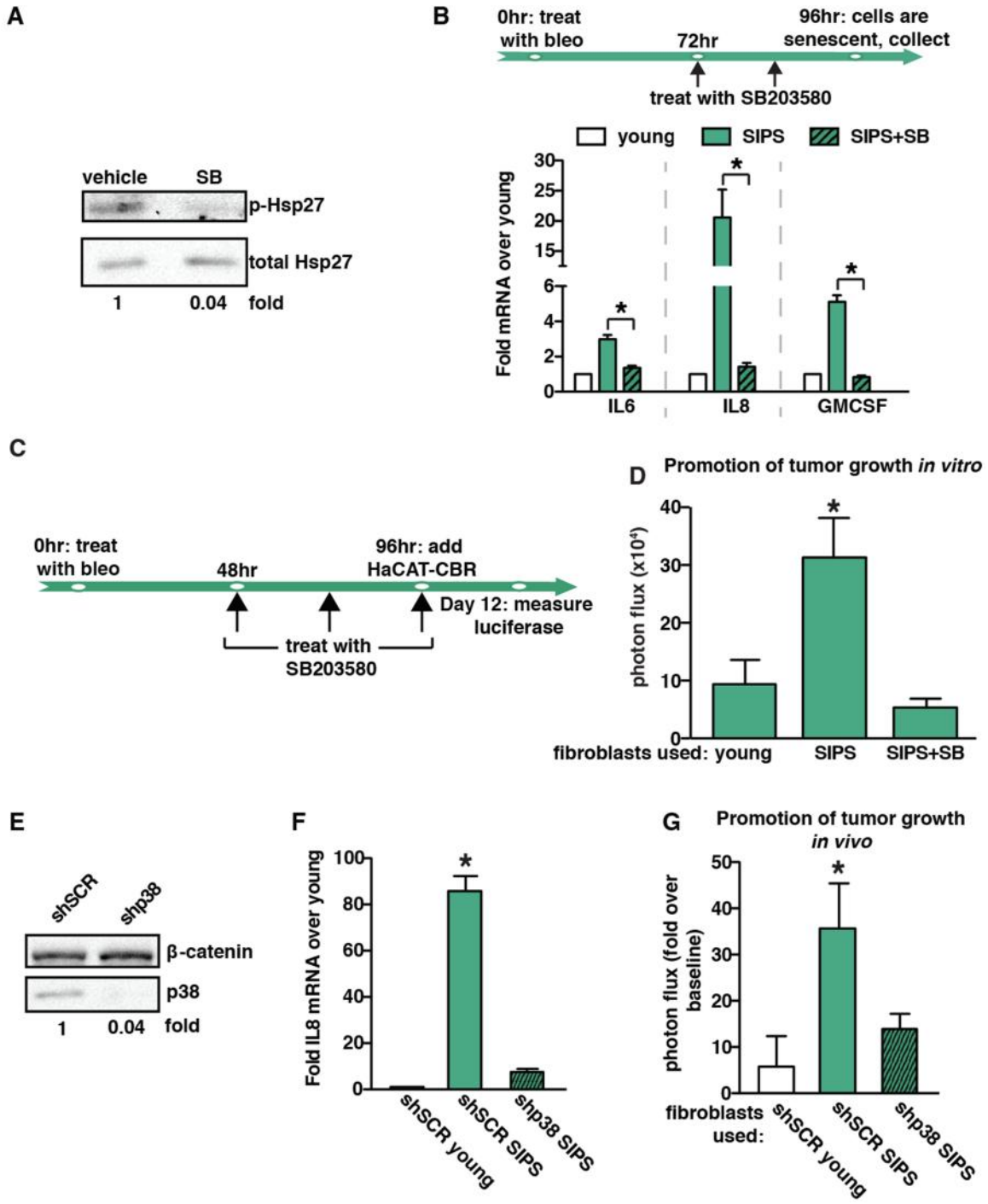

Fig. 3.1: p38MAPK activity controls the pro-tumorigenic properties of the SASP A) Western blot analysis demonstrating that SB203580 treatment inhibits p38MAPK activity. SB203580 treatment significantly impacts phosphorylation of p38MAPK's direct downstream target, Hsp27. B) Schematic of protocol to generate SIPS in BJ fibroblasts.

Cells were treated with bleomycin for 24 hours. SB203580 (SB) treatment or vehicle control was initiated 48 hours after removal of bleomycin (bleo). 96 hours after bleomycin treatment, cells were collected for expression analysis of IL6, IL8, and GMCSF by qRT-PCR. Representative experiment, n=4. C) Timeline of bleomycin (bleo) and SB203580 treatment of BJ fibroblasts in (D). SB203580 was replenished daily until co-culture with HaCAT-CBR cells was initiated. D) Growth of human keratinocytes expressing click beetle red (HaCaT-CBR) measured 8 days following initiation of co-culture with indicated fibroblast populations. Representative experiment, n=3. E) BJ fibroblasts were depleted of p38MAPK through the expression of shRNA (shp38) or control shRNA (shSCR). p38 depletion was verified by western blot analysis. F) Expression of IL8 was analyzed by qRT-PCR 96 hours following bleomycin treatment in p38MAPK-depleted (shp38) or control (shSCR) fibroblasts and represented relative to young fibroblasts expressing shSCR control. Representative experiment, n=3. G) BJ fibroblasts expressing shp38 or shSCR were treated with bleomycin for 72 hours prior to injection. Indicated fibroblast populations were admixed with preneoplastic epithelial cells expressing click beetle red (BPH1-CBR cells) and injected subcutaneously into the rear flanks of female NcR nude mice. Luciferase activity was measured using live, whole-animal imaging to monitor BPH1 cell growth relative to baseline signal. Data represents mean + SEM, n=8. Data represents mean + SD unless otherwise stated. * indicates $p<0.05$. SIPS: stress induced premature senescence.

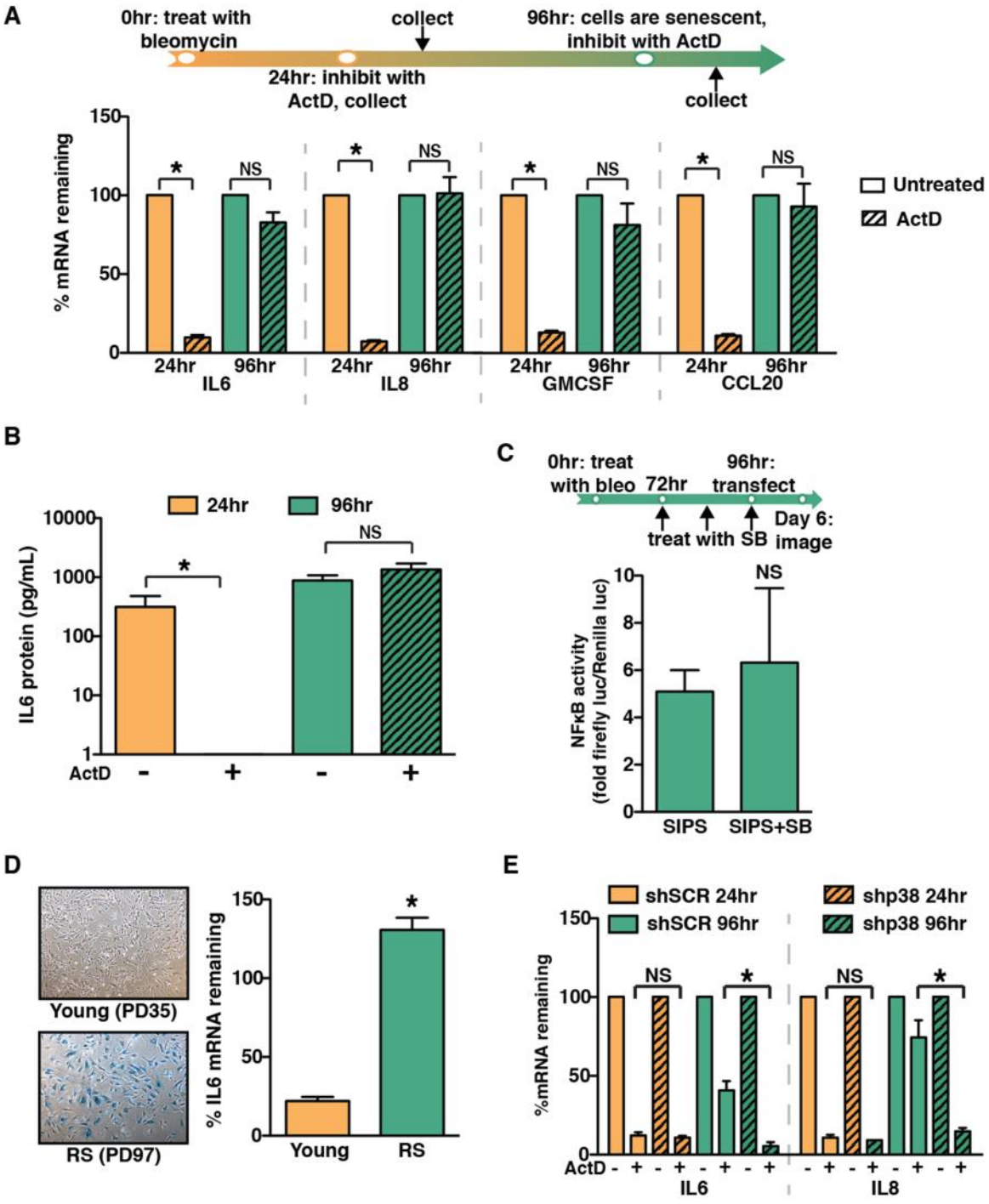

Fig. 3.2: p38MAPK post-transcriptionally regulates the SASP A) Schematic of protocol to generate SIPS in BJ fibroblasts. Cells were treated with bleomycin for 24 hours. Cells were subsequently treated with actinomycin D (ActD) for 24 hours. The ActD treatment was initiated 24 or 96 hours after the completion of bleomycin treatment.

IL6, IL8, GMCSF, and CCL20 mRNA levels were analyzed by qRT-PCR. To account for changes in gene expression, levels mRNA in ActD-treated cells were normalized to the levels observed in untreated cells from the respective time points (% mRNA remaining). Representative experiment, n=3. B) ELISA analysis of IL6 protein levels in conditioned media from cells treated as in (A). Representative experiment, n=4. C) BJ fibroblasts were treated with bleomycin (bleo) for 24 hours and with SB203580 (SB) as indicated. 96 hours post bleomycin treatment cells were transiently transfected with an NFκB activity luciferase reporter. Luciferase activity was measured by live-cell imaging 48 hours post transfection. Representative experiment, n=2. D) Young BJ fibroblasts (35 population doublings, PD) or replicatively senescent BJ fibroblasts (PD97) were stained for senescence-associated β-galactosidase to confirm senescent phenotype (left). Cells were treated with ActD and IL6 mRNA levels were analyzed by qRT-PCR. Representative experiment, n=3. E) BJ fibroblasts expressing a control hairpin (shSCR) or shp38 were treated for 24 hours with ActD at 24 or 96 hours after the completion of bleomycin treatment. IL6 and IL8 mRNA levels were analyzed by qRT-PCR. Representative experiment, n=2.

Data represent mean + SD. * indicates $p<0.05$. SIPS: stress-induced premature senescence.

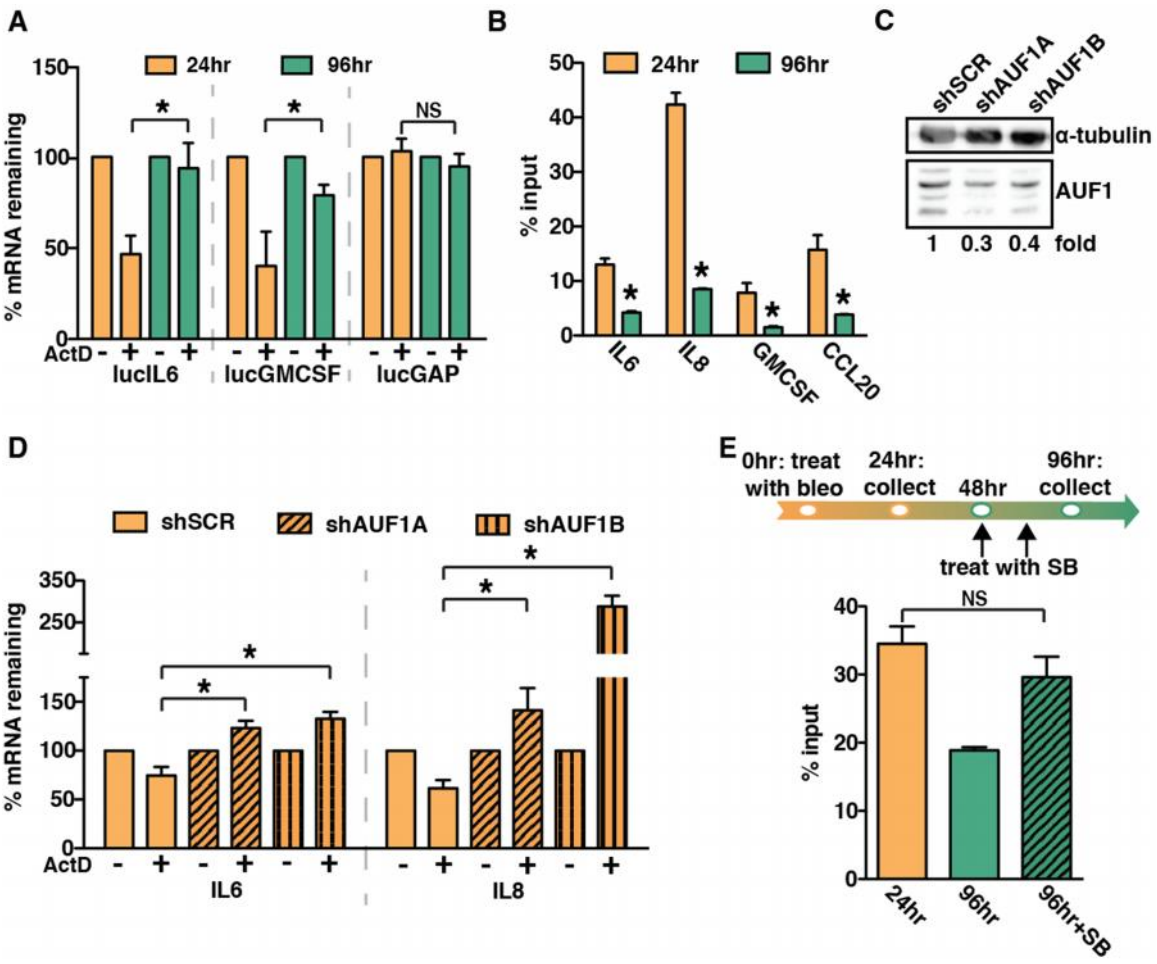

Fig. 3.3: AUF1 directly binds to SASP factor mRNA and modulates SASP factor stabilization A) BJ fibroblasts were stably transduced with luciferase constructs fused to the 3' untranslated regions (UTR) of IL6, GMCSF, and GAPDH (lucIL6, lucGMCSF, and lucGAP). Cells were treated with ActD at 24 or 96 hours following bleomycin treatment. Luciferase mRNA levels were analyzed by qRT-PCR. Representative experiment, n=3. B) RNA immunoprecipitation was performed for AUF1 using BJ fibroblast cell lysates collected 24 or 96 hours after bleomycin treatment. IL6, IL8, GMCSF, and CCL20 mRNA levels in immunoprecipitations were analyzed by qRT-PCR. Representative experiment, n=4. C) BJ fibroblasts were transduced with shRNAs to deplete AUF1 (shAUF1A and shAUF1B) or a control shRNA (shSCR). Protein levels

were analyzed by western blot analysis. Note: there are four AUF1 isoforms present and α-tubulin was used as a loading control. D) 24 hours following bleomycin treatment, BJ fibroblasts expressing a control hairpin shSCR, shAUF1A, or shAUF1B were treated with ActD for 1 hour. IL6 and IL8 mRNA levels were analyzed by qRT-PCR. Representative experiment, n=2. E) RNA immunoprecipitation for AUF1 was performed on BJ fibroblasts treated with bleomycin (bleo) and SB203580 (SB) as indicated. The level of IL8 mRNA in the AUF1 immunoprecipitation was measured by qRT-PCR. Representative experiment, n=3. Data represent mean + SD. * indicates $p<0.05$.

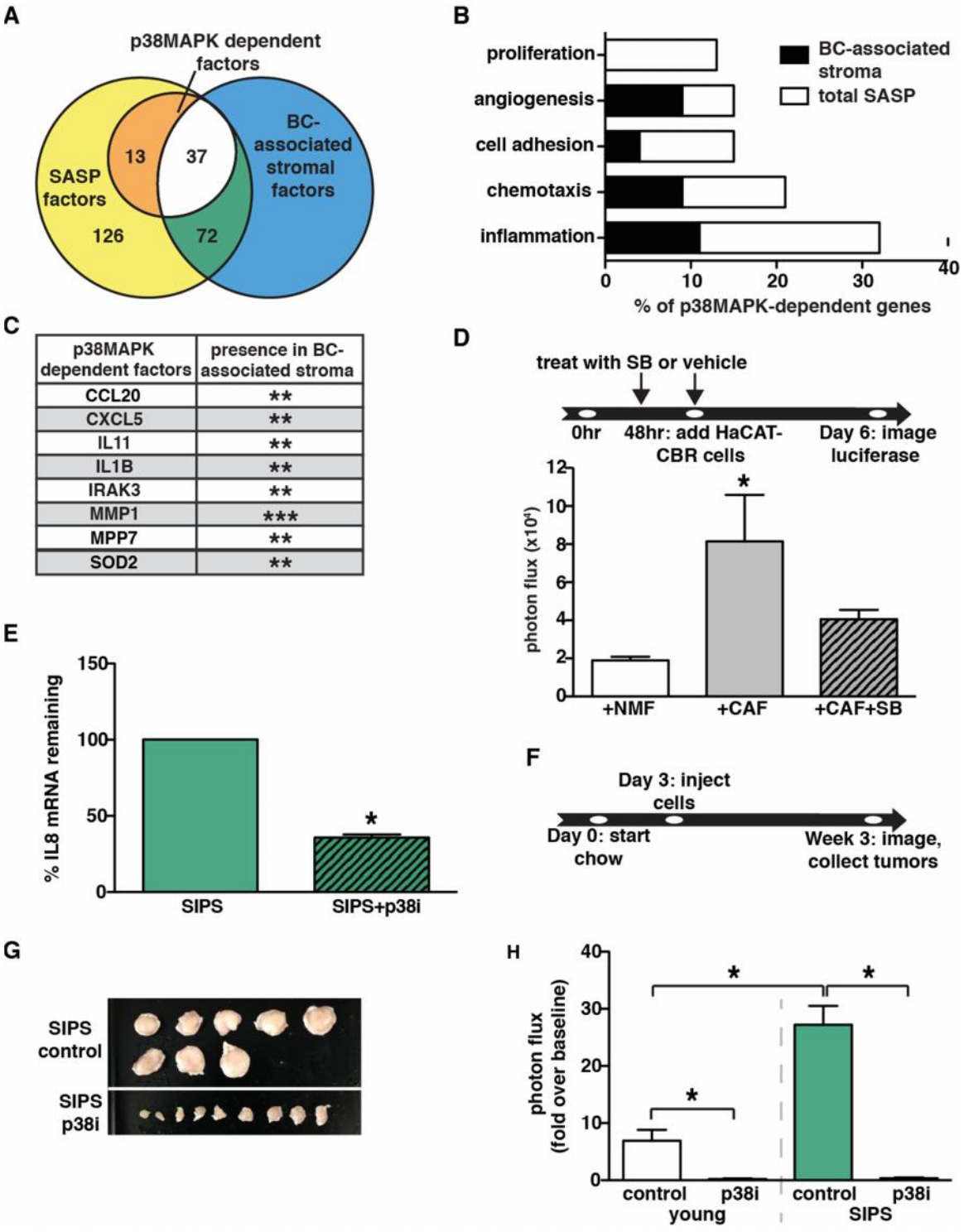

Fig. 3.4: p38MAPK-dependent factors are expressed in the TME of breast cancer lesions A) RNA-seq analysis was performed on young fibroblasts, senescent fibroblasts, and senescent fibroblasts treated with SB203580. RNA-seq results were

analyzed to determine the number of factors upregulated in response to senescence (SASP factors) and the number of p38MAPK-dependent factors. These results were also analyzed for overlap with the expression profiles of breast cancer (BC)-associated stroma. B) GO processes analysis was performed on p38MAPK-dependent SASP factors. Results are presented as the percent of p38MAPK-depenedent genes assigned to the processes shown. Black regions of the bars represent the percent of p38MAPK-dependent SASP factors assigned to each process that are also expressed in BC-associated stroma. The significance threshold was set at $p < 0.05$. C) p38MAPK-dependent SASP factors that are expressed in more than one BC-associated stroma data set. **indicates expression in 2 BC-associated stroma datasets, ***indicates expression in 3 BC-associated stroma datasets. D) Tumor-educated human CAFs and their normal isogenic counterparts (NMF) were treated with SB203580 (SB) or vehicle as indicated and replenished daily until co-culture with HaCAT-CBR preneoplastic keratinocytes was initiated. Luciferase activity was measured using live-cell imaging 4 days following initiation of co-culture to monitor HaCaT cell growth. Representative experiment, n=2. E) Senescent BJ fibroblasts in matrigel were injected subcutaneously into the rear flanks of nude mice fed either control or p38i chow. Cells were removed 10 days after injection and IL8 mRNA levels were measured using qRT-PCR. Representative experiment, n=4. F,G and H) Xenografts of BPH1-CBR cells co-injected with senescent BJ fibroblasts (SIPS) into female NcR nude mice. Control or the p38i compounded chow were performed as outlined in (F). Tumor are shown in (G). Tumor growth was analyzed by bioluminescence imaging (H). Data represent mean + SEM, n=8.

Data represent mean + SD unless otherwise stated. * indicates $p<0.05$. SIPS: stress induced premature senescence.

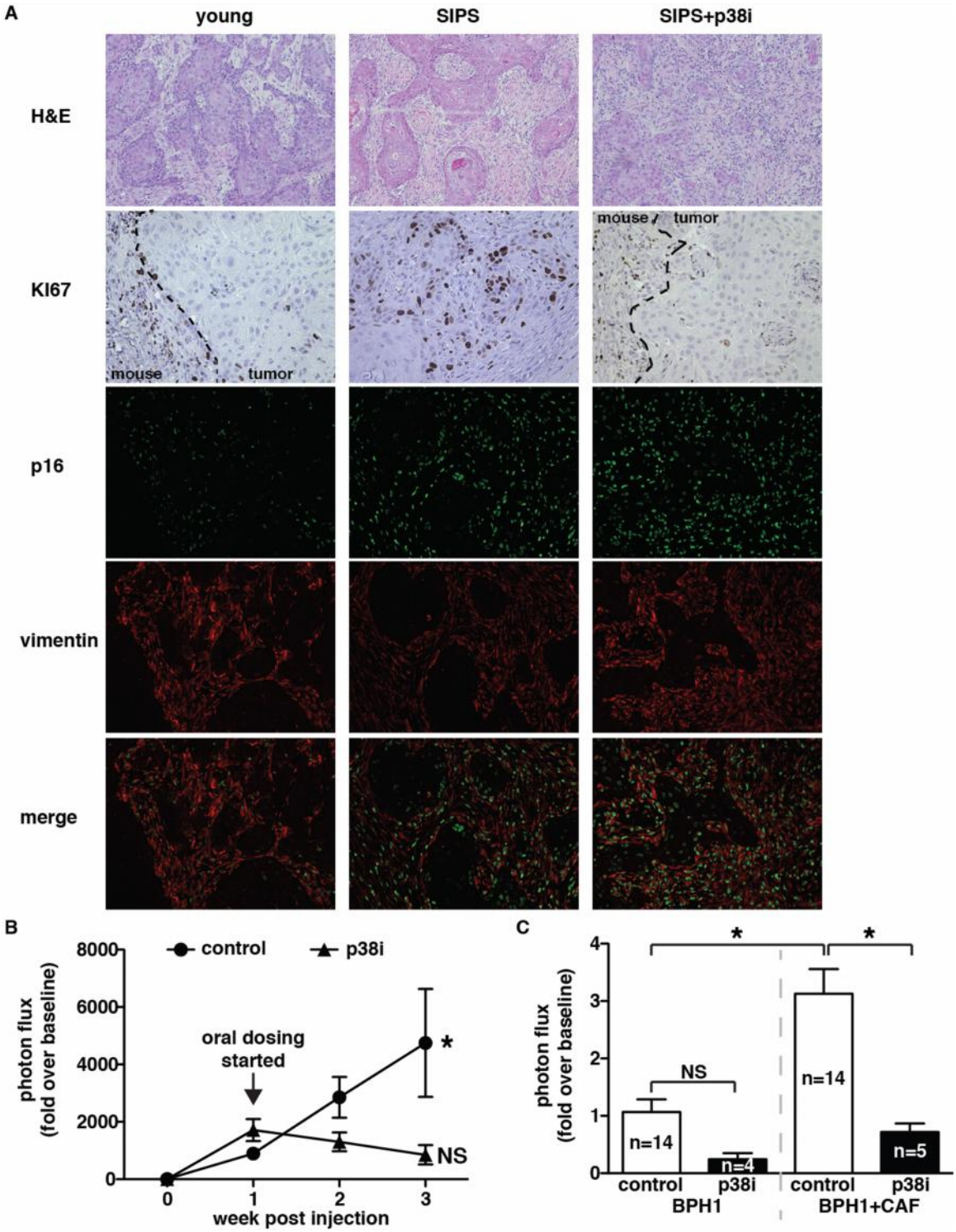

Fig. 3.5: p38MAPK inhibition is effective in both senescent fibroblast and CAF-driven tumors A) Tumors were removed at the endpoint of the experiment described in (Fig. 3.4F) and stained for Ki67 (dashed line demarks the margin between the mouse

and xenograft), p16, and vimentin. H&E images were captured with a 10X objective, all other images were captured with a 20X objective. Representative images, n=2. B) Xenograft growth of BPH1-CBR cells co-injected with senescent BJ fibroblasts (SIPS) into female NcR nude mice. Tumors were allowed to grow for 1 week after injection, at which time mice were placed on control or p38i-compounded chow. Tumor growth was analyzed by bioluminescence imaging. Data represent mean + SEM, n=16. * indicates significance between 1 and 3 weeks post-injection in mice fed control chow. C) Xenografts of BPH1-CBR cells co-injected with pCAFs into female NcR nude mice. Mice were fed control or p38i chow as outlined for the experiment in Fig. 3.4F. Tumor growth was analyzed by bioluminescence imaging. Data represent mean + SEM, n is indicated for each sample. * indicates $p<0.05$. NS: not significant.

Supplemental Table 3.1: p38MAPK dependent SASP factors and their overlap with BC-associated stroma

p38MAPK-dependent SASP	overlap with Finak	overlap with Ma	overlap with Karnoub
ABCA6	ABCA6	AKR1B1	AKR1B1
AKR1B1	BDKRB2	C1QTNF1	CCL20
ANKRD30BL	C1QTNF1	CCL20	GMCSF
BDKRB2	C8orf4	CXCL 5	IRAK3
C1QTNF1	CARD6	FOXE1	MMP1
C8orf4	CD36	IL11	MPP7
CARD6	CH25H	IL1A	NAMPT
CCL20	CXCL 2	IL1B	
CD36	CXCL 5	IL8	
CH25H	CYP26B1	LACC1	
CXCL 1	CYP7B1	LPXN	
CXCL 2	FOXE1	MMP1	
CXCL 5	FRMD6	MMP3	
CYP26B1	GCSF	NAMPT	
CYP7B1	GDNF	NEK10	
ERRFI1	GREM2	PSG1	
FAM43A	IL11	SFRP1	
FOXE1	IL13RA2	SOD2	
FRMD6	IL1B		
GCSF	IL24		
GDF15	IRAK3		
GDNF	KCNJ2		
GMCSF	MMP1		
GREM2	MPP7		
HAS2	MYEOV		
IL11	PLCH1		
IL13RA2	PSG1		
IL1A	SOD2		
IL1B	XDH		
IL24			
IL6			
IL8			
IRAK3			
KCNJ2			
LACC1			
LPXN			
MMP1			
MMP3			
MPP7			
MYEOV			
NAMPT			
NAMPTL			
NEK10			
PLA2G4A			
PLCH1			
PSG1			
SFRP1			
SOD2			
TFPI2			
TNFSF18			
USP53			
XDH			

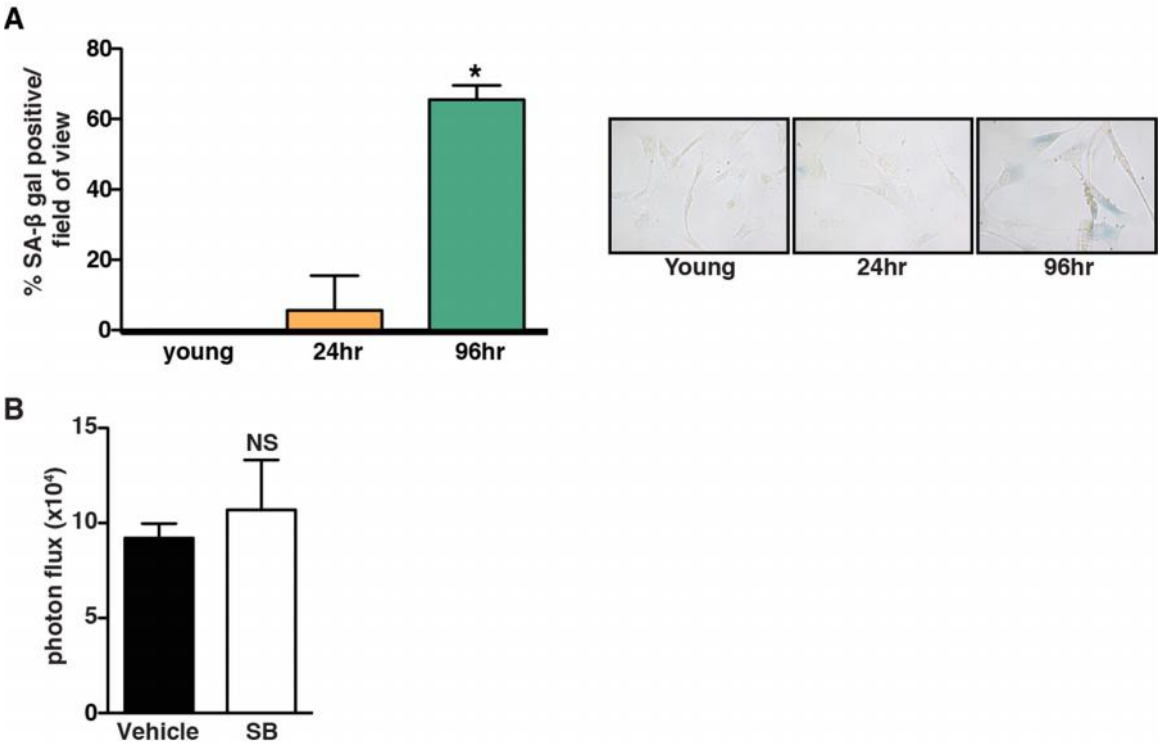

Supplemental Fig. 3.1: p38MAPK activity controls the pro-tumorigenic properties of the SASP A) BJ fibroblasts were fixed for senescence-associated β-galactosidase 24 or 96 hours after treatment with bleomycin. n=3. B) HaCAT-CBR preneoplastic skin keratinocytes were treated with SB203580 or vehicle for 72 hours. Representative experiment, n=3. Data is presented as mean ± SD. * indicates $p \leq 0.05$.

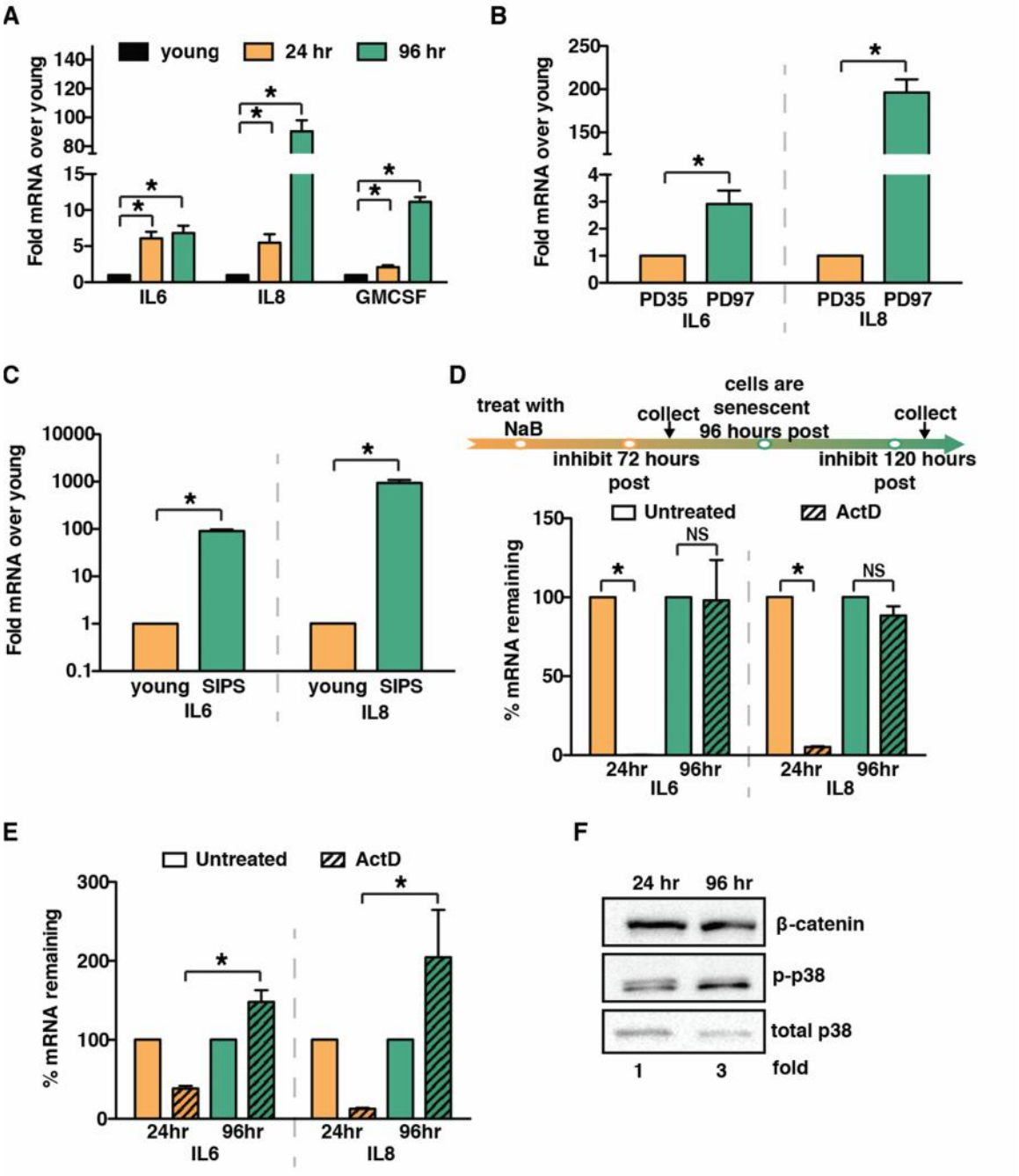

Supplemental Fig. 3.2: p38MAPK post-transcriptionally regulates the SASP A) BJ fibroblasts were treated with bleomycin for 24 hours. Cells were collected either 24 or 96 hours after treatment with bleomycin and upregulation of SASP factors IL6, IL8 and GMCSF was verified by qRT-PCR. Representative experiment, n=3. B) BJ fibroblasts were induced to senesce through telomere attrition (replicative senescence, RS).

Upregulation of SASP factors IL6 and IL8 was verified by qRT-PCR. Representative experiment, n=3. C) BJ fibroblasts were treated with sodium butyrate (NaB) for 120 hours. Upregulation of SASP factors IL6 and IL8 was verified by qRT-PCR. Representative experiment, n=3. D) BJ fibroblasts were treated with NaB for 72 or 120 hours followed by actinomycin D (ActD) at the time points indicated. IL6 and IL8 expression was quantified by qRT-PCR. Representative experiment, n=3. E) IMR90 human lung fibroblasts were treated with bleomycin and ActD as described in **Fig. 3.2B**. IL6 and IL8 expression was quantified by qRT-PCR. Representative experiment, n=2. F) BJ fibroblast cell lysates 24 or 96 hours post bleomycin treatment were analyzed for phosphorylation of p38MAPK (p-p38). Total p38MAPK was used as a loading control. Representative experiment, n=3. Data is presented as mean + SD. * indicates $p \leq 0.05$. SIPS: stress-induced premature senescence.

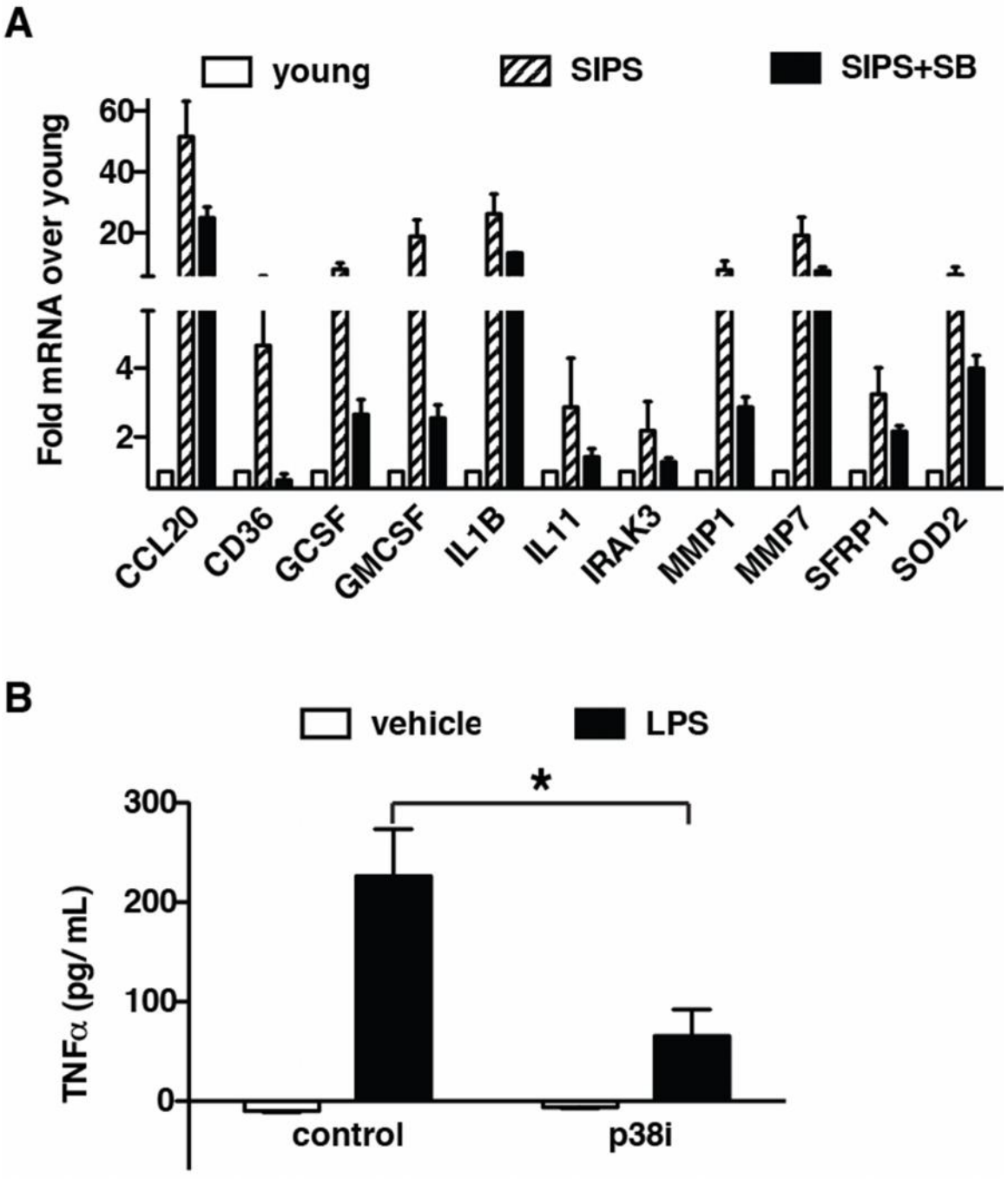

Supplemental Fig. 3.3: p38MAPK-dependent factors are expressed in the stromal compartment of breast cancer lesions A) A subset of p38MAPK-dependent SASP factors was validated by qRT-PCR in young, senescent or senescent fibroblasts treated with SB203580. Data represent mean + SD. B) Female NcR nude mice were given

control or p38i chow for 3 days prior to challenging with 100ng LPS. 1 hour post LPS injection, mice were sacrificed and serum was collected for analysis by TNFα ELISA. Data represent mean + SEM, n=3. * indicates $p \leq 0.05$. SIPS: stress-induced premature senescence.

REFERENCES

1. Finak G, Bertos N, Pepin F, Sadekova S, Souleimanova M, Zhao H, Chen H, Omeroglu G, Meterissian S, Omeroglu A, Hallett M, Park M. Stromal gene expression predicts clinical outcome in breast cancer. Nat Med. 2008;14(5):518-27.

2. Ma XJ, Dahiya S, Richardson E, Erlander M, Sgroi DC. Gene expression profiling of the tumor microenvironment during breast cancer progression. Breast Cancer Res. 2009;11(1):R7.

3. Karnoub AE, Dash AB, Vo AP, Sullivan A, Brooks MW, Bell GW, Richardson AL, Polyak K, Tubo R, Weinberg RA. Mesenchymal stem cells within tumour stroma promote breast cancer metastasis. Nature. 2007;449(7162):557-63. Epub 2007/10/05.

4. Olumi AF, Grossfeld GD, Hayward SW, Carroll PR, Tlsty TD, Cunha GR. Carcinoma-associated fibroblasts direct tumor progression of initiated human prostatic epithelium. Cancer research. 1999;59(19):5002-11.

5. Dimri GP, Lee X, Basile G, Acosta M, Scott G, Roskelley C, Medrano EE, Linskens M, Rubelj I, Pereira-Smith O, et al. A biomarker that identifies senescent human cells in culture and in aging skin *in vivo*. Proceedings of the National Academy of Sciences of the United States of America. 1995;92(20):9363-7.

6. Bavik C, Coleman I, Dean JP, Knudsen B, Plymate S, Nelson PS. The gene expression program of prostate fibroblast senescence modulates neoplastic epithelial cell proliferation through paracrine mechanisms. Cancer research. 2006;66(2):794-802.

7. Parrinello S, Coppe JP, Krtolica A, Campisi J. Stromal-epithelial interactions in aging and cancer: senescent fibroblasts alter epithelial cell differentiation. Journal of cell science. 2005;118(Pt 3):485-96.

8. Krtolica A, Parrinello S, Lockett S, Desprez PY, Campisi J. Senescent fibroblasts promote epithelial cell growth and tumorigenesis: a link between cancer and aging. Proceedings of the National Academy of Sciences of the United States of America. 2001;98(21):12072-7.

9. Coppe JP, Patil CK, Rodier F, Sun Y, Munoz DP, Goldstein J, Nelson PS, Desprez PY, Campisi J. Senescence-associated secretory phenotypes reveal

cell-nonautonomous functions of oncogenic RAS and the p53 tumor suppressor. PLoS biology. 2008;6(12):2853-68.

10. Elkabets M, Gifford AM, Scheel C, Nilsson B, Reinhardt F, Bray MA, Carpenter AE, Jirstrom K, Magnusson K, Ebert BL, Ponten F, Weinberg RA, McAllister SS. Human tumors instigate granulin-expressing hematopoietic cells that promote malignancy by activating stromal fibroblasts in mice. The Journal of clinical investigation. 2011;121(2):784-99. Epub 2011/01/27.

11. Orimo A, Gupta PB, Sgroi DC, Arenzana-Seisdedos F, Delaunay T, Naeem R, Carey VJ, Richardson AL, Weinberg RA. Stromal fibroblasts present in invasive human breast carcinomas promote tumor growth and angiogenesis through elevated SDF-1/CXCL12 secretion. Cell. 2005;121(3):335-48.

12. Erez N, Truitt M, Olson P, Arron ST, Hanahan D. Cancer-Associated Fibroblasts Are Activated in Incipient Neoplasia to Orchestrate Tumor-Promoting Inflammation in an NF-kappaB-Dependent Manner. Cancer cell. 2010;17(2):135-47. Epub 2010/02/09.

13. Hu M, Polyak K. Microenvironmental regulation of cancer development. Current opinion in genetics & development. 2008;18(1):27-34. Epub 2008/02/20.

14. Allinen M, Beroukhim R, Cai L, Brennan C, Lahti-Domenici J, Huang H, Porter D, Hu M, Chin L, Richardson A, Schnitt S, Sellers wR, Polyak K. Molecular characterization of the tumor microenvironment in breast cancer. Cancer cell. 2004;6(1):17-32.

15. Pazolli E, Alspach E, Milczarek A, Prior J, Piwnica-Worms D, Stewart SA. Chromatin remodeling underlies the senescence-associated secretory phenotype of tumor stromal fibroblasts that supports cancer progression. Cancer research. 2012;72(9):2251-61. Epub 2012/03/17.

16. Rodier F, Coppe JP, Patil CK, Hoeijmakers WA, Munoz DP, Raza SR, Freund A, Campeau E, Davalos AR, Campisi J. Persistent DNA damage signalling triggers senescence-associated inflammatory cytokine secretion. Nature cell biology. 2009;11(8):973-9.

17. Kuilman T, Michaloglou C, Vredeveld LC, Douma S, van Doorn R, Desmet CJ, Aarden LA, Mooi WJ, Peeper DS. Oncogene-induced senescence relayed by an interleukin-dependent inflammatory network. Cell. 2008;133(6):1019-31.

18. Chien Y, Scuoppo C, Wang X, Fang X, Balgley B, Bolden JE, Premsrirut P, Luo W, Chicas A, Lee CS, Kogan SC, Lowe SW. Control of the senescence-

associated secretory phenotype by NF-kappaB promotes senescence and enhances chemosensitivity. Genes & development. 2011;25(20):2125-36. Epub 2011/10/08.

19. Freund A, Patil CK, Campisi J. p38MAPK is a novel DNA damage response-independent regulator of the senescence-associated secretory phenotype. Embo J.

20. Winzen R, Kracht M, Ritter B, Wilhelm A, Chen CY, Shyu AB, Muller M, Gaestel M, Resch K, Holtmann H. The p38 MAP kinase pathway signals for cytokine-induced mRNA stabilization via MAP kinase-activated protein kinase 2 and an AU-rich region-targeted mechanism. The EMBO journal. 1999;18(18):4969-80. Epub 1999/09/16.

21. Zhao W, Liu M, Kirkwood KL. p38alpha stabilizes interleukin-6 mRNA via multiple AU-rich elements. The Journal of biological chemistry. 2008;283(4):1778-85. Epub 2007/11/29.

22. Knapinska AM, Gratacos FM, Krause CD, Hernandez K, Jensen AG, Bradley JJ, Wu X, Pestka S, Brewer G. Chaperone Hsp27 modulates AUF1 proteolysis and AU-rich element-mediated mRNA degradation. Molecular and cellular biology. 2011;31(7):1419-31. Epub 2011/01/20.

23. Pazolli E, Luo X, Brehm S, Carbery K, Chung JJ, Prior JL, Doherty J, Demehri S, Salavaggione L, Piwnica-Worms D, Stewart SA. Senescent Stromal-Derived Osteopontin Promotes Preneoplastic Cell Growth. Cancer research. 2009.

24. Liu D, Hornsby PJ. Senescent human fibroblasts increase the early growth of xenograft tumors via matrix metalloproteinase secretion. Cancer research. 2007;67(7):3117-26.

25. Freund A, Patil CK, Campisi J. p38MAPK is a novel DNA damage response-independent regulator of the senescence-associated secretory phenotype. The EMBO journal. 2011;30(8):1536-48. Epub 2011/03/15.

26. Cuenda A, Rouse J, Doza YN, Meier R, Cohen P, Gallagher TF, Young PR, Lee JC. SB 203580 is a specific inhibitor of a MAP kinase homologue which is stimulated by cellular stresses and interleukin-1. FEBS letters. 1995;364(2):229-33. Epub 1995/05/08.

27. Guhaniyogi J, Brewer G. Regulation of mRNA stability in mammalian cells. Gene. 2001;265(1-2):11-23. Epub 2001/03/20.

28. Paschoud S, Dogar AM, Kuntz C, Grisoni-Neupert B, Richman L, Kuhn LC. Destabilization of interleukin-6 mRNA requires a putative RNA stem-loop structure, an AU-rich element, and the RNA-binding protein AUF1. Molecular and cellular biology. 2006;26(22):8228-41. Epub 2006/09/07.

29. Raineri I, Wegmueller D, Gross B, Certa U, Moroni C. Roles of AUF1 isoforms, HuR and BRF1 in ARE-dependent mRNA turnover studied by RNA interference. Nucleic acids research. 2004;32(4):1279-88. Epub 2004/02/21.

30. Sarkar S, Han J, Sinsimer KS, Liao B, Foster RL, Brewer G, Pestka S. RNA-binding protein AUF1 regulates lipopolysaccharide-induced IL10 expression by activating IkappaB kinase complex in monocytes. Molecular and cellular biology. 2011;31(4):602-15. Epub 2010/12/08.

31. Strieter RM, Burdick MD, Gomperts BN, Belperio JA, Keane MP. CXC chemokines in angiogenesis. Cytokine & growth factor reviews. 2005;16(6):593-609. Epub 2005/07/28.

32. Liu J, Zhang N, Li Q, Zhang W, Ke F, Leng Q, Wang H, Chen J, Wang H. Tumor-associated macrophages recruit CCR6+ regulatory T cells and promote the development of colorectal cancer via enhancing CCL20 production in mice. PloS one. 2011;6(4):e19495. Epub 2011/05/12.

33. Ernst M, Najdovska M, Grail D, Lundgren-May T, Buchert M, Tye H, Matthews VB, Armes J, Bhathal PS, Hughes NR, Marcusson EG, Karras JG, Na S, Sedgwick JD, Hertzog PJ, Jenkins BJ. STAT3 and STAT1 mediate IL-11-dependent and inflammation-associated gastric tumorigenesis in gp130 receptor mutant mice. The Journal of clinical investigation. 2008;118(5):1727-38. Epub 2008/04/24.

34. Apte RN, Dotan S, Elkabets M, White MR, Reich E, Carmi Y, Song X, Dvozkin T, Krelin Y, Voronov E. The involvement of IL-1 in tumorigenesis, tumor invasiveness, metastasis and tumor-host interactions. Cancer metastasis reviews. 2006;25(3):387-408. Epub 2006/10/18.

35. Uhlirova M, Bohmann D. JNK- and Fos-regulated Mmp1 expression cooperates with Ras to induce invasive tumors in Drosophila. The EMBO journal. 2006;25(22):5294-304. Epub 2006/11/04.

36. Cohen P. Protein kinases--the major drug targets of the twenty-first century? Nature reviews Drug discovery. 2002;1(4):309-15. Epub 2002/07/18.

37. Saklatvala J. The p38 MAP kinase pathway as a therapeutic target in inflammatory disease. Curr Opin Pharmacol. 2004;4(4):372-7. Epub 2004/07/15.

38. Burnette BL, Selness S, Devraj R, Jungbluth G, Kurumbail R, Stillwell L, Anderson G, Mnich S, Hirsch J, Compton R, De Ciechi P, Hope H, Hepperle M, Keith RH, Naing W, Shieh H, Portanova J, Zhang Y, Zhang J, Leimgruber RM, Monahan J. SD0006: a potent, selective and orally available inhibitor of p38 kinase. Pharmacology. 2009;84(1):42-60. Epub 2009/07/11.

39. Coppe JP, Kauser K, Campisi J, Beausejour CM. Secretion of vascular endothelial growth factor by primary human fibroblasts at senescence. The Journal of biological chemistry. 2006;281(40):29568-74.

40. Gilbert LA, Hemann MT. DNA damage-mediated induction of a chemoresistant niche. Cell. 2010;143(3):355-66. Epub 2010/10/30.

41. Cahu J, Bustany S, Sola B. Senescence-associated secretory phenotype favors the emergence of cancer stem-like cells. Cell death & disease. 2012;3:e446. Epub 2012/12/21.

42. Coppe JP, Boysen M, Sun CH, Wong BJ, Kang MK, Park NH, Desprez PY, Campisi J, Krtolica A. A role for fibroblasts in mediating the effects of tobacco-induced epithelial cell growth and invasion. Molecular cancer research : MCR. 2008;6(7):1085-98.

43. Moss BL, Gross S, Gammon ST, Vinjamoori A, Piwnica-Worms D. Identification of a ligand-induced transient refractory period in nuclear factor-kappaB signaling. The Journal of biological chemistry. 2008;283(13):8687-98. Epub 2008/01/22.

44. Hahn WC, Counter CM, Lundberg AS, Beijersbergen RL, Brooks MW, Weinberg RA. Creation of human tumour cells with defined genetic elements. Nature. 1999;400(6743):464-8.

45. Beissbarth T, Speed TP. GOstat: find statistically overrepresented Gene Ontologies within a group of genes. Bioinformatics. 2004;20(9):1464-5. Epub 2004/02/14.

CHAPTER 4

Conclusions and Future Directions

Conclusions

Over the last decade, extensive research has greatly increased our understanding of the SASP, its physiological and pathological roles, and its regulation. It is now apparent that the SASP is not a uniform, unchanging phenotype, but rather a complex response to various stresses which is highly context-dependent. The factors that make up the SASP vary depending on the cell type, the senescence-inducer, and the environment. Further, the magnitude of induction of individual factors is also dependent on the context.

The complexity and variability of SASP induction is reflected by the complexity of the regulatory networks which induce and restrain the many SASP factors. This work further illustrates that the SASP is not regulated by any single pathway, but rather by a complex network of interrelated stress-responders, kinases, transcription factors, mRNA-stability proteins, and other signaling and effector molecules. The SASP is initially upregulated via transcription, and multiple transcription factors are required to induce the many SASP factors. NF-κB and C/EBPβ are the canonical SASP-inducing transcription factors, but many SASP-factors are upregulated independently of their action (1–4). Chapter Two of this dissertation focuses on understanding the regulation of the SASP factor OPN. OPN was previously known to be independent of NF-κB in response to senescence (4). We identified C/EBPβ as a necessary regulator of OPN, illustrating that while NF-κB and C/EBPβ regulate many of the same SASP factors, their target gene sets are not identical (**Fig 2.2**). Further, we showed that C/EBPβ directly binds to the OPN promoter and that binding of exogenous LAP2, the full-length

activating C/EBPβ isoform, increases at the OPN promoter as well as the promoters of known C/EBPβ targets IL-6 and IL-8 (**Fig 2.3**).

Given the potent pro-tumor potential of senescent stromal-derived OPN, I sought to understand how it was regulated in senescent fibroblasts. Through this work, we identified the novel SASP regulator c-Myb (**Fig 2.4**). C-Myb binds to the OPN promoter and this binding is required for promoter activation in response to senescence (**Fig 2.5**). C-Myb also binds to the promoters of IL-6 and IL-8. Further, using a combination of a microarray and RNAi approach, I identified 59 additional putative c-Myb targets (**Fig 2.6**). Of these 59 putative c-Myb targets, 47 were also putative C/EBPβ targets. The high degree of overlap between these two gene sets suggests that c-Myb and C/EBPβ often co-regulate many SASP factors. Although it has not been shown in this system, c-Myb and C/EBPβ can directly interact and co-activate transcription, raising the possibility that such a mechanism may be at play here (5). Given the importance of this interaction in other systems, a key avenue of future research will be to explore whether c-Myb and C/EBPβ interact directly in senescent cells, whether this interaction is required for transcriptional activation of SASP factors, and how this interaction is regulated. Underscoring the importance of c-Myb and C/EBPβ for the induction of many important SASP factors, I found that fibroblasts depleted of either c-Myb or C/EBPβ had significantly reduced ability to promote preneoplastic epithelial cell growth in cocultures (**Fig 2.7**).

While transcription plays a critical role in the induction of SASP factors, post-transcriptional stabilization of SASP factor mRNA is also important for the robust induction of the SASP. In Chapter 3, we identified this post-transcriptional regulatory mechanism and described its importance for the induction of SASP factors including IL-6, IL-8, and GM-CSF (**Fig 3.2**). It is not known whether OPN is regulated in this manner, as OPN mRNA is extremely stable at basal conditions, making it difficult to assess whether it is further stabilized in senescent cells (6, 7). Interestingly, while transcriptional induction of SASP mRNA occurs relatively quickly following exposure to a senescence-inducing stimulus, the stabilization of SASP factor mRNAs occurs only after the full establishment of cellular senescence days later.

The increase in the stability of many SASP factor mRNAs is dependent on p38MAPK (**Fig 3.2**). In response to senescence, p38MAPK is activated by phosphorylation and plays at least two distinct roles in SASP factor induction. First, p38MAPK is important for the transcriptional induction of SASP factors via initiation of NF-κB activity (2). Second, p38MAPK is required for the stabilization of SASP factor mRNAs in fully senescent cells. However, the transcription pathway is distinct from the post-transcriptional stabilization pathway, and p38MAPK is not required for the continued activity of NF-κB once senescence is fully established. In fully senescent cells, p38MAPK activity results in the removal of AUF1 from the 3'UTRs of SASP mRNAs (**Fig 3.3**). AUF1 is an mRNA destabilizing protein which binds to 3'-UTRs and causes mRNA ubiquitination and degradation.

Given the twofold nature of p38MAPK's regulation of many important pro-tumorigenic SASP factors, it is a promising potential therapeutic target. We found that depletion or inhibition of p38MAPK in senescent fibroblasts abrogates growth promotion of preneoplastic epithelial cells by senescent fibroblasts in cocultures and xenograft models (**Figs 3.1**). Further, cancer-associated fibroblasts (CAFs) have a similar expression profile to senescent fibroblasts and also promote growth of epithelial cells. Treatment of CAFs with p38MAPK inhibitors inhibits their ability to promote the growth of cocultured epithelial cells (**Fig 3.4**). Furthermore, p38MAPK inhibitors are effective at preventing the growth of established tumors growing in senescent fibroblast- or CAF-supported microenvironments (**Fig 3.5**). Many of the p38MAPK-dependent SASP factors are present in human breast cancer patients' stroma, suggesting that targeting p38MAPK is a viable potential patient therapy (**Fig 3.4**). The similarities between senescent fibroblasts and CAFs in their expression profiles, shared regulation by p38MAPK, and ability to promote epithelial cell growth underscore the notion that senescent fibroblasts and CAFs are in essence two different types of activated fibroblasts.

Future Directions

In Chapter 2, we established the transcription factor c-Myb as a regulator of a subset of the SASP. Further, we confirmed previous reports that C/EBPβ also regulates the SASP, and we identified new SASP factor targets of C/EBPβ including OPN. However, the mechanism by which c-Myb and C/EBPβ regulate SASP factors remains incompletely understood. One important question is whether c-Myb and C/EBPβ are

functioning independently to activate many of the same genes or whether they are working in a coordinated fashion. In other systems, c-Myb and C/EBPβ interact as a heterocomplex between one c-Myb molecule and a C/EBPβ dimer (5). It is not clear whether c-Myb and C/EBPβ are interacting in our system, nor whether there is a difference in the degree of interaction between non-senescent and senescent cells. Co-immunoprecipitations of c-Myb and C/EBPβ would help elucidate whether the genes are interacting. Further, we have synthesized a mutant form of C/EBPβ in which several of the key residues in the c-Myb binding domain are mutated. To test whether the putative interaction between c-Myb and C/EBPβ is important, expression of this construct in an endogenous C/EBPβ knockdown cell or mutation of the endogenous locus using CRISPR/Cas9 would be followed by measurement of SASP factors such as OPN, IL-6, and IL-8. If the interaction is important, the SASP factor mRNA induction should be inhibited.

While c-Myb and C/EBPβ both bind DNA separately, it is not clear whether this DNA binding is required prior to the interaction between the two proteins, or if one or both of the transcription factors can interact with and recruit the other protein to bind to the DNA. While there is no significant increase in c-Myb or C/EBPβ binding to the SASP promoters we studied in response to senescence, exogenously expressed LAP2, a full length isoform of C/EBPβ does increase binding in response to senescence. This raises the possibility that in response to senescence there is a change in C/EBPβ isoform binding to SASP promoters despite there being no change in overall C/EBPβ binding. The isoforms derive from alternative translation initiation sites, and there are

no available antibodies to carry out the needed ChIPs to answer this provocative question, so alternative methods such as mass-spectrometry are needed. This isoform switch could facilitate activation of SASP genes if the inhibitory isoform LIP is replaced by LAP2 or LAP1, both of which activate transcription. If there is a change in C/EBPβ isoform binding, a further question of interest is whether c-Myb facilitates or is necessary for this switch.

Also of interest are the upstream activators of c-Myb and C/EBPβ. C/EBPβ protein levels increase in response to senescence (data not shown and ref. 3). However, we do not observe an increase in binding to SASP promoters. It has been reported that ERK phosphorylates C/EBPβ in response to senescence. This may activate C/EBPβ and even drive interactions with c-Myb. Likewise, c-Myb is subject to multiple post-translational modifications, including phosphorylation, acetylation, and sumoylation (8–12). It remains to be seen if c-Myb is modified in response to senescence and whether this modification is important for the activation of the SASP.

An additional question that remains unclear is whether p38MAPK regulates OPN in response to senescence. Preliminary data gave inconsistent results depending on the means of p38MAPK depletion or inhibition, sometimes even yielding an increase in OPN mRNA levels (data not shown). P38MAPK regulates the SASP via a transcriptional and a post-transcriptional mechanism and does so differentially depending on the stage of senescence induction or maintenance. This transition and the importance of timing may explain the variable data. Given that p38MAPK

transcriptionally activates SASP factors via NF-κB, which does not regulate OPN in senescence, it is unlikely that p38MAPK is required for transcriptional activation of OPN. Further, OPN mRNA has a long half-life, and thus it is difficult to measure increases in its stability (6, 7). Nonetheless, it is possible that p38MAPK regulates OPN in response to senescence.

Inhibiting p38MAPK does significantly reduce the induction of many SASP factors, including IL-6, IL-8, and GM-CSF. Further, this inhibition is a promising therapeutic avenue and can significantly reduce primary tumor growth in xenograft models. In addition, preliminary data indicate that p38MAPK inhibition can reduce bone and visceral metastasis in PyMT breast cancer metastasis model (data not shown). Around 90% of all cancer deaths are caused by metastasis. In addition, bone metastases dramatically decrease quality of life. Thus, it is important to continue to study p38MAPK's role in metastasis and whether treatment with p38MAPK inhibitors, in conjunction with chemotherapy, is an effective therapy option. Importantly, our data indicate that p38MAPK act on the tumor and metastatic microenvironment, not directly on the tumor cells (**Supp. Fig 3.1.b, Fig 3.1,** & data not shown).

However, p38MAPK has also been reported to enforce tumor cell dormancy (13, 14). Dormant tumor cells tend to be resistant to chemotherapy and may represent a significant source of tumor recurrence. While it is possible that inhibiting p38MAPK could have negative outcomes via activation of otherwise dormant tumor cells, it is also likely that treatment with p38MAPK inhibitors could sensitize dormant tumor cells to

chemotherapy by limiting their stromal support and/or driving them into the cell cycle. Effective targeting of dormant tumor cells may reduce the chances of tumor recurrence. To better assess the potential for p38MAPK inhibitors as anti-cancer therapeutics, more work is needed to understand tumor dormancy and the microenvironment's role in it, metastasis, and the effects of p38MAPK inhibition.

REFERENCES

1. Salminen A, Kauppinen A, Kaarniranta K. 2012. Emerging role of NF-κB signaling in the induction of senescence-associated secretory phenotype (SASP). Cell Signal 24:835–45.

2. Freund A, Patil CK, Campisi J. 2011. p38MAPK is a novel DNA damage response-independent regulator of the senescence-associated secretory phenotype. EMBO J 30:1536–48.

3. Kuilman T, Michaloglou C, Vredeveld LCW, Douma S, van Doorn R, Desmet CJ, Aarden L a, Mooi WJ, Peeper DS. 2008. Oncogene-induced senescence relayed by an interleukin-dependent inflammatory network. Cell 133:1019–31.

4. Pazolli E, Alspach E, Milczarek A, Prior J, Piwnica-Worms D, Stewart SA. 2012. Chromatin remodeling underlies the senescence-associated secretory phenotype of tumor stromal fibroblasts that supports cancer progression. Cancer Res 72:2251–61.

5. Tahirov TH, Sato K, Ichikawa-Iwata E, Sasaki M, Inoue-Bungo T, Shiina M, Kimura K, Takata S, Fujikawa A, Morii H, Kumasaka T, Yamamoto M, Ishii S, Ogata K. 2002. Mechanism of c-Myb-C/EBP beta cooperation from separated sites on a promoter. Cell 108:57–70.

6. Emani S, Zhang J, Guo L, Guo H, Kuo PC. 2008. RNA Stability Regulates Differential Expression Of The Metastasis Protein, Osteopontin, In Hepatocellular Cancer 143:803–812.

7. Noda M, Yoon K, Prince CW, Butler WT, Rodan GA. 1988. Transcriptional regulation of osteopontin production in rat osteosarcoma cells by type beta transforming growth factor. J Biol Chem 263:13916–21.

8. Molvaersmyr A-K, Saether T, Gilfillan S, Lorenzo PI, Kvaløy H, Matre V, Gabrielsen OS. 2010. A SUMO-regulated activation function controls synergy of c-Myb through a repressor-activator switch leading to differential p300 recruitment. Nucleic Acids Res 38:4970–84.

9. Dahle O, Andersen TO, Nordgard O, Matre V, Del Sal G, Gabrielsen OS. 2003. Transactivation properties of c-Myb are critically dependent on two SUMO-1 acceptor sites that are conjugated in a PIASy enhanced manner. Eur J Biochem 270:1338–1348.

10. Miglarese MR, Richardson a F, Aziz N, Bender TP. 1996. Differential regulation of c-Myb-induced transcription activation by a phosphorylation site in the negative regulatory domain. J Biol Chem 271:22697–705.

11. Pani E, Menigatti M, Schubert S, Hess D, Gerrits B, Klempnauer K-H, Ferrari S. 2008. Pin1 interacts with c-Myb in a phosphorylation-dependent manner and

regulates its transactivation activity. Biochim Biophys Acta 1783:1121–8.

12. Amaru Calzada A, Todoerti K, Donadoni L, Pellicioli A, Tuana G, Gatta R, Neri A, Finazzi G, Mantovani R, Rambaldi A, Introna M, Lombardi L, Golay J. 2012. The HDAC inhibitor Givinostat modulates the hematopoietic transcription factors NFE2 and C-MYB in JAK2(V617F) myeloproliferative neoplasm cells. Exp Hematol 40:634–45.e10.

13. Bragado P, Estrada Y, Parikh F, Krause S, Capobianco C, Farina HG, Schewe DM, Aguirre-Ghiso JA. 2013. TGF-β2 dictates disseminated tumour cell fate in target organs through TGF-β-RIII and p38α/β signalling. Nat Cell Biol 15:1351–61.

14. Aguirre-Ghiso JA. 2008. Models, mechanisms and clinical evidence for cancer dormancy. Nat Rev Cancer 7:834–846.